Passive Acoustic Monitoring for Marine Mammals in the SOCAL Range Complex April 2020–2021 and Abundance and Density Estimates from CalCOFI Visual Surveys 2004–2021

Ally C. Rice, Jennifer S. Trickey, Ashlyn Giddings, Macey A. Rafter, Sean M. Wiggins, Kaitlin E. Frasier, Simone Baumann-Pickering, John A. Hildebrand

Marine Physical Laboratory
Scripps Institution of Oceanography
University of California San Diego
La Jolla, CA 92037

Cuvier's beaked whale, Photo by Gustavo Cárdenas-Hinojosa

MPL TECHNICAL MEMORANDUM #657
February 2022

Suggested Citation:

Rice, A.C., Trickey, J.S., Giddings, A., Rafter, M.A., Wiggins, S.M., Frasier, K.E., Baumann-Pickering, S., and Hildebrand, J.A. (2022) “Passive Acoustic Monitoring for Marine Mammals in the SOCAL Range Complex April 2020–2021 and Abundance and Density Estimates from CalCOFI visual surveys 2004–2021,” Marine Physical Laboratory, Scripps Institution of Oceanography, University of California San Diego, La Jolla, CA, MPL Technical Memorandum #657 under Cooperative Ecosystems Study Unit Cooperative Agreement N62473-21-2-0012 for U.S. Navy, U.S. Pacific Fleet, Pearl Harbor, HI.

Author contributions:

A.C.R. wrote and edited report, produced all plots of acoustic results, finalized CalCOFI plots, and conducted ambient soundscape and sonar metric analysis. J.S.T. conducted beaked whale and MFA sonar analysis. A.G. produced all CalCOFI density estimates and associated figures. M.A.R. conducted explosion analysis. S.M.W. contributed to algorithm development. K.E.F., S.B.P., and J.A.H. developed and managed the project.

Table of Contents

List of Tables

List of Figures

Executive Summary

Passive acoustic monitoring was conducted in the Navy's Southern California Range Complex from April 2020 to 2021 to detect marine mammal and anthropogenic sounds. High-frequency Acoustic Recording Packages (HARPs) recorded sounds between 10 Hz and 100 kHz at four locations: two west of San Clemente Island (1,300 m depth, site E and 1,100 m depth, site H) and two southwest of San Clemente Island (1,300 m depth, site N and 1,200 m depth, site U). With the offshore expansion of the SOCAL range, future noise monitoring will be improved by the deployment of a recorder west of San Nicolas Island (site SN). This new site will replace site U, which is located in the Mexican Exclusive Economic Zone where instrument deployment is difficult.

While a typical southern California marine mammal assemblage is consistently detected in these recordings (Hildebrand *et al.*, 2012), only beaked whales were analyzed for this report. The low-frequency ambient soundscape and the presence of Mid-Frequency Active (MFA) sonar and explosions are also reported.

Ambient sound levels were highest for frequencies greater than ~200 Hz at site E and lowest at site U, likely related to local wind. Peaks in sound levels at all sites during the fall and winter are related to the seasonally increased presence of blue whales and fin whales, respectively.

For marine mammal and anthropogenic sounds, data analysis was performed using automated computer algorithms. Frequency modulated (FM) echolocation pulses from Cuvier's beaked whales were regularly detected at all sites, but were detected in much higher numbers at sites E and H. At site E, detections were highest in December 2020, while at site H they peaked in October and November 2020. Hubbs' beaked whale FM pulses (previously referred to as BW37V; Rice *et al.*, 2021) were only detected at site H in November 2020 and January 2021. The FM pulse type, BW43, thought to be produced by Perrin's beaked whale (Baumann-Pickering *et al.*, 2014), was detected intermittently at sites H and N, and throughout the recording period at site U. No other beaked whale signal types were detected.

Two anthropogenic signals were detected: MFA sonar and explosions. MFA sonar was detected at all sites with peaks in May and November 2020 and in February and April 2021. Site H had the most MFA sonar packet detections normalized per year, while site N had the highest cumulative sound exposure levels. Site E had the lowest number of sonar packet detections, while site H had the lowest maximum cumulative sound exposure level. Explosions were detected at all sites, but were highest in December 2020 and February 2021 at site H. At site H, temporal and spectral parameters suggest association with fishing, specifically with the use of seal bombs.

Cetacean distribution, density, and abundance in the Southern California Bight were assessed through visual surveys during quarterly California Cooperative Oceanic Fisheries Investigations (CalCOFI) cruises from 2004 to 2021. Abundance and density estimates were developed for nine commonly-sighted marine mammal species. Fin whales were the most often sighted mysticete species, while short-beaked common dolphins were the most often sighted odontocete. Blue and fin whale abundance was highest in summer and fall, while humpback and grey whale abundance, as well as abundance for all odontocete species, was highest in winter and spring. In the CalCOFI

study area, humpback whales, bottlenose dolphins, and common dolphins show a potential increase in abundance over time, while Dall's porpoise abundance has declined in recent years.

Project Background

The Navy's Southern California (SOCAL) Range Complex is located in the Southern California Bight and the adjacent deep waters to the west. This region has a highly productive marine ecosystem due to the southward flowing California Current and associated coastal current system. A diverse array of marine mammals is found here, including baleen whales, beaked whales, and other toothed whales and pinnipeds.

In January 2009, an acoustic monitoring effort was initiated within the SOCAL Range Complex with support from the U.S. Pacific Fleet. The goal of this effort was to characterize the vocalizations of marine mammal species present in the area, determine their seasonal presence, and evaluate the potential for impact from naval training. In this current effort, the goal was to explore the seasonal presence of beaked whales. In addition, the low-frequency ambient soundscape, as well as the presence of Mid-Frequency Active (MFA) sonar and explosions, was analyzed.

California Cooperative Oceanic Fisheries Investigations (CalCOFI) cruises are conducted quarterly in the Southern California Bight to provide a valuable assessment of cetacean abundance, density, distribution and habitat use patterns in an area that is also the location of extensive naval training (Campbell *et al.*, 2015). Cetacean surveys have been integrated into the cruises since 2004, using both visual and acoustic detection methods (Soldevilla *et al.*, 2006; Campbell *et al.*, 2015; Debich *et al.*, 2017; Trickey *et al.*, 2020). The objectives of the cetacean monitoring program are to make seasonal, annual and long-term estimates of cetacean density and abundance, to determine the temporal and spatial patterns of cetacean distribution, to provide data for habitat-based density modeling, to quantify differences in vocalizations between cetacean species, and to compare visual and acoustic survey methods and results.

This report documents the analysis of data recorded by High-frequency Acoustic Recording Packages (HARPs) that were deployed at four sites within the SOCAL Range Complex and collected data between April 2020 and 2021 (Table 1; Table 2; Table 3; Table 4). The four recording sites include two to the west (sites E and H) and two to the south (sites N and U) of San Clemente Island (Figure 1; Figure 2). This report also documents the distribution, abundance, and density for the marine mammal species most commonly sighted during quarterly CalCOFI cruises in the Southern California Bight from 2004 to 2021.

Table 1. SOCAL Range Complex acoustic monitoring at site E since January 2009.
Periods of instrument deployment analyzed in this report are shown in bold. Deployment 66 did not record due to implosion of instrument floats during deployment.

Deployment #	Monitoring Period	# Hours
31	1/13/09 – 3/9/09	1302
32	3/13/09 – 5/7/09	1302
33	5/19/09 – 7/12/09	1302
34	7/24/09 – 9/16/09	1302
61	3/5/17 – 7/10/17	3063
62	7/11/17 – 2/10/18	5148
63	3/15/18 – 7/11/18	2843
64	7/12/18 – 11/28/18	3356
65	11/29/18 – 5/7/19	3838
66	-	-
67	11/9/19 – 5/8/20	4362
68	**5/9/20–10/29/20**	**4170**
69	**10/29/20–4/24/21**	**4247**

Table 2. SOCAL Range Complex acoustic monitoring at site H since January 2009. Periods of instrument deployment analyzed in this report are shown in bold. Missing deployments are the result of hydrophone failures.

Deployment #	Monitoring Period	# Hours
31	1/13/09 – 3/8/09	1320
32	3/14/09 – 5/7/09	1320
33	5/19/09 – 6/13/09	600
34	7/23/09 – 9/15/09	1296
35	9/25/09 – 11/18/09	1320
36	12/6/09 – 1/29/10	1296
37	1/30/10 – 3/22/10	1248
38	4/10/10 – 7/22/10	2472
40	7/23/10 – 11/8/10	2592
41	12/6/10 – 4/17/11	3192
44	5/11/11 – 10/12/11	2952
45	10/16/11 – 3/5/12	3024
46	3/25/12 – 7/21/12	2856
47	8/10/12 – 12/20/12	3192
48	12/21/12 – 4/30/13	3140
49	-	-
50	9/10/13 – 1/6/14	2843
51	1/7/14 – 4/3/14	2082
52	4/4/14 – 7/30/14	2814
53	7/30/14 – 11/5/14	2340
54	11/5/14 – 2/4/15	2198
55	2/5/15 – 6/1/15	2800
56	6/2/15 – 10/3/15	2952
57	-	-
58	11/21/15 – 4/25/16	3734
59	7/6/16 – 11/9/16	3011
60	-	-
61	2/22/17 – 6/6/17	2518
62	6/7/17 – 10/4/17	2879
63	10/5/17 – 11/3/17	707
65	7/9/18 – 11/28/18	3413
66	11/29/18 – 5/5/19	3784
67	6/1/19 – 12/8/19	4557
68	12/8/19 – 5/8/20	3644
69	**5/9/20–10/29/20**	**4172**
70	**10/29/20–4/24/21**	**4245**

Table 3. SOCAL Range Complex acoustic monitoring at site N since January 2009. Periods of instrument deployment analyzed in this report are shown in bold. Dates in italics were only used for high frequency analysis. Deployment 50 yielded no usable data due to flooding of the instrument from a hardware failure.

Deployment #	Monitoring Period	# Hours
31	1/14/09 – 3/9/09	1296
32	3/14/09 – 5/7/09	1320
33	5/19/09 – 7/12/09	1296
34	7/22/09 – 9/15/09	1320
35	9/26/09 – 11/19/09	1296
36	12/6/09 – 1/26/10	1224
37	1/31/10 – 3/26/10	1296
38	4/11/10 – 7/18/10	2352
40	7/23/10 – 11/8/10	2592
41	12/7/10 – 4/9/11	2952
44	5/12/10 – 9/23/11	3216
45	10/16/11 – 2/13/12	2904
46	3/25/12 – 8/5/12	3216
47	8/10/12 – 12/6/12	2856
48	12/20/12 – 5/1/13	3155
49	5/2/13 – 9/11/13	3156
50	-	-
51	1/7/14 – 2/16/14	956
52	4/4/14 – 7/30/14	2817
53	7/30/14 – 11/5/14	2342
54	11/4/14 -2/5/15	2196
55	2/5/15 – 2/23/15	433
56	6/2/15 – 10/3/15	2966
57	10/3/15 – 11/21/15	1168
58	*11/21/15 – 4/18/16*	*3578*
59	7/7/16 – 11/8/16	2999
60	11/9/16 – 2/21/17	2457
61	2/21/17 – 6/7/17	2528
62	6/7/17 – 12/21/17	4723
63	2/4/18 – 7/9/18	3722
64	7/9/18 – 11/28/18	3417
65	11/29/18 – 5/5/19	3768
66	5/5/19 – 11/7/19	4481
67	11/8/19 – 4/29/20	4148
68	**4/29/20–10/15/20**	**4058**
69	**11/6/20–4/15/21**	**3861**

Table 4. SOCAL Range Complex acoustic monitoring at site U since November 2018. Periods of instrument deployment analyzed in this report are shown in bold.

Deployment #	Monitoring Period	# Hours
01	11/18/18 – 6/11/19	4936
02	11/6/19 – 1/16/20	1689
03	**4/29/20–11/02/20**	**4488**
04	**11/06/20–1/19/21**	**1796**

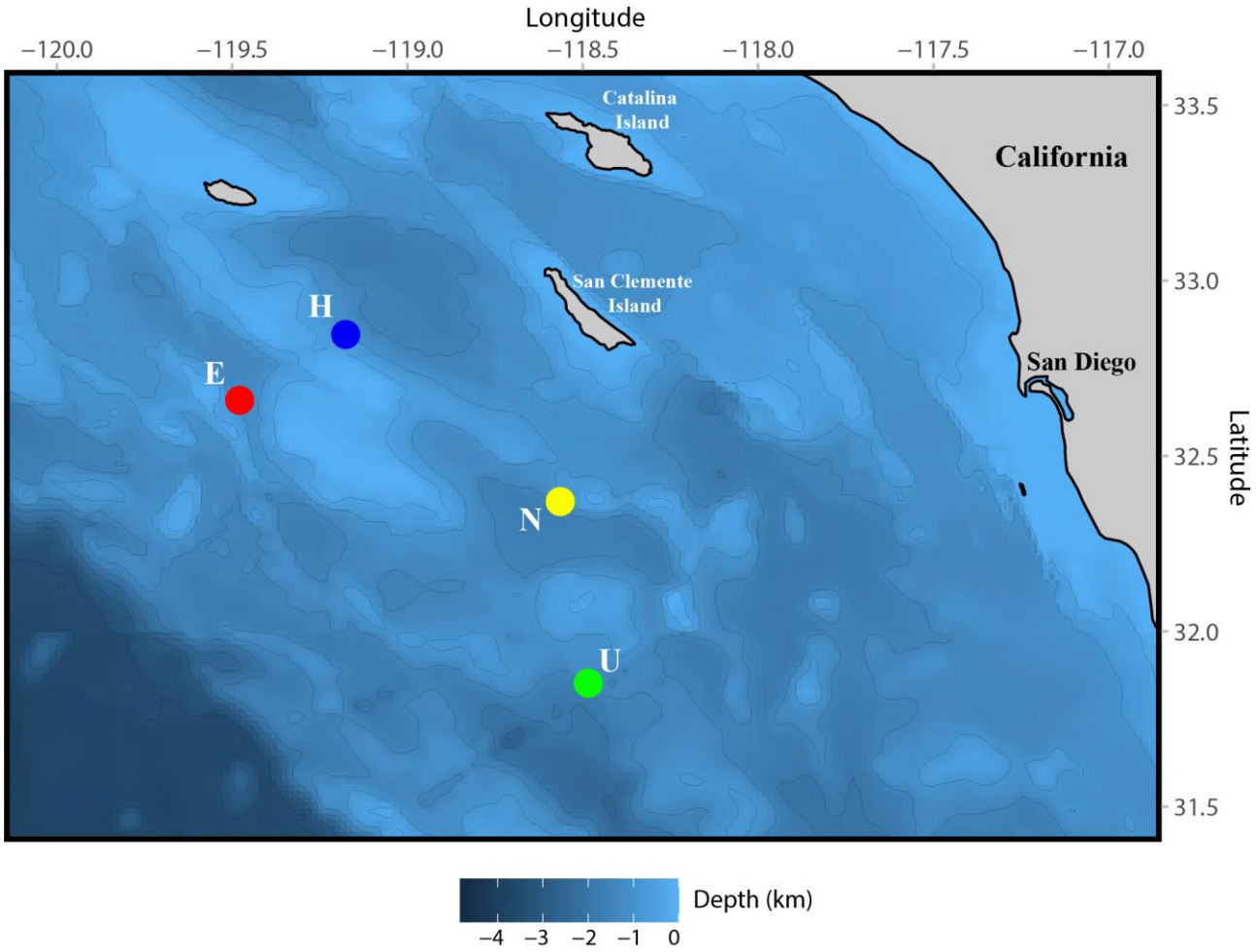

Figure 1. Locations of High-frequency Acoustic Recording Package (HARP) deployment sites E, H, N, and U (circles) in the SOCAL study area from April 2020 through 2021. Color indicates bathymetric depth. Contour lines represent 500 m depth increments.

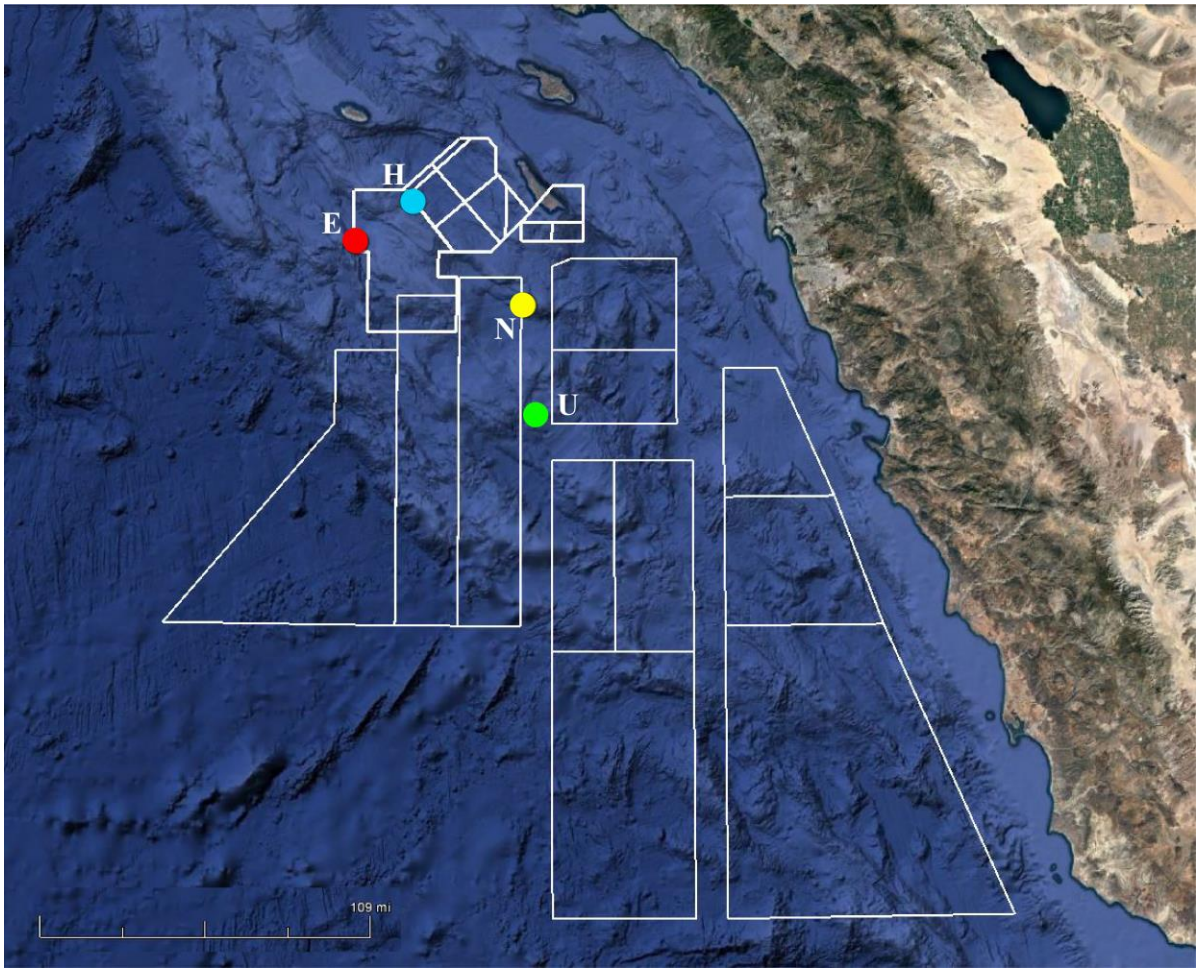

Figure 2. Locations of High-frequency Acoustic Recording Package (HARP) deployments in the SOCAL study area (colored circles) and US Naval Operation Areas (white boxes).

Methods

Passive Acoustic Monitoring

High-frequency Acoustic Recording Package (HARP)

HARPs were used to record the low-frequency ambient soundscape as well as marine mammal and anthropogenic sounds in the SOCAL area. HARPs can autonomously record underwater sounds from 10 Hz up to 160 kHz and are capable of up to approximately one year of continuous data storage. The HARPs were deployed in a seafloor mooring configuration with the hydrophones suspended at least 10 m above the seafloor. Each HARP hydrophone is calibrated in the laboratory to provide a quantitative analysis of the received sound field. Representative data loggers and hydrophones were also calibrated at the Navy's Transducer Evaluation Center facility to verify the laboratory calibrations (Wiggins and Hildebrand, 2007).

Data Collected

Acoustic recordings have been collected within the SOCAL Range Complex near San Clemente Island since 2009 (Table 1; Table 2; Table 3) using HARPs sampling at 200 kHz. The sites analyzed in this report are designated site E (32° 39.56' N, 119° 28.76' W, depth 1,300 m), site H

(32° 51.27'N, 119° 08.95' W, depth 1,100 m), site N (32° 22.18' N, 118° 33.90' W, depth 1,300 m), and site U (31° 51.1' N, 118° 29.07' W, depth 1,200 m).

Site E recorded from May 9, 2020 to April 24, 2021, but there were gaps from June 6 to July 4, 2020 and again from December 25, 2020 to February 19, 2021 due to disk imaging errors. Site H recorded from May 9, 2020 to April 24, 2021. Site N recorded from April 29, 2020 to October 15, 2020 and again from November 6, 2020 to April 15, 2021. Site U recorded from April 29 to November 2, 2020 and again from November 6, 2020 to January 19, 2021. During the second deployment, the recording at Site U ended early due to a bad connection to the battery case. For all four sites, a total of 31,037 h (1,293 days) of acoustic data were recorded in the deployments analyzed in this report.

Data Analysis

Recording over a broad frequency range of 10 Hz to 100 kHz allows quantification of the low-frequency ambient soundscape, detection of baleen whales (mysticetes), toothed whales (odontocetes), and anthropogenic sounds. Analyses were conducted using appropriate automated detectors for whale and anthropogenic sound sources. Analysis was focused on Cuvier's beaked whales (*Ziphius cavirostris*). In addition, the data were screened for signals from Blainville's (*Mesoplodon densirostris*) and Stejneger's (*M. stejnegeri*) beaked whales, as well as for frequency-modulated (FM) pulse types known as BW43 and BW70, which may belong to Perrin's (*M. perrini*) and pygmy beaked whales (*M. peruvianus*), respectively (Baumann-Pickering *et al.*, 2014). A recently identified beaked whale signal type (Griffiths *et al.*, 2018), which has now been confirmed to belong to Hubbs' beaked whale (*M. carlhubbsi*; Ballance *et al.*, 2022, in prep.), was found during this reporting period. This signal type was previously referred to as BW37V during the previous monitoring period (Rice *et al.*, 2021). A description of relevant signal types can be found below. Individual beaked whale echolocation clicks, as well as MFA sonar and explosion occurrence and levels were detected automatically using computer algorithms. For analysis of the low-frequency ambient soundscape, data were decimated by a factor of 100 for an effective bandwidth of 10 Hz to 1 kHz and long-term spectral averages (LTSAs) were created using a time average of 5 seconds and frequency bins of 1 Hz. For analysis of MFA sonar, data were decimated by a factor of 20 for an effective bandwidth of 10 Hz to 5 kHz and LTSAs were created using a time average of 5 seconds and frequency bins of 10 Hz. Full bandwidth data were used for the analysis of beaked whale signals and LTSAs were created using a time average of 5 seconds and a frequency bin size of 100 Hz. Details of all detection methods are described below.

Low-frequency Ambient Soundscape

HARPs write sequential 75-s acoustic records, from which sound pressure levels were calculated. Five, 5-s, 1-Hz sound pressure spectrum levels from the middle of each 75-s acoustic record were averaged to avoid system self-noise (specifically hard drive disk writes). Spectra from each day were subsequently combined as daily spectral averages.

Beaked Whales

Beaked whales potentially found in the Southern California Bight include Baird's (*Berardius bairdii*), Cuvier's, Blainville's, Stejneger's, Hubbs', Perrin's, and pygmy beaked whales (Jefferson *et al.,* 2008; Jefferson *et al.,* 2015).

Beaked whales can be identified acoustically by their echolocation signals (Baumann-Pickering *et al.,* 2014). These signals are FM upswept pulses, which appear to be species specific and are distinguishable by their spectral and temporal features. Identifiable signals are known for Baird's, Blainville's, Cuvier's, Hubbs', and likely Stejneger's beaked whales (Baumann-Pickering *et al.,* 2013b; Griffiths *et al.,* 2018; Ballance *et al.,* 2022, in prep.).

Other beaked whale signals detected in the Southern California Bight include FM pulses known as BW43 and BW70, which may belong to Perrin's and pygmy beaked whales, respectively (Baumann-Pickering *et al.,* 2013a; Baumann-Pickering *et al.,* 2014). During this reporting period, only Cuvier's, Hubbs', and BW43 signals were detected. These signals are described below in more detail.

Beaked whale FM pulses were detected with an automated method. This automated effort was for all identifiable signals found in Southern California except for those produced by Baird's beaked whales, as they have a signal with lower frequency content than is typical of other beaked whales and therefore are not reliably identified by the detector used. Therefore, there was no detection effort for Baird's beaked whales. After all echolocation signals were identified with a Teager Kaiser energy detector (Soldevilla *et al.,* 2008; Roch *et al.,* 2011b), an expert system discriminated between delphinid clicks and beaked whale FM pulses based on the parameters described below.

A decision about presence or absence of beaked whale signals was based on detections within a 75-s segment. Only segments with more than seven detections were used in further analysis. All echolocation signals with a peak and center frequency below 32 and 25 kHz, respectively, a duration less than 355 μs, and a sweep rate of less than 23 kHz/ms were deleted. If more than 13% of all initially detected echolocation signals remained after applying these criteria, the segment was classified to have beaked whale FM pulses. This threshold was chosen to obtain the best balance between missed and false detections. A third classification step, based on computer assisted manual decisions by a trained analyst, labeled the automatically detected segments to pulse type and rejected false detections (Baumann-Pickering *et al.,* 2013a). The rate of missed segments for this approach is typically ~5%. The start and end of each segment containing beaked whale signals was logged and their durations were added to estimate cumulative weekly presence.

Cuvier's Beaked Whales

Cuvier's beaked whale echolocation signals (Figure 3) are well differentiated from other species' acoustic signals as polycyclic, with a characteristic FM pulse upsweep, peak frequency around 40 kHz, and uniform inter-pulse interval of about 0.4–0.5 s (Johnson *et al.*, 2004; Zimmer *et al.*, 2005). An additional feature that helps with the identification of Cuvier's beaked whale FM pulses is that they have characteristic spectral peaks around 17 and 23 kHz.

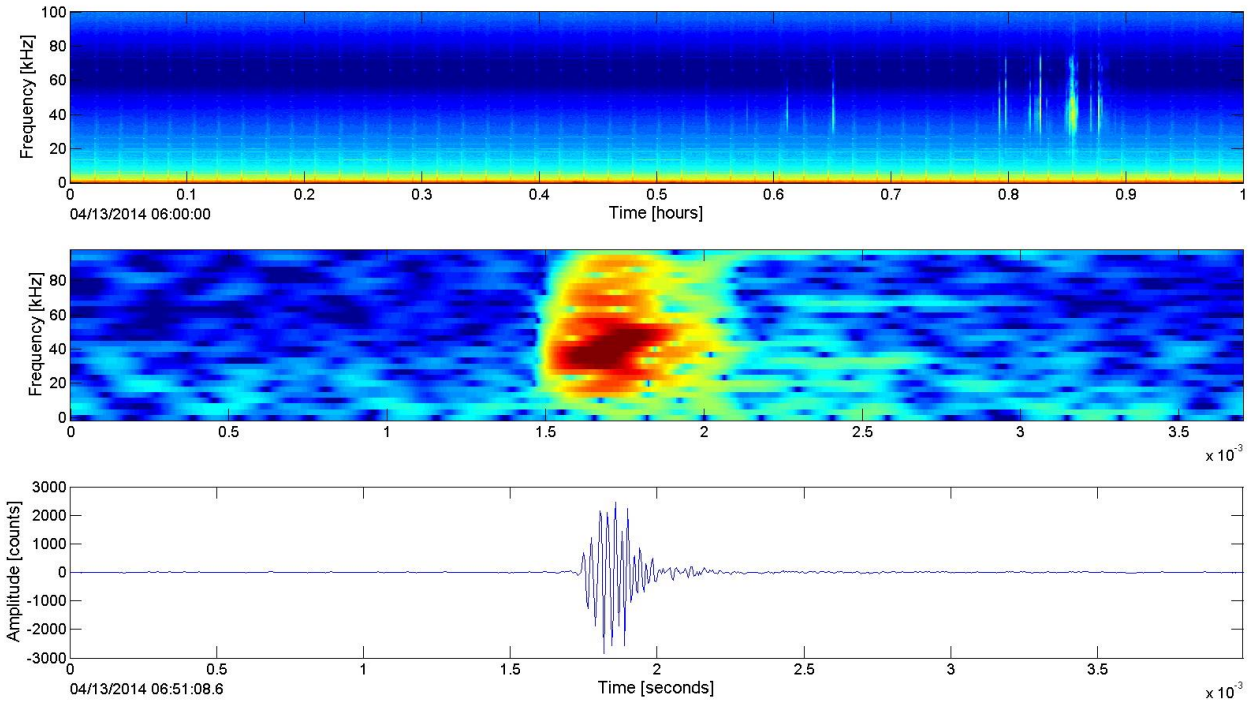

Figure 3. Echolocation sequence of Cuvier's beaked whale in an LTSA (top) and example FM pulse in a spectrogram (middle) and corresponding time series (bottom) previously recorded at site N.

Hubbs' Beaked Whales

Hubbs' beaked whale echolocation signals (Figure 4) are distinct from other beaked whale species' signals in their bimodal frequency distribution, which shows a prominent spectral peak around 35 kHz, a spectral notch at 37 kHz, and an upper peak at 48 kHz (Griffiths *et al.*, 2018). This signal type has a stable inter-pulse interval of approximately 0.13 s. This pulse type was previously referred to as BW37V (Griffiths *et al.*, 2018), but has recently been confirmed to be produced by Hubbs' beaked whale (Ballance *et al.*, 2022, in prep.).

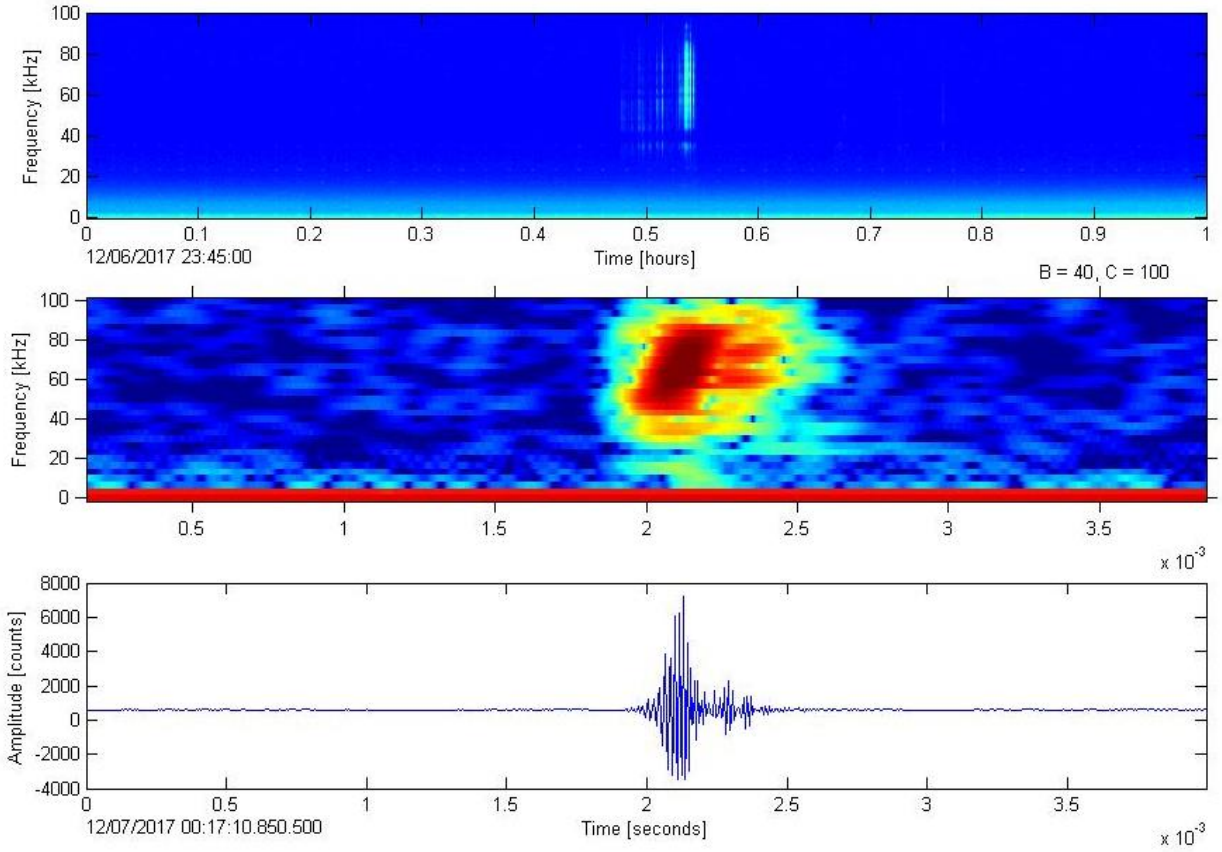

Figure 4. Echolocation sequence of Hubbs' beaked whale in an LTSA (top) and example FM pulse in a spectrogram (middle) and corresponding time series (bottom) previously recorded at site E.

BW43

The BW43 FM pulse type (Figure 5) has yet to be positively linked to a specific species. These FM pulses are distinguishable from other species' signals by their peak frequency around 43 kHz and uniform inter-pulse interval around 0.2 s (Baumann-Pickering *et al.*, 2013a). A candidate species for producing this FM pulse type may be Perrin's beaked whale (Baumann-Pickering *et al.*, 2014).

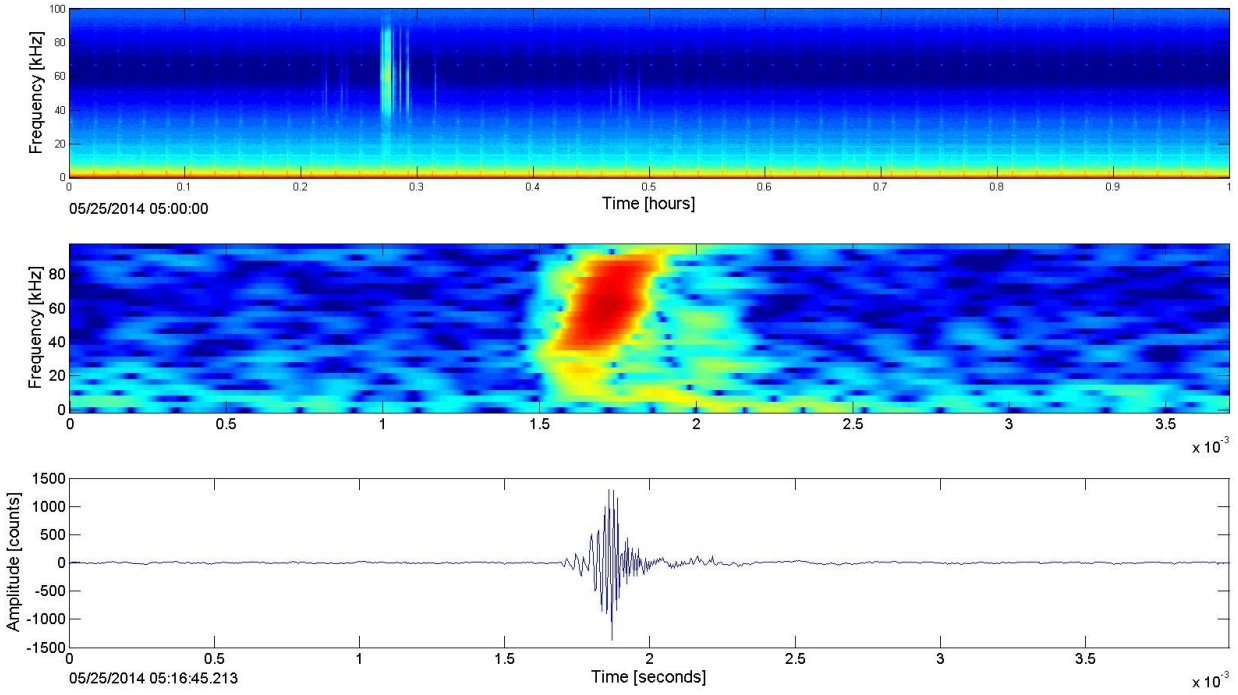

Figure 5. Echolocation sequence of BW43 in an LTSA (top) and example FM pulse in a spectrogram (middle) and corresponding time series (bottom) previously recorded at site N.

Anthropogenic Sounds

Two anthropogenic sounds were monitored for this report: Mid-Frequency Active (MFA) sonar and explosions. Both sounds were detected by computer algorithms. For MFA sonar, the start and end of each sound or session was logged and their durations were added to estimate cumulative weekly presence. For explosions, individual explosions were detected and weekly totals are reported.

Mid-Frequency Active Sonar

Sounds from MFA sonar vary in frequency (1–10 kHz) and are composed of pulses of both frequency modulated (FM) sweeps and continuous wave (CW) tones that have durations ranging from less than 1 s to greater than 5 s. Groups of pulses, or pings, constitute a packet while a wave train, or an event, is a group of packets that are separated from other MFA sonar packets by at least 1 h. Packets are transmitted repetitively as wave trains with inter-packet-intervals typically greater than 20 s (Figure 6). In the SOCAL Range Complex, the most common MFA sonar signals are between 2 and 5 kHz and are more generically known as '3.5-kHz' sonar.

In the first stage of MFA sonar detection, we used a modified version of the *Silbido* detection system (Roch *et al.*, 2011a), originally designed for characterizing toothed whale whistles. The

algorithm identifies peaks in time-frequency distributions (e.g., spectrogram) and determines which peaks should be linked into a graph structure based on heuristic rules that include examining the trajectory of existing peaks, tracking intersections between time-frequency trajectories, and allowing for brief signal dropouts or interfering signals. Detection graphs are then examined to identify individual tonal contours looking at trajectories from both sides of time-frequency intersection points. For MFA sonar detection, parameters were adjusted to detect tonal contours at or above 2 kHz in data decimated to a 10-kHz sample rate with time-frequency peaks with signal to noise ratios of 5 dB or above and contour durations of at least 200 ms with a frequency resolution of 100 Hz.

The detector frequently triggered on noise produced by instrument disk writes that occurred at 75-s intervals. Over periods of several months, these disk-write detections dominated the number of detections and could be eliminated using an outlier detection test. Histograms of the detection start times that remained once disk write periods were removed were constructed and outliers were discarded. This removed some valid detections that occurred during disk writes, but as the disk writes and sonar signals are uncorrelated, this is expected to only have a minor impact on analysis. As the detector did not distinguish between sonar and non-anthropogenic tonal signals within the operating band (e.g., humpback whales), human analysts examined detection output and accepted or rejected contiguous sets of detections, thereby removing any false detections. Start and end times of these cleaned sonar events were then used in further processing.

In the second stage of MFA sonar detection, these start and end times of MFA events from both methods were then used to read segments of waveforms upon which a 2.4 to 4.5 kHz bandpass filter and a simple time series energy detector was applied to detect and measure various packet parameters after correcting for the instrument calibrated transfer function (Wiggins, 2015). For each packet, maximum peak-to-peak (pp) received level (RL), sound exposure level (SEL), root-mean-square (RMS) RL, date/time of packet occurrence, and packet RMS duration (for RL_{pp} -10dB) were measured and saved.

Various filters were applied to the detections to limit the MFA sonar detection range to ~20 km for off-axis signals from an AN/SQS 53C source, which resulted in a RL detection threshold of 130 dB pp re 1 µPa (Wiggins, 2015). Instrument maximum received level was ~165 dB pp re 1 µPa, above which waveform clipping occurred. Packets were grouped into wave trains separated by more than 1 h. Packet received levels were plotted along with the number of packets and cumulative SEL (CSEL) in each wave train over the study period. Wave train duration and total packet duration were also calculated. Wave train duration is the difference between the first and last packet detections in an event. The total packet duration of a wave train is the sum of the individual packet (i.e., group of pings) durations, which is measured as the period of the waveform that is 0 to 10 dB less than the maximum peak-to-peak received level of the ping group.

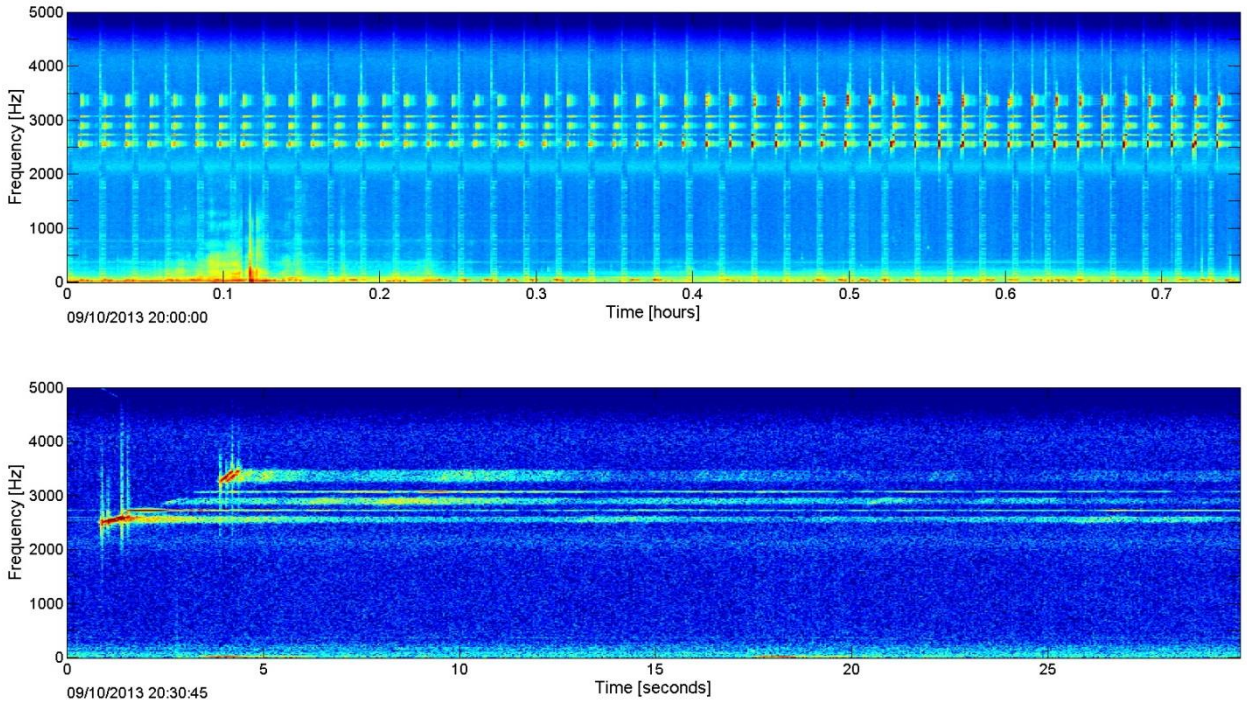

Figure 6. MFA sonar previously recorded at site H and shown as a wave train event in a 45-minute LTSA (top) and as a single packet with multiple pulses in a 30 second spectrogram (bottom).

Explosions

Effort was directed toward finding explosive sounds in the recordings including military explosions, shots from geophysical exploration, and seal bombs used by the fishing industry. Explosions have energy as low as 10 Hz and often extend up to 2,000 Hz or higher, lasting for a few seconds including the reverberation. An explosion appears as a vertical spike in the LTSA that, when expanded in the spectrogram, has a sharp onset with a reverberant decay (Figure 7). Explosions were detected automatically for all deployments using a matched filter detector on data decimated to a 10-kHz sampling rate.

The explosion detector starts by filtering the time series with a 10^{th} order Butterworth bandpass filter between 200 and 2,000 Hz. Next, cross-correlation was computed between 75 s of the envelope (i.e., Hilbert transform low pass filter) of the filtered time series and the envelope of a filtered example explosion (0.7 s, Hann windowed) as the matched filter signal. The cross correlation was squared to 'sharpen' peaks of explosion detections. A floating threshold was calculated by taking the median cross correlation value over the current 75 s of data to account for detecting explosions within noise, such as shipping. A cross-correlation threshold of above the median was set. When the correlation coefficient reached above the threshold, the time series was inspected more closely.

Consecutive explosions were required to have a minimum time distance of 0.5 s to be detected. A 300-point (0.03 s) floating average energy across the detection was computed. The start and end of the detection above threshold was determined when the energy rose by more than 2 dB above the median energy across the detection. Peak-to-peak and RMS RL were computed over the potential detection period and a time series of the length of the explosion template before and after the detection.

The potential detection was classified as false and deleted if: 1) the dB difference pp and RMS between signal and time AFTER the detection was less than 4 dB or 1.5 dB, respectively; 2) the dB difference pp and RMS between signal and time BEFORE signal was less than 3 dB or 1 dB, respectively; and 3) the detection was shorter than 0.03 or longer than 0.55 seconds. The thresholds were evaluated based on the distribution of histograms of manually verified true and false detections. By design, this detector produces a low number of false-negative detections but a high number of false-positive detections (>85%). To reduce the number of false-positive detections, each automated detection was manually reviewed and verified by a trained analyst.

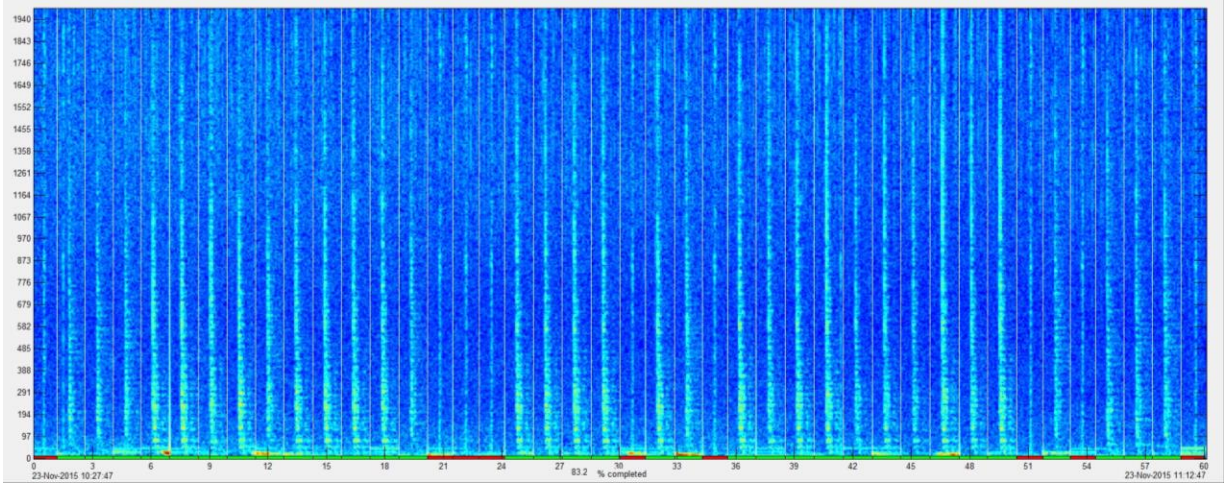

Figure 7. Explosions previously detected at site H in the analyst verification stage where events are concatenated into a single spectrogram.
Green along the bottom indicates true and red indicates false detections.

Abundance and Density Estimates from Visual Surveys

California Cooperative Oceanic Fisheries Investigations (CalCOFI) Visual Surveys

Visual surveys of marine mammals were conducted on quarterly CalCOFI cruises according to the protocol outlined in Campbell *et al.* (2015). Briefly, visual surveys were conducted by two observers (except for the fall 2019 cruise, where only one observer was present) using 7x50 Fujinon binoculars during daylight transit between CalCOFI oceanographic stations (Figure 8). Sightings were logged systematically including supporting information such as Beaufort sea state. Visual observations were conducted on each quarterly CalCOFI cruise from the summer of 2004 to fall of 2021. No visual survey was conducted on the spring 2010 cruise nor were visual surveys conducted due to COVID-related restrictions from spring 2020 through spring 2021.

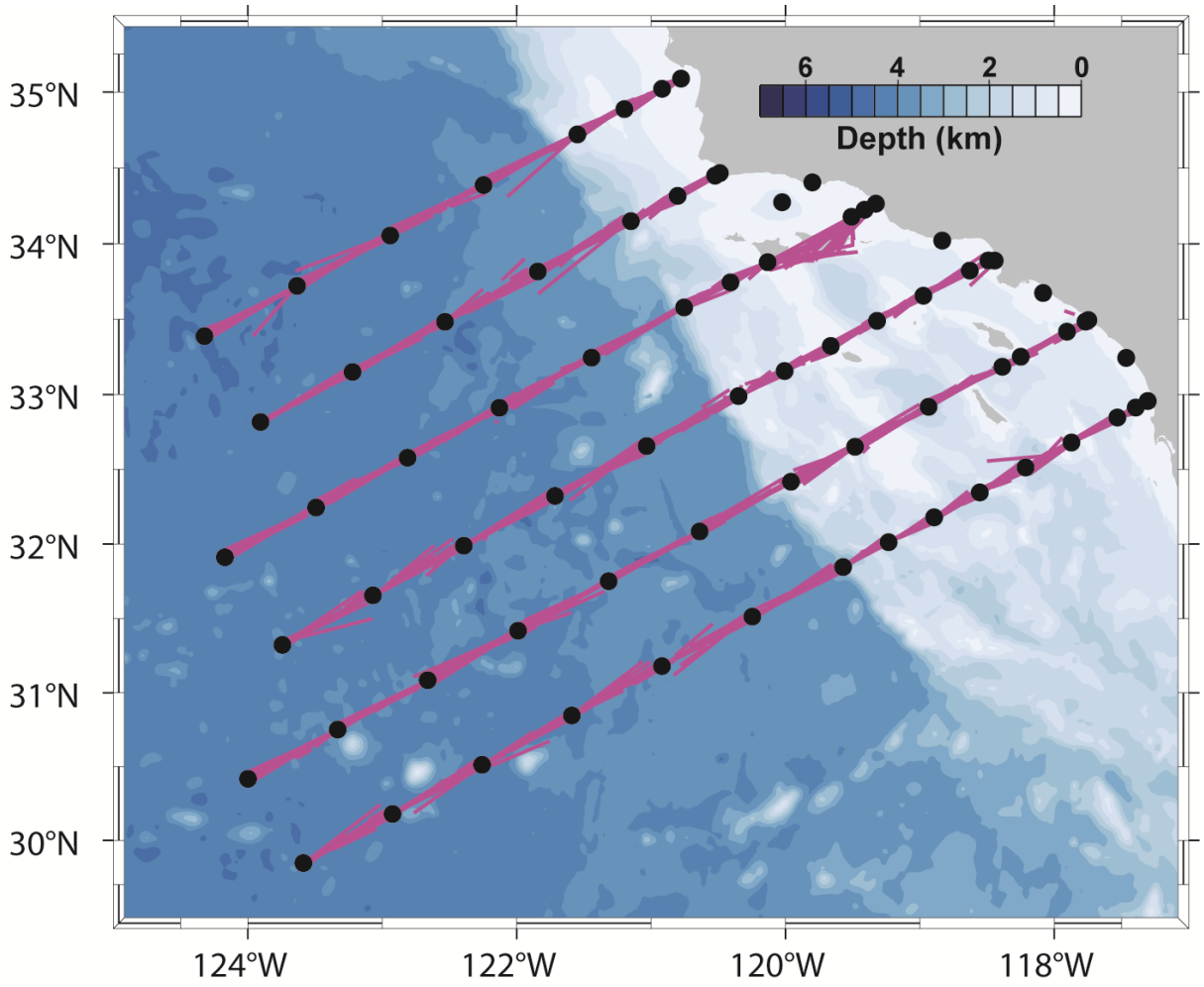

Figure 8. On-effort survey track lines (purple lines) and locations of CalCOFI oceanographic stations (black dots) from 2004 to 2021. Track lines are extrapolated from coordinates at the start and end of transits between stations. Color indicates bathymetric depth. Contour lines represent 500 m depth increments.

Abundance and Density Estimates

Abundance and density estimates were calculated for the southern CalCOFI region using distance sampling techniques with the 'distance' package in R (Miller *et al.*, 2019). The analysis included only sightings that were "on-effort" as well as "on-transect" as per the criteria in Campbell *et al.* (2015). Transects were defined as segments between oceanographic stations perpendicular to the coast. A minimum of 60 "on-effort" and "on-transect" sightings is recommended for proper detection function fitting (Buckland *et al.*, 2001). When pooling detections across all CalCOFI cruises, eight species met this requirement: blue whale (*Balaenoptera musculus*), fin whale (*B. physalus*), humpback whale (*Megaptera novaeangliae*), gray whale (*Eschrichtius robustus*), common dolphin (*Delphinus delphis*), Pacific white-sided dolphin (*Lagenorhynchus obliquidens*), Risso's dolphin (*Grampus griseus*), and Dall's porpoise (*Phocoenoides dalli*). A ninth species (bottlenose dolphin [*Tursiops truncates*]) was also analyzed, although only 59 sightings met the "on-effort" and "on-transect" requirements. Common dolphins were split into two subspecies: long-beaked common dolphin (*D. delphis bairdii*) and short-beaked common dolphin (*D. delphis delphis*). As the group size of common dolphins varies widely and this could have an impact on detection probability, short-beaked common dolphins were further divided based on group size: less than or equal to 20 dolphins or greater than 20 dolphins per group. Such group-sized stratification

was not possible for long-beaked common dolphins because very few sightings occurred with group sizes below 21 dolphins.

We were unable to measure the detection probability directly on the track line, as doing so requires two independent teams of observers, and thus relied on previous estimates of track line detection probability (*g(0)*) in the region (Barlow and Forney, 2007). It is worth noting that these estimates were calculated for observers using greater magnification (25x vs 7x in the present study) and thus are likely to have some positive bias. Truncation was selected using the Cramer-von Mises goodness-of fit test and was based either on distance to the sighting (e.g. truncation of sightings further than 2400 m away) or data percentage (e.g. truncating data further away than 90% of the recorded observed distances) and used to determine the effective strip width (Buckland *et al.*, 2001). Both truncation methods were tested for each species and the method that produced the highest Cramer-von Mises score was used in subsequent modeling. Sea state, season, and group size were investigated as covariates (Marques *et al.*, 2007). Detection function models were selected using the Akaike's information criterion and Cramer-von Mises goodness-of-fit tests. Pacific white-sided dolphin, Dall's porpoise, bottlenose dolphin, and common dolphin have been shown to have responsive movement (e.g. ship attraction), which can cause a positive bias in density and abundance estimation. Hazard-rate models for these species exacerbate this positive bias with a large spike in detection probability at small distances. To counteract this issue, we selected only among half-normal models for these species. Confidence intervals were calculated using a log-normal distribution.

CalCOFI surveys are conducted in "passing mode" with the ship remaining on the transect line throughout the survey. This results in larger numbers of unidentified individuals than in other survey designs. To counteract the potential negative bias to our abundance estimates, we applied a correction factor following the protocol in Becker *et al.* (2017; equation 1, below).

Equation 1

$$c = 1 + \frac{t_{unid}}{t_{tgt} + t_{oth}}$$

In this equation, t_{tgt} is the number of identified individuals in the target species, t_{oth} is the number of identified individuals of closely related species, and t_{unid} is the number of unidentified individuals in the species group (Becker *et al.*, 2017). We used this correction factor for two groups: unidentified large baleen whales (either blue, fin, or humpback whales) and common dolphins not identified at the subspecies level (either long-beaked or short-beaked common dolphins). This correction factor was then multiplied by the abundance estimate (equation 2, Buckland *et al.*, 2001; Becker *et al.*, 2017) obtained through the distance sampling protocol for large whales (blue, fin, and humpback whales) and for common dolphins (long- and short-beaked common dolphins) in order to obtain our finalized abundance estimates for these species.

Equation 2

$$D = \frac{n \cdot s \cdot c}{L \cdot ESW \cdot g(0)}$$

In this equation, *D* is the density (animals per km^2), *n* is the number of sightings, *s* is the mean group size, *c* is the unidentified animal correction factor (equation 1; set to *c*=1 when no correction was applied), *L* is the length surveyed, *ESW* is the effective strip width, and *g(0)* is the probability of detection on the track line.

Results

Passive Acoustic Monitoring

The results of acoustic data analysis at sites E, H, N, and U from April 2020 to 2021 are summarized below.

We describe the low-frequency ambient soundscape and the seasonal occurrence and relative abundance of beaked whale acoustic signals and anthropogenic sounds of interest.

Low-frequency Ambient Soundscape

- The underwater ambient soundscape at all sites had spectral shapes with higher levels at low frequencies (Figure 9) owing to the dominance of ship noise at frequencies below 100 Hz and local wind and waves above 100 Hz (Hildebrand, 2009).
- Site H generally had lower spectrum levels, compared to the other sites, below 100 Hz (Figure 9). This is expected because site H is away from shipping routes and is located in a basin shielded from the deep ocean (McDonald *et al.*, 2008). However, spectrum levels below 15 Hz during spring months appear to have been influenced by strumming related to tidal flow (Figure 9).
- Sites E, N, and U generally had spectrum levels around 3 dB higher than site H at 10–100 Hz, owing to greater exposure to open-ocean shipping noise (Figure 9).
- Prominent peaks in sound spectrum levels observed in the frequency band 15–30 Hz during fall and winter at all sites were related to the seasonally increased presence of fin whale calls. The highest levels during this period occurred at site E (Figure 9).
- Spectral peaks around 45 Hz from July to December at all sites were related to blue whale B calls. The highest levels during this period occurred at site U. The peaks at 15 and 30 Hz at site U were also a result of blue whale B calls (Figure 9).

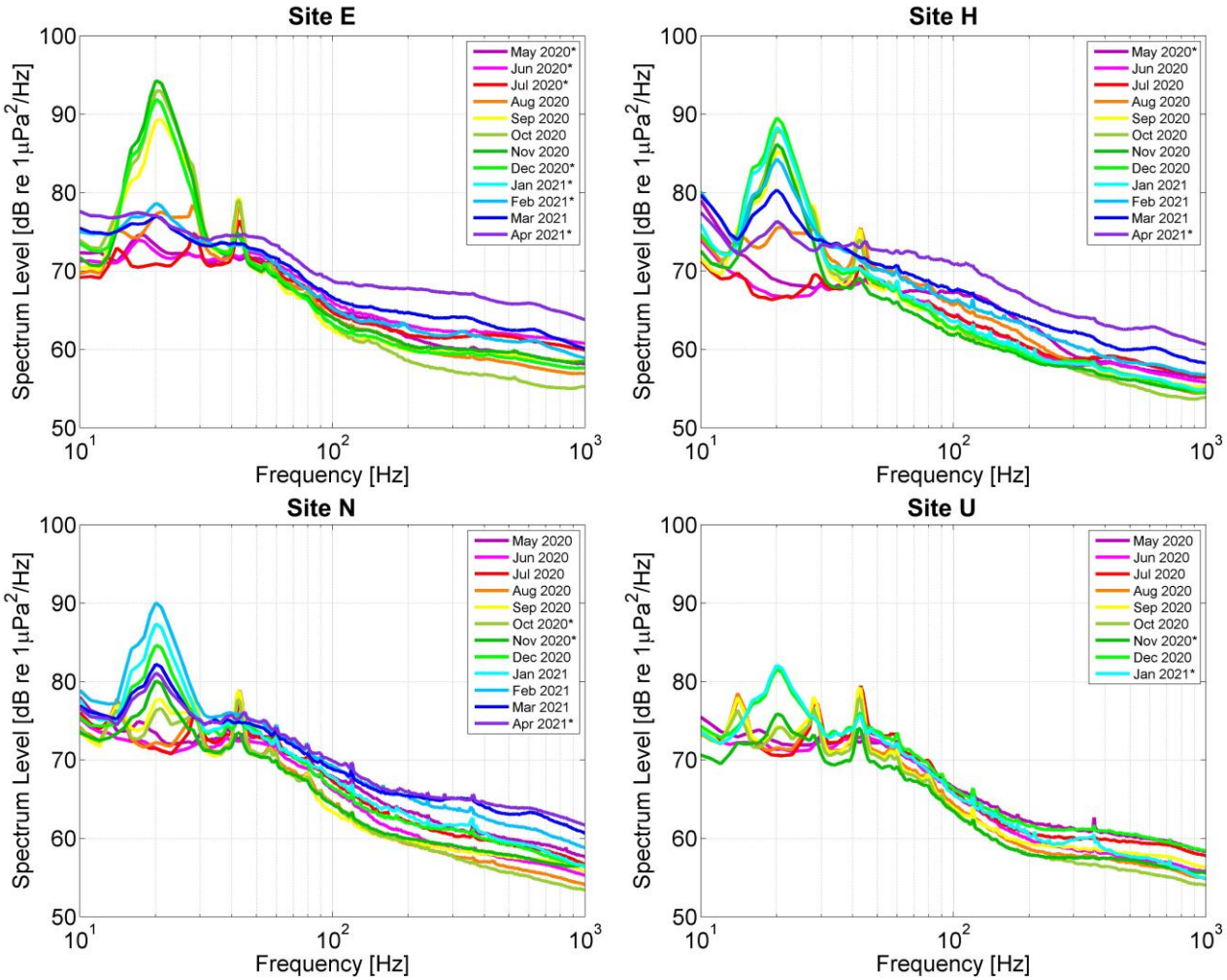

Figure 9. Monthly averages of sound spectrum levels at sites E, H, N, and U. Legend gives color-coding by month. * denotes months with partial (< 90%) effort.

Beaked Whales

Cuvier's beaked whales were detected throughout the monitoring period at all four sites. Hubbs' beaked whales were detected only during November and January at site H. The FM pulse type, BW43, possibly produced by Perrin's beaked whales (Baumann-Pickering *et al.*, 2014), was detected in low numbers intermittently at sites H and N, and throughout the monitoring period at site U. No other beaked whale species were detected during this recording period. More details of each species' presence at the four sites are given below.

Cuvier's Beaked Whales

Cuvier's beaked whale was the most commonly detected beaked whale.

- Cuvier's beaked whale FM pulses were detected most at sites E and H and least at site U (Figure 10).
- At site E, detections were low in September and showed a slight increase in December 2020. At site H, detections were relatively consistent throughout the monitoring period, with a peak during October and November 2020. Detections were low throughout the monitoring periods for sites N and U, except for an increase in detections in January 2021 at site N (Figure 10).
- There was no discernable diel pattern for Cuvier's beaked whale detections (Figure 11).
- Detections were generally consistent with previous reports, although the January 2021 peak in detections at site N was higher than during previous monitoring periods (Kerosky *et al.*, 2013; Debich *et al.*, 2015a; Debich *et al.*, 2015b; Širović *et al.*, 2016; Rice *et al.*, 2017; Rice *et al.*, 2018; Rice *et al.*, 2019; Rice *et al.*, 2020; Rice *et al.*, 2021).

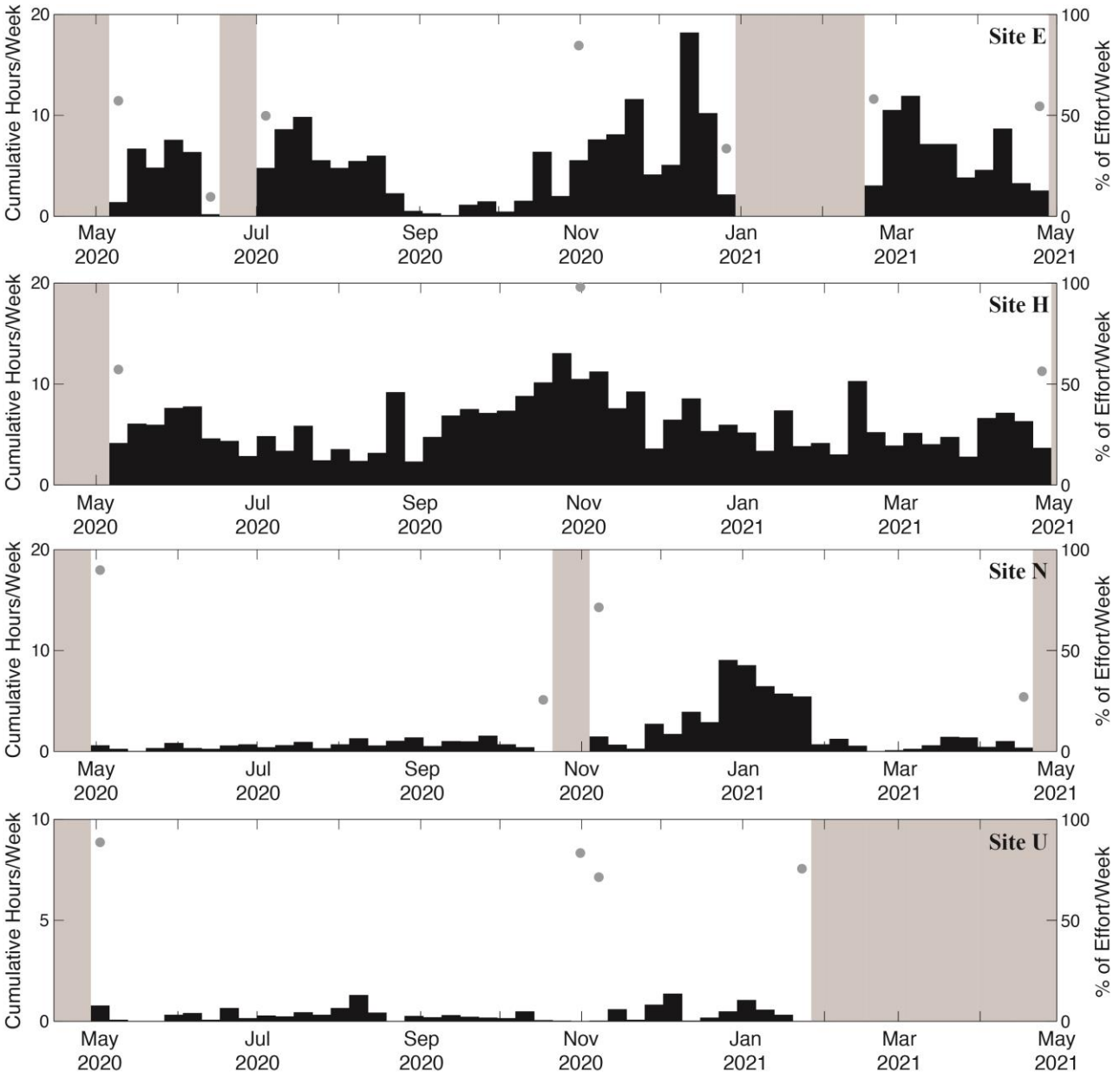

Figure 10. Weekly presence of Cuvier's beaked whale FM pulses between April 2020 and 2021 at sites E, H, N, and U.

Gray dots represent percent of effort per week in weeks with less than 100% recording effort, and gray shading represents periods with no recording effort. Where gray dots or shading are absent, full recording effort occurred for the entire week. Note the lower y-axis value for site U.

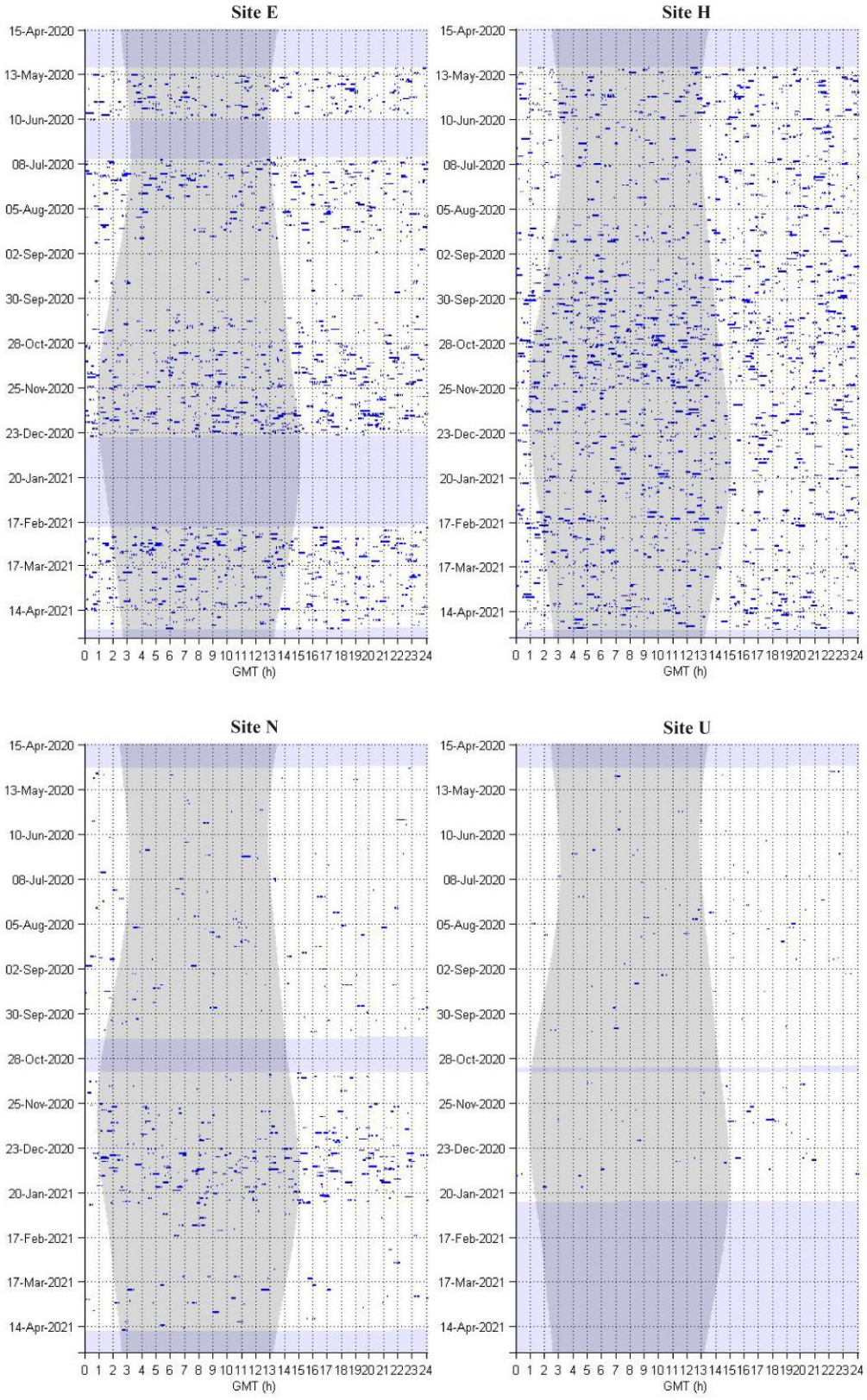

Figure 11. Cuvier's beaked whale FM pulses, indicated by blue dots, in one-minute bins at sites E, H, N, and U.
Gray vertical shading denotes nighttime and light purple horizontal shading denotes absence of acoustic data.

Hubbs' Beaked Whales

Hubbs' beaked whale FM pulses, previously referred to as BW37V FM pulses, were detected in low numbers at site H.

- Hubbs' beaked whale FM pulses were detected at site H on only one day in November 2020 and one day in January 2021. There were no detections at sites E, N, and U (Figure 12).
- All Hubbs' beaked whale detections occurred at night, but there were not enough detections to determine if there was a diel pattern (Figure 13).
- Detections at site H were lower than during the previous monitoring period (Rice *et al.*, 2021), but were consistent with detections in past reports (Rice *et al.*, 2019; Rice *et al.*, 2020). However, there were no detections at site E or N, as there were during previous monitoring periods (Rice *et al.*, 2019; Rice *et al.*, 2020; Rice *et al.*, 2021).

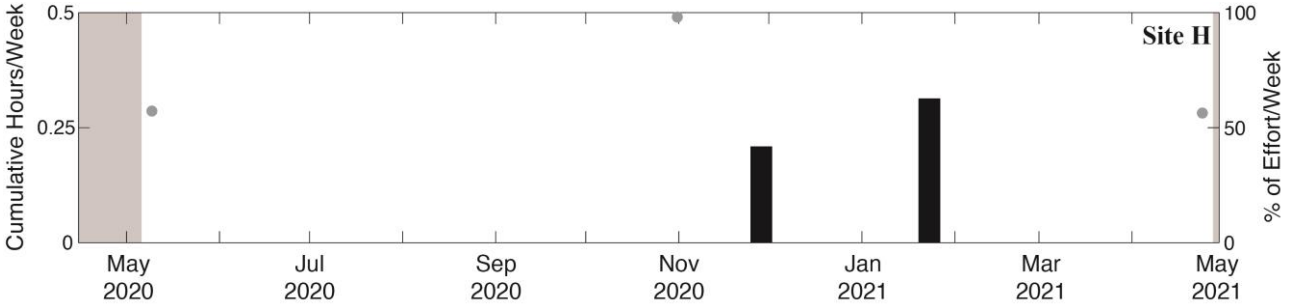

Figure 12. Weekly presence of Hubbs' beaked whale FM pulses between April 2020 and 2021 at site H. Gray dots represent percent of effort per week in weeks with less than 100% recording effort, and gray shading represents periods with no recording effort. Where gray dots or shading are absent, full recording effort occurred for the entire week.

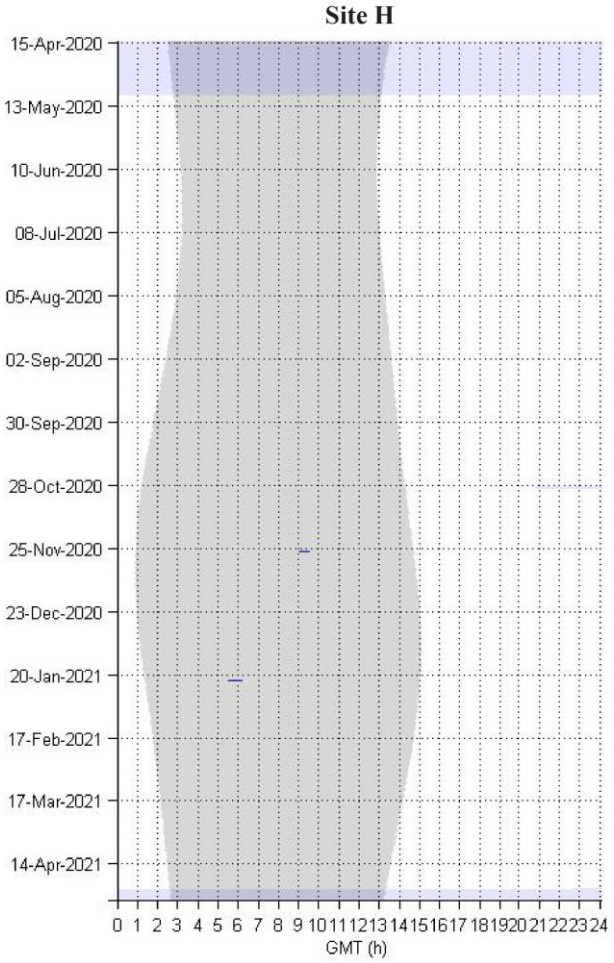

Figure 13. Hubbs' beaked whale FM pulses, indicated by blue dots, in ten-minute bins at site H. Gray vertical shading denotes nighttime and light purple horizontal shading denotes absence of acoustic data.

BW43

BW43 FM pulses were detected intermittently at sites H and N and throughout the recording period at site U.

- BW43 FM pulses were detected at sites H, N, and U. At site H, detections occurred on one day in July and on two days in December 2020. At site N, detections occurred from June to August, and on one day each in October and December 2020, and in February 2021. At site U detections occurred throughout the monitoring period, with a peak in August 2020 (Figure 14). There were no detections at site E.
- There was no discernable diel pattern for BW43 detections (Figure 15).
- The overall number of detections is consistent with previous reports (Kerosky *et al.*, 2013; Debich *et al.*, 2015a; Debich *et al.*, 2015b; Širović *et al.*, 2016; Rice *et al.*, 2017; Rice *et al.*, 2018; Rice *et al.*, 2019; Rice *et al.*, 2020; Rice *et al.*, 2021). However, there were no detections at site E, as there was during one previous monitoring period (Rice *et al.*, 2020).

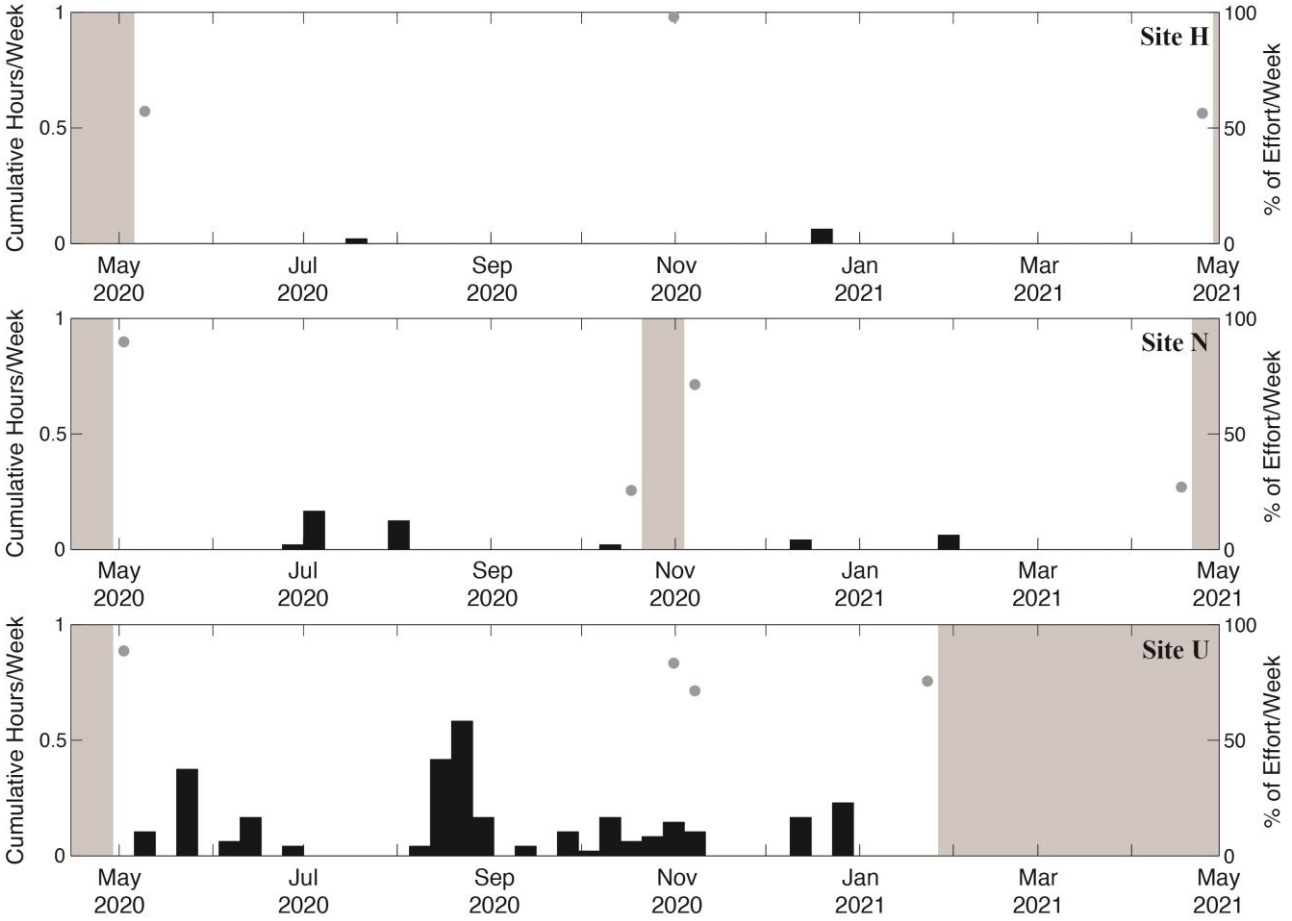

Figure 14. Weekly presence of BW43 FM pulses between April 2020 and 2021 at sites H, N, and U. Gray dots represent percent of effort per week in weeks with less than 100% recording effort, and gray shading represents periods with no recording effort. Where gray dots or shading are absent, full recording effort occurred for the entire week.

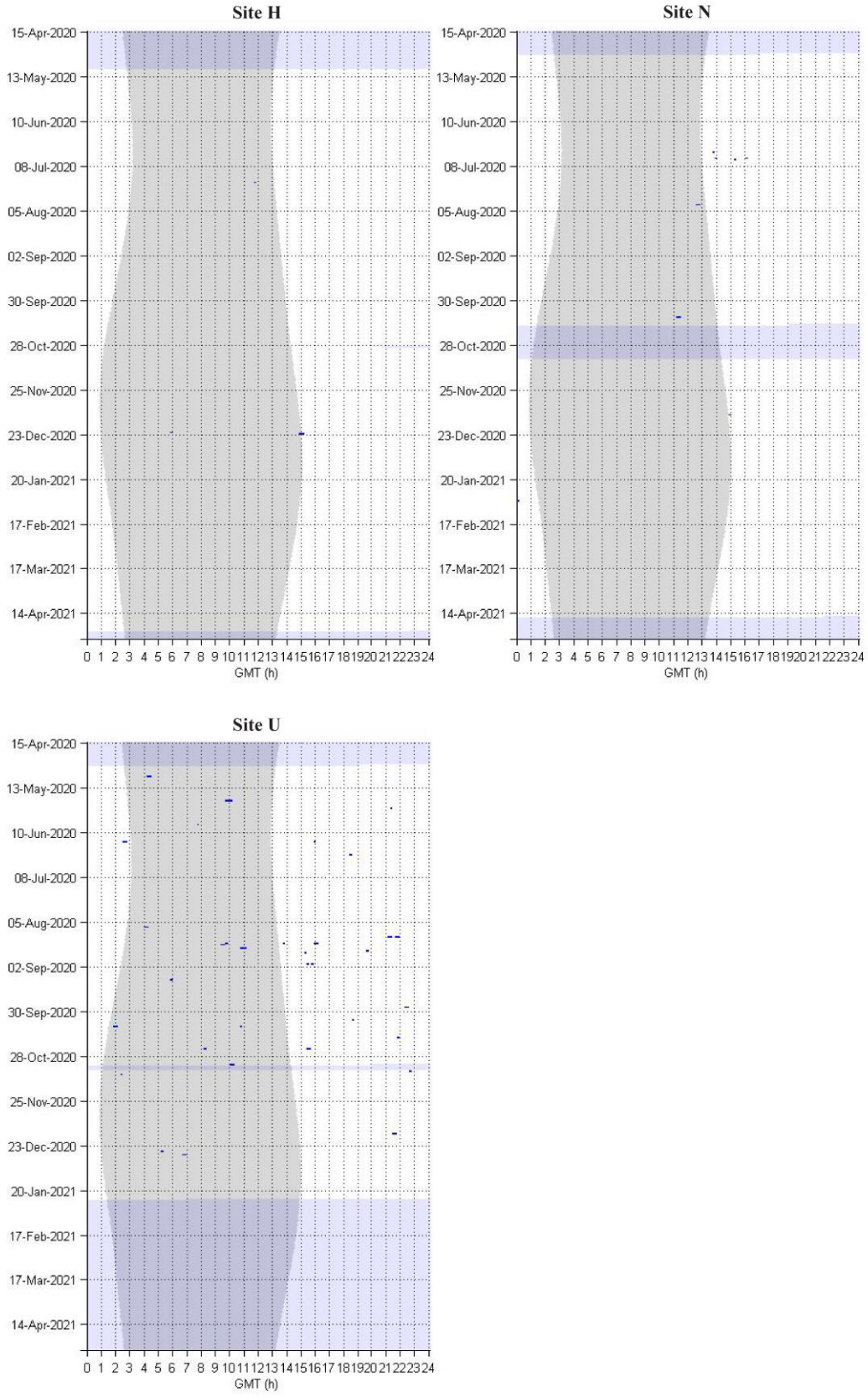

Figure 15. BW43 FM pulses, indicated by blue dots, in ten-minute bins at sites H, N, and U. Gray vertical shading denotes nighttime and light purple horizontal shading denotes absence of acoustic data.

Anthropogenic Sounds

Anthropogenic sounds from MFA sonar (2.4–4.5 kHz) and explosions, between April 2020 and 2021, were analyzed for this report.

Mid-Frequency Active Sonar

MFA sonar was a commonly detected anthropogenic sound. The dates of major naval training exercises that were conducted in the SOCAL region between April 2020 and 2021 are listed in Table 5 (C. Johnson, personal communication). Sonar usage outside of designated major exercises is likely attributable to unit-level training. The automatically detected packets and wave trains show the highest level of MFA sonar activity (> 130 dB_{pp} re 1 µPa) when normalized per year at site H, while site E showed the lowest levels (Table 6).

- MFA sonar was detected throughout the recording period at all four sites. In general, the highest number of detections occurred in May and November 2020 and in February and April 2021 (Figure 16).
- Although MFA sonar was detected during both night and day, there was a general decrease in detections in the hours before sunrise at all sites. (Figure 17).
- At site E, a total of 283 packets were detected, with a maximum received level of 164 dB_{pp} re 1 µPa (Figure 18). Total wave train duration was 6.4 h (Figure 21), but the total packet duration was only about 0.3 h (947.8 s; Table 6; Figure 22).
- At site H, a total of 13,290 packets were detected, with a maximum received level of 170 dB_{pp} re 1 µPa (Figure 18). Total wave train duration was 226.4 h (Figure 21), but the total packet duration was only about 8 h (29,491.1 s; Table 6; Figure 22).
- At site N, a total of 4,345 packets were detected, with a maximum received level of 166 dB_{pp} re 1 µPa (Figure 18). Total wave train duration was 89.8 h (Figure 21), but the total packet duration was only 3 h (11,305.7 s; Table 6; Figure 22).
- At site U, a total of 1,681 packets were detected, with a maximum received level of 166 dB_{pp} re 1 µPa (Figure 18). Total wave train duration was 33.8 h (Figure 21), but the total packet duration was only about 1.5 h (5,209 s; Table 6; Figure 22).
- Maximum cumulative sound exposure levels of wave trains occurred during October 2020 and January 2021 at sites U and N, respectively, and were greater than 175 dB re 1 μPa^2-s. At sites H and E, maximum levels occurred in February and March 2021, respectively, and were greater than 170 dB re 1 μPa^2-s (Figure 19).
- The peak in MFA sonar that occurred in May 2020 overlapped with a major training exercise (Table 5), but most MFA detections occurred when there was no training exercise taking place (Figure 20).

Table 5. Major naval training exercises in the SOCAL region between April 2020 and 2021.

Exercise Dates
May 6 to June 2, 2020
December 7 to 22, 2020

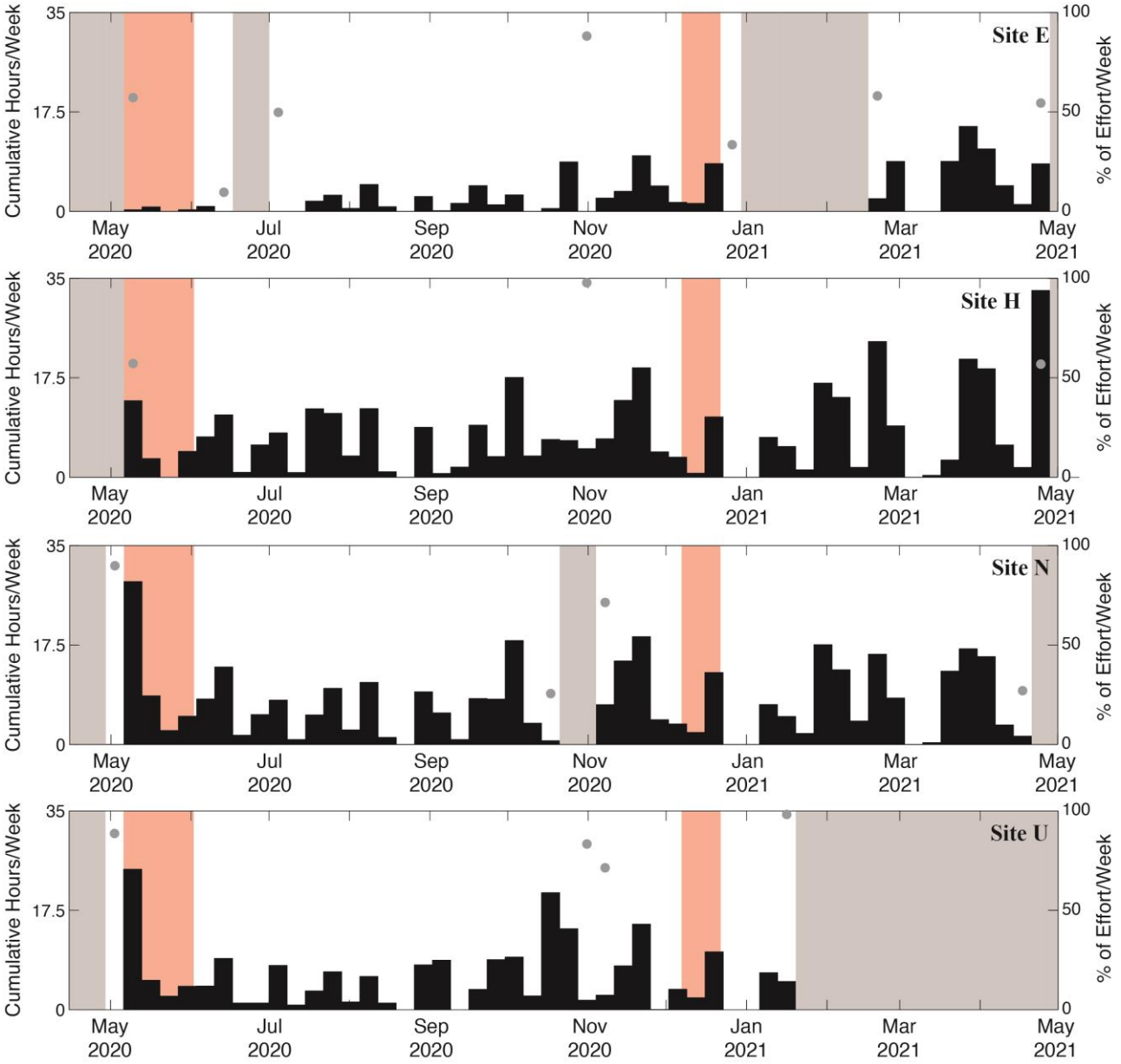

Figure 16. Major naval training events (shaded light red, from Table 5) overlaid on weekly presence of MFA sonar < 5kHz from the *Silbido* detector between April 2020 and 2021 at sites E, H, N, and U. Gray dots represent percent of effort per week in weeks with less than 100% recording effort, and gray shading represents periods with no recording effort. Where gray dots or shading are absent, full recording effort occurred for the entire week.

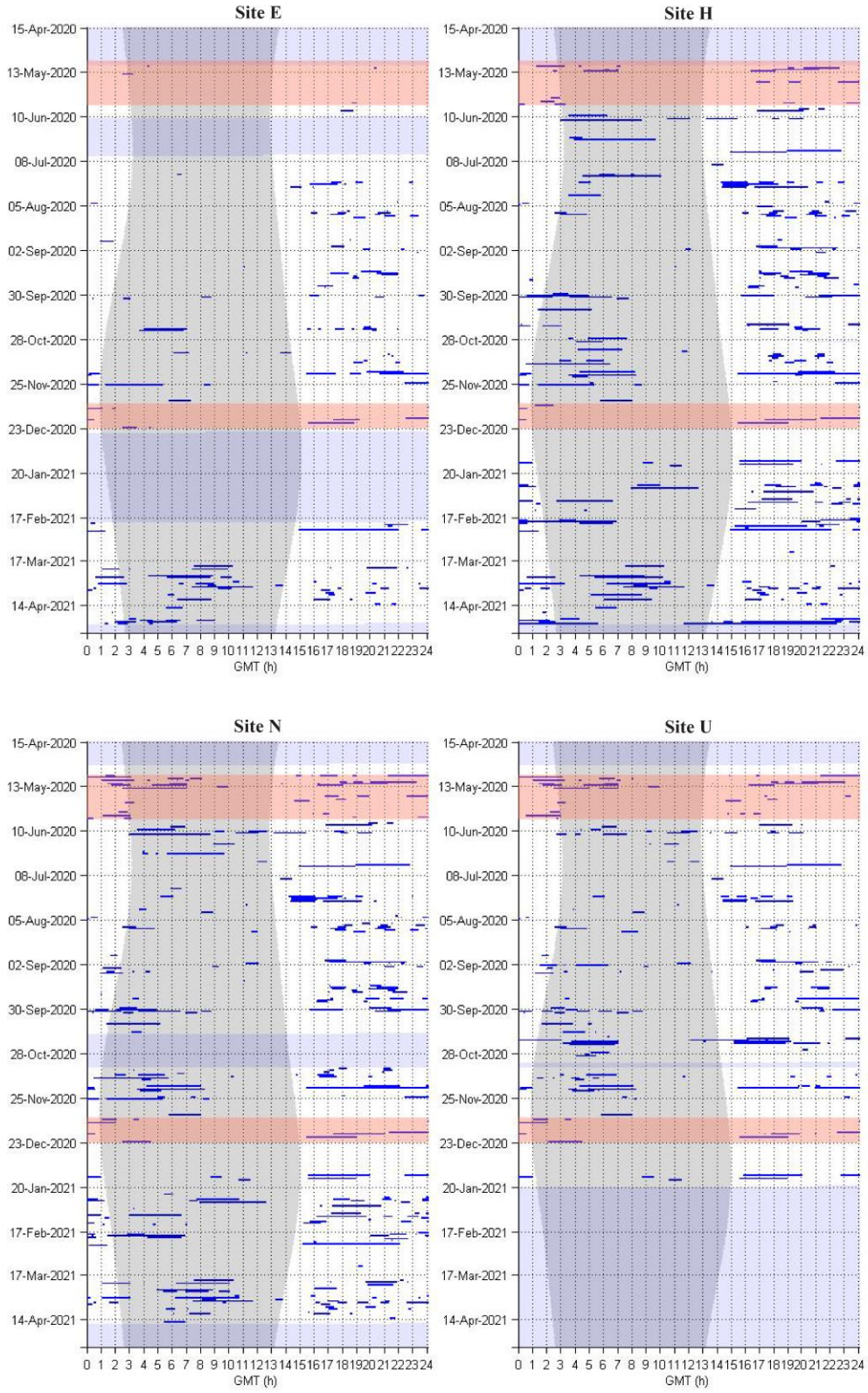

Figure 17. Major naval training events (shaded light red, from Table 5) overlaid on MFA sonar < 5 kHz signals from the *Silbido* detector, indicated by blue dots, in one-minute bins at sites E, H, N, and U.
Gray vertical shading denotes nighttime and light purple horizontal shading denotes absence of acoustic data.

Table 6. MFA sonar automated detector results for sites E, H, N, and U.
Total effort at each site in days (years), number of and extrapolated yearly estimates of wave trains and packets at each site (> 130 dB_{pp} re 1 µPa), total wave train duration, and total packet duration.

Site	Period Analyzed Days (Years)	Number of Wave Trains	Wave Trains per year	Number of Packets	Packets per year	Total Wave Train Duration (h)	Total Packet Duration (s)
E	351 (0.96)	5	5	283	295	6.4	947.8
H	351 (0.96)	128	133	13,290	13,844	226.4	29,491.1
N	330 (0.90)	60	67	4,345	4,828	89.8	11,305.7
U	262 (0.72)	25	35	1,681	2,335	33.8	5,209

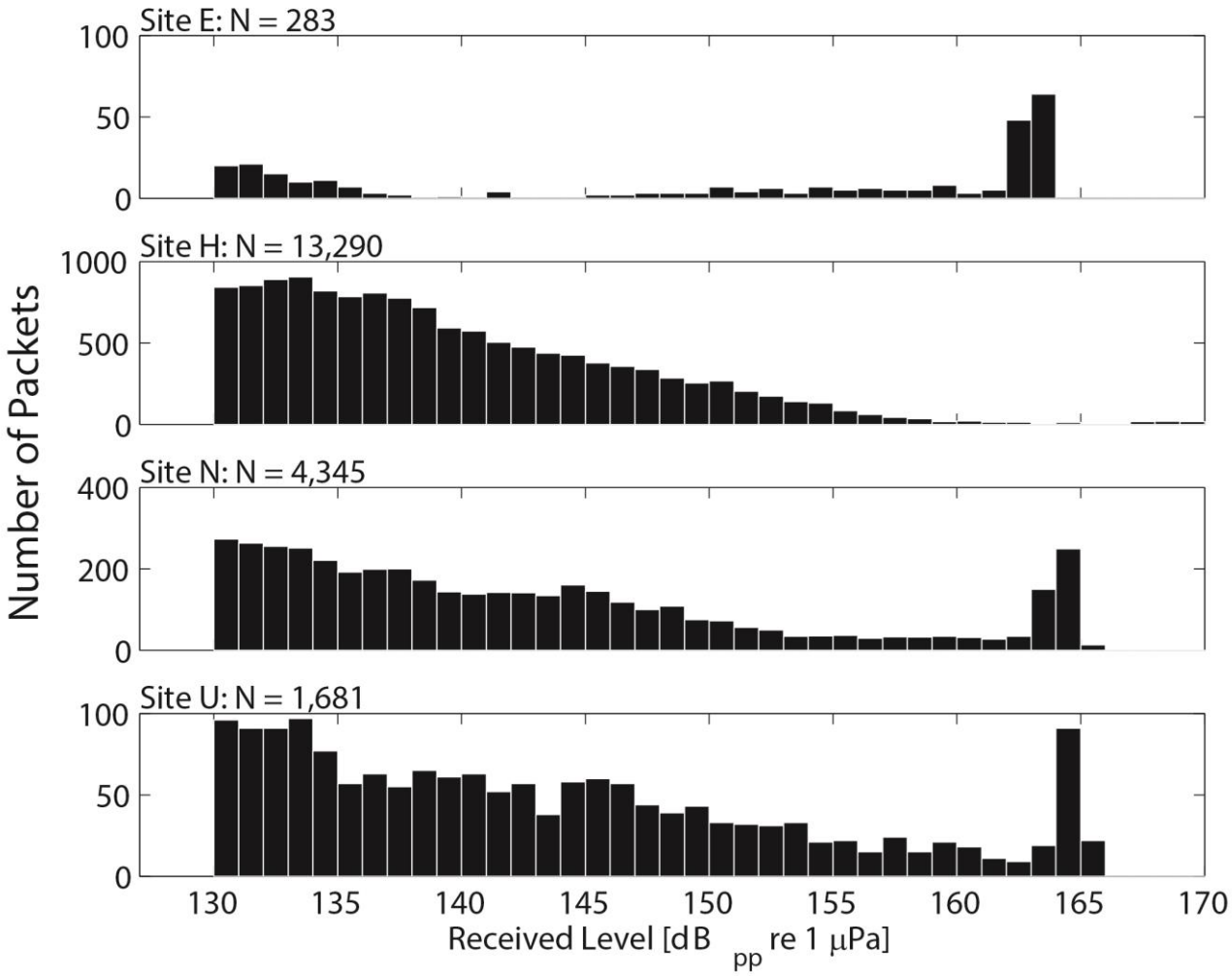

Figure 18. MFA sonar packet peak-to-peak received level distributions for sites E, H, N, and U. The total number of packets detected at each site is given in the upper left corner of each panel. Instrument clipping levels typically occur around 165 dB_{pp} re 1 µPa, but were higher at site H. Note the vetical axes are at different scales.

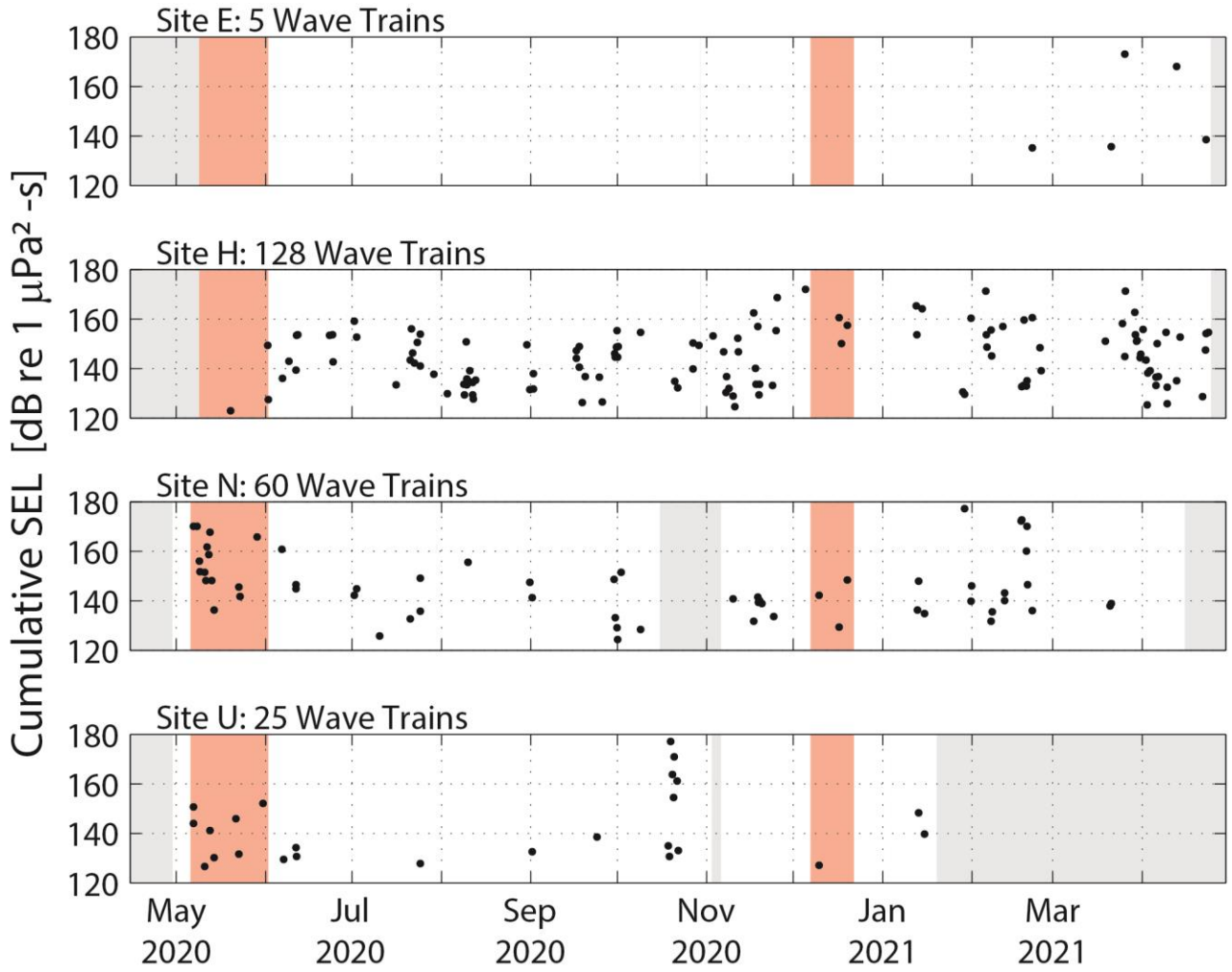

Figure 19. Cumulative sound exposure level for each wave train at sites E, H, N, and U. Light red shading indicates major naval training events (Table 5).

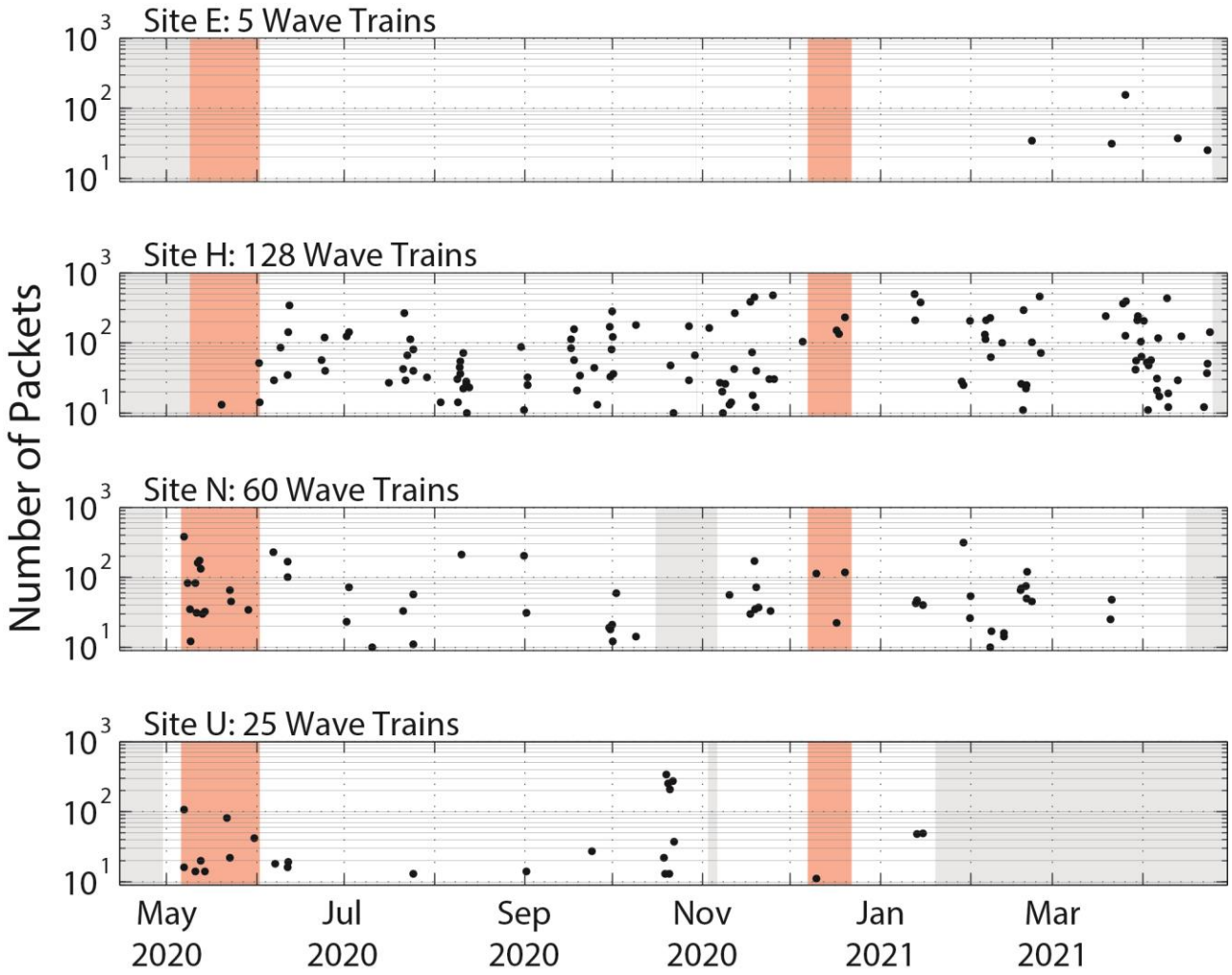

Figure 20. Number of MFA sonar packets for each wave train at sites E, H, N, and U. Light red shading indicates major naval training events (Table 5). Note the vertical axes are logarithmic base-10.

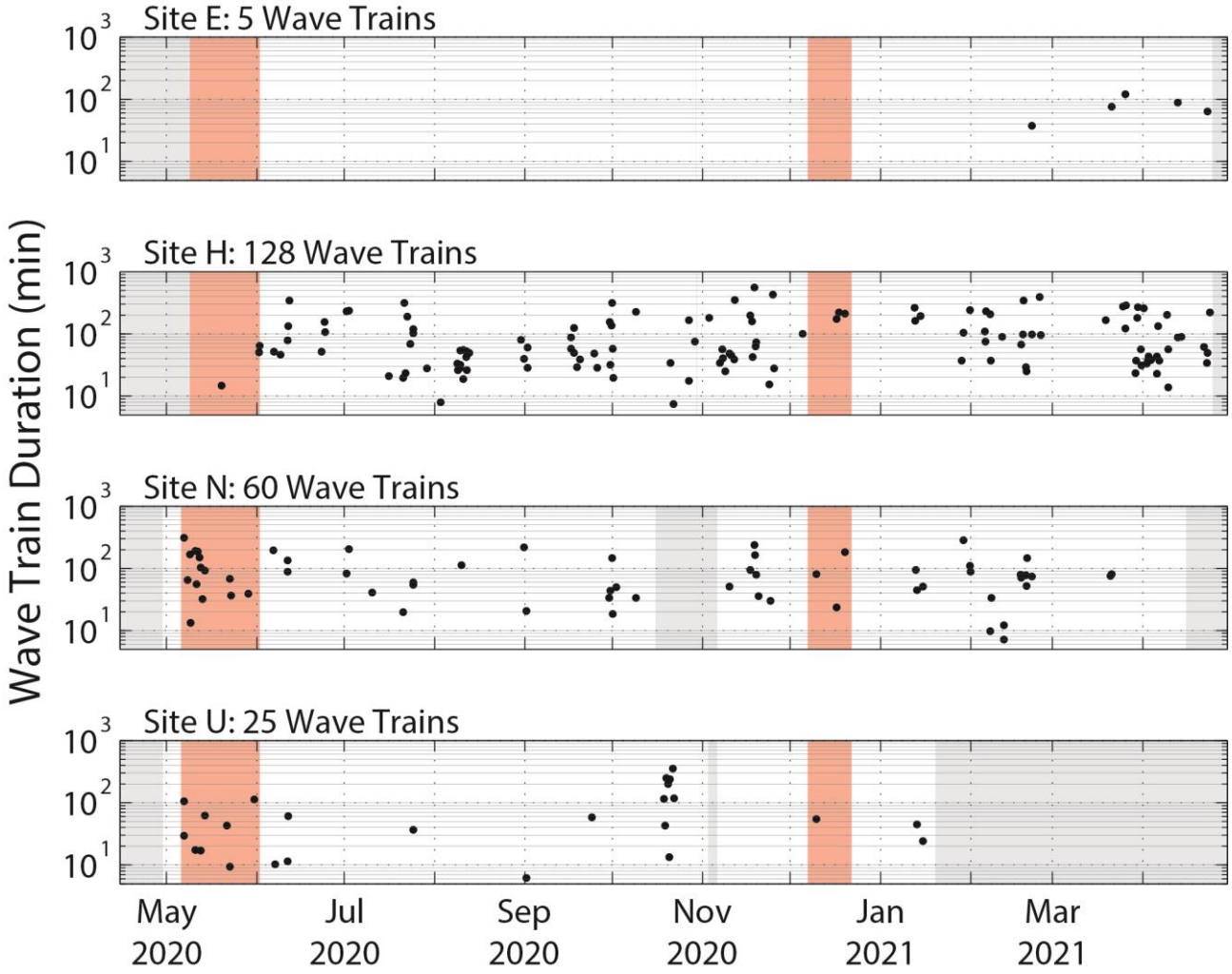

Figure 21. Wave train duration at sites E, H, N, and U.
Light red shading indicates major naval training events (Table 5). Note the vertical axes are logarithmic base-10.

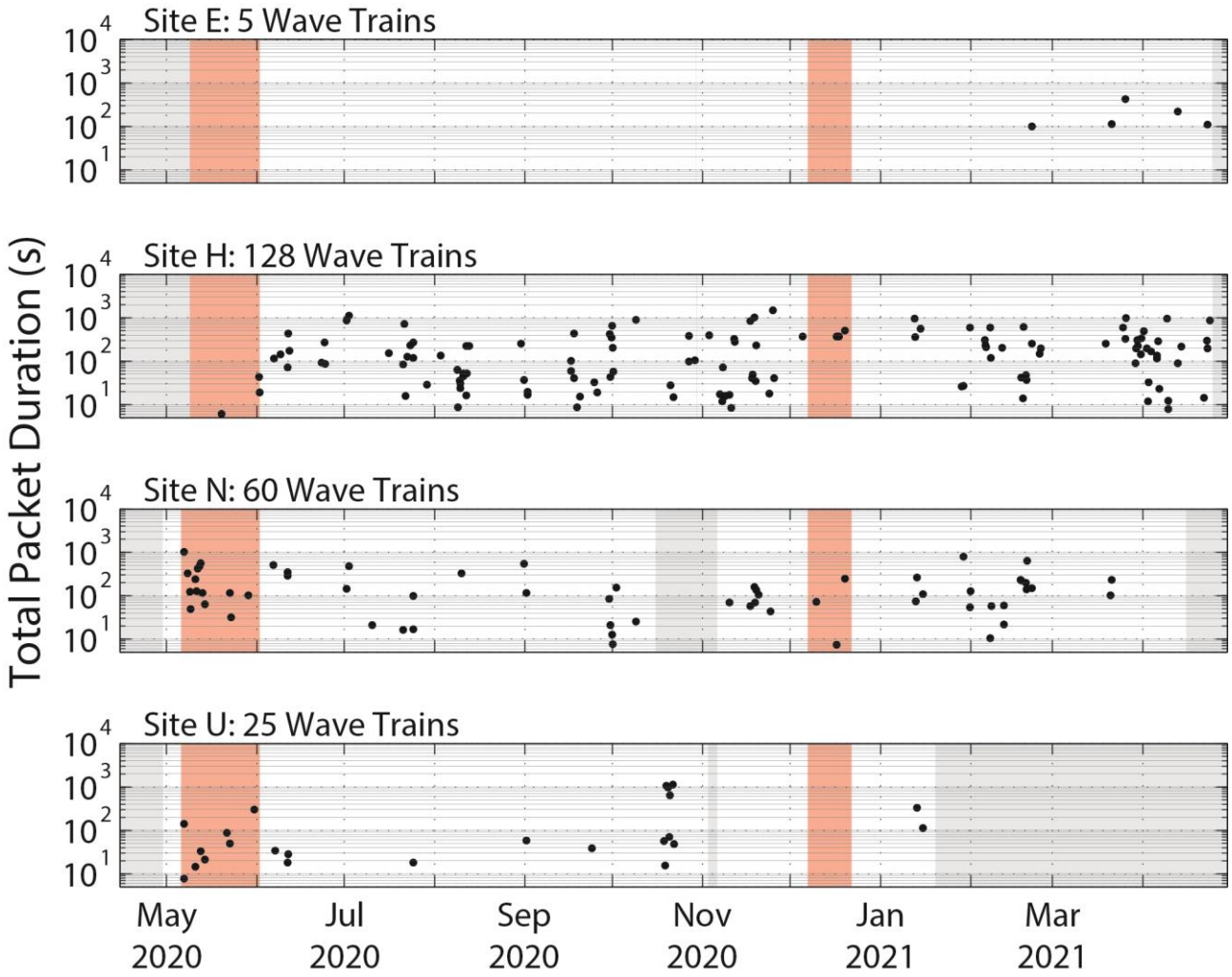

Figure 22. Total packet duration for each wave train at sites E, H, N, and U. Light red shading indicates major naval training events (Table 5). Note the vertical axes are logarithmic base-10.

Explosions

Explosions were detected at all four sites.

- Explosions occurred throughout the monitoring periods at all sites. The highest number of explosions occurred at site H, with a peak in December 2020 and again in February 2021. The lowest number of detections occurred at site E (Figure 23).
- Total explosion counts at each site were as follows:
    - 232 at site E
    - 2,219 at site H
    - 1,526 at site N
    - 1,865 at site U
- There was no clear diel pattern at sites E, N, or U. At site H, there were more explosions at night, particularly for about the first six hours after sunset (Figure 24).
- The predominant nighttime pattern at site H suggests potential use of seal bombs by the squid fishery. However, daytime use at all sites may indicate another fishery using seal bombs.
- The overall number of detections at site H was lower than during the last reporting period (Rice *et al.*, 2021), but was generally comparable with previous reports (Debich *et al.*, 2015a; Debich *et al.*, 2015b; Širović *et al.*, 2016; Rice *et al.*, 2017; Rice *et al.*, 2018; Rice *et al.*, 2019; Rice *et al.*, 2020).

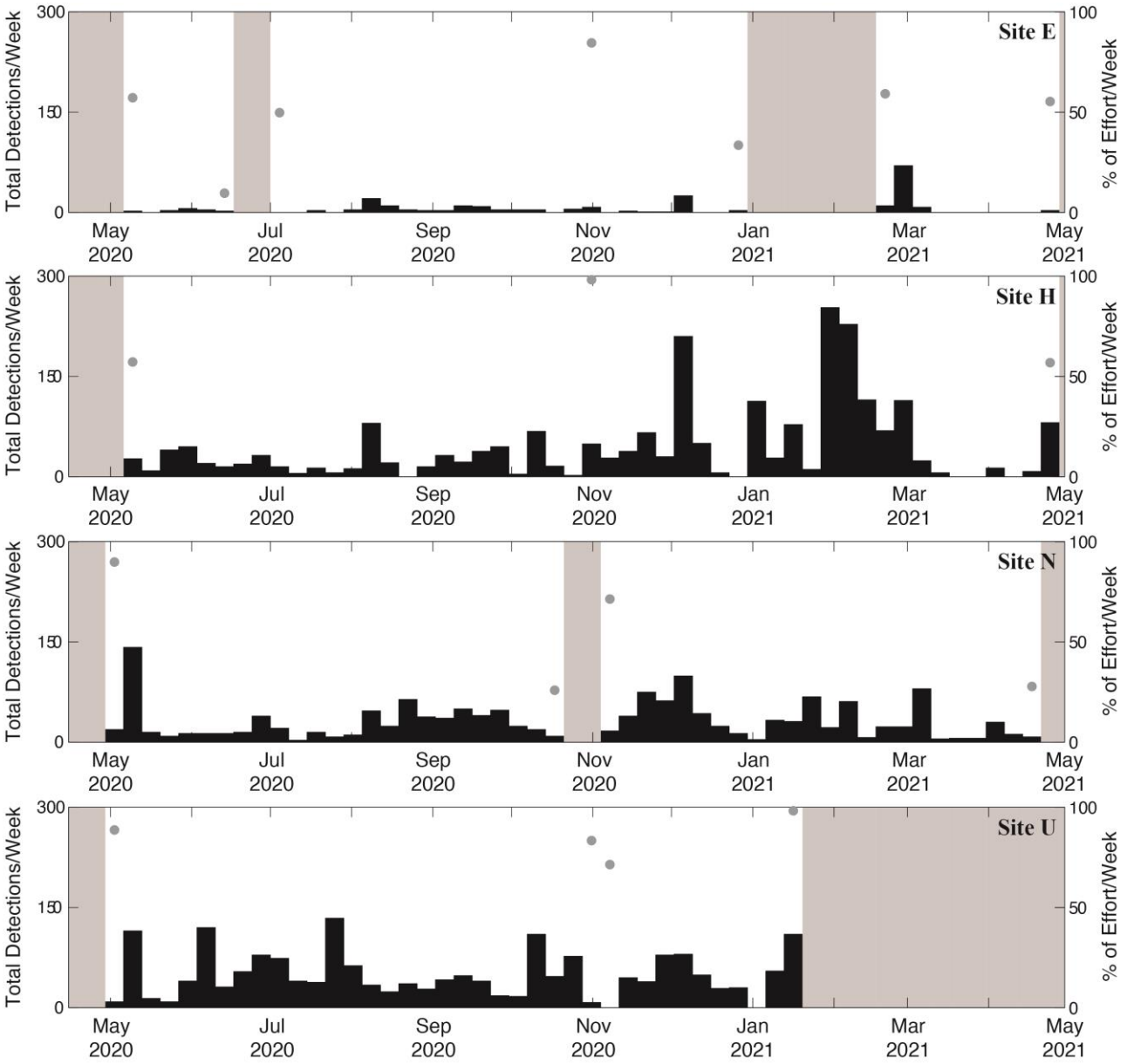

Figure 23. Weekly presence of explosions between April 2020 and 2021 at sites E, H, N, and U. Gray dots represent percent of effort per week in weeks with less than 100% recording effort, and gray shading represents periods with no recording effort. Where gray dots or shading are absent, full recording effort occurred for the entire week.

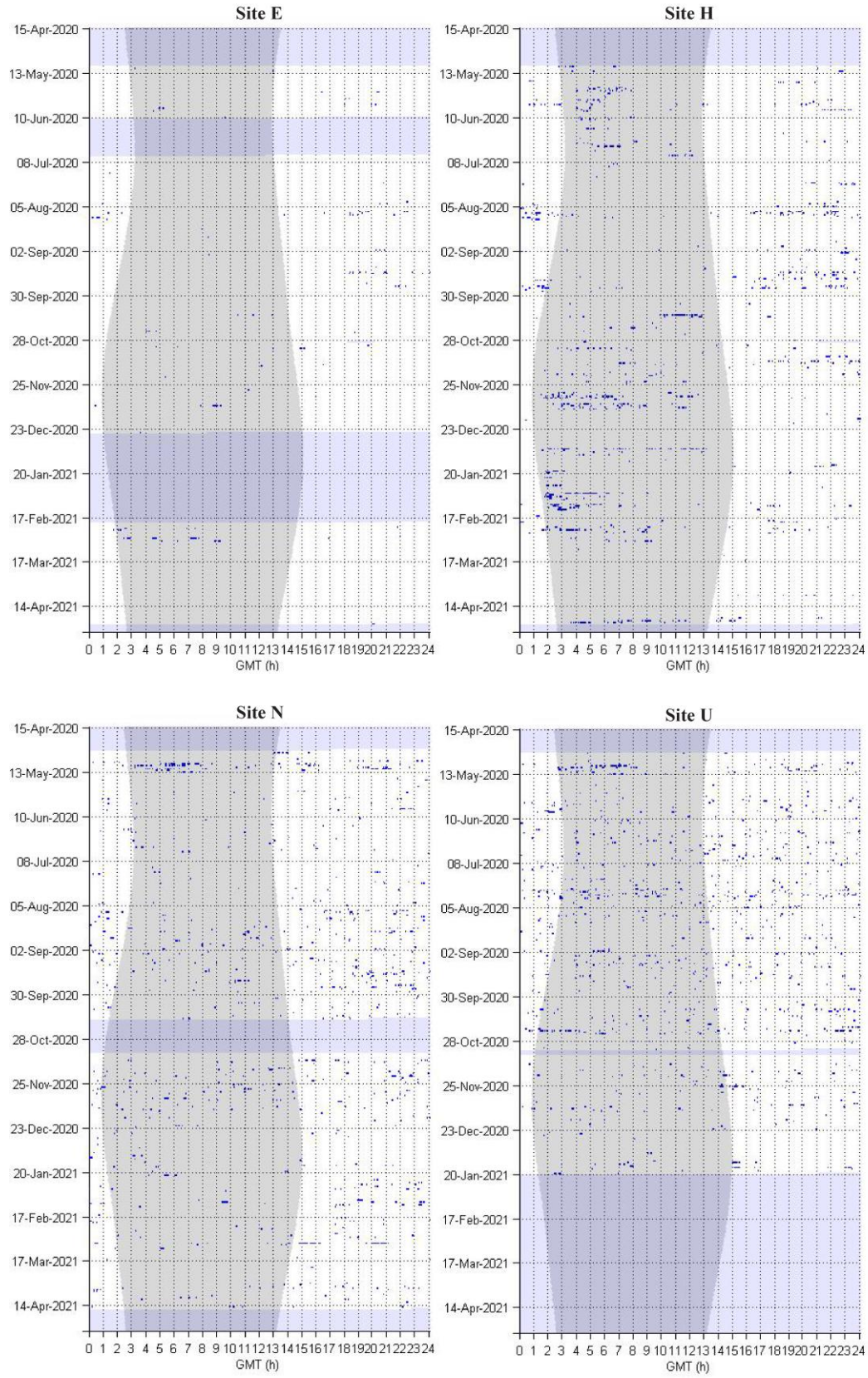

Figure 24. Explosion detections, indicated by blue dots, in five-minute bins at sites E, H, N, and U. Gray vertical shading denotes nighttime and light purple horizontal shading denotes absence of acoustic data.

Abundance and Density Estimates from Visual Surveys

The results of abundance and density estimation based on CalCOFI visual surveys from 2004 to 2021 are summarized below.

We describe the seasonal visual sightings, modeled detection probabilities, and seasonal and yearly abundance for nine marine mammal species. Values for detection function models (Table 7), seasonal abundance (Table 8), and yearly abundance (Table 9) are also provided.

Table 7. Detection function model summary from CalCOFI visual surveys from 2004 to 2021. For each species, the truncation (based on either distance or data percentage), model (adjusted to account for responsive movement of some species), and covariates (sea state, season, and group size) used are provided along with resulting trackline detection probabilities and Cramer-von Mises p-values. Short-beaked common dolphins are divided by group size (≤ 20 or > 20 individuals). Abbreviations: PWS = Pacific white-sided, LBC = long-beaked common, and SBC = short-beaked common.

	Truncation	Model	Covariates	Trackline detection probability	Cramer-von Mises p-value
Blue whale	2400 m	Half-normal	-	0.921	0.9552
Fin whale	10%	Hazard-rate	Sea state	0.921	0.9046
Humpback whale	2700 m	Half-normal with cosine adjustment term of order 2	-	0.921	0.7239
Gray whale	2400 m	Half-normal with cosine adjustment term of order 2	-	0.921	0.9970
Bottlenose dolphin	10%	Half-normal with cosine adjustment terms of order 2,3	-	0.856	0.8790
Risso's dolphin	-	Hazard-rate	Sea state	0.856	0.9844
PWS dolphin	400 m	Half-normal	Sea state	0.856	0.1808
LBC dolphin	700 m	Half-normal	-	0.97	0.9003
SBC dolphin, ≤ 20	400 m	Half-normal with cosine adjustment term of order 2	-	0.856	0.1162
SBC dolphin, > 20	700 m	Half-normal with cosine adjustment terms of order 2,3	-	0.97	0.5714
Dall's porpoise	700 m	Half-normal with cosine adjustment term of order 2	-	0.822	0.2224

Table 8. Seasonal abundance estimates from CalCOFI visual surveys from 2004 to 2021. The abundance, lower (L) and upper (U) 95% confidence intervals (CI), density (animals/1000 km^2), coefficient of variation (cv) and unidentified individual correction factor (c) for each species 2004–2021. There were no cruises for winter or spring in 2004, for spring in 2010, for spring, summer, or fall in 2020, or for winter or spring in 2021. Short-beaked common dolphins are divided by group size (≤ 20 or > 20 individuals). Abbreviations: PWS = Pacific white-sided, LBC = long-beaked common, and SBC = short-beaked common.

	Season			
	Winter	**Spring**	**Summer**	**Fall**
Blue whale				
Abundance	39	64	1524	201
95% CI (L)	9	25	1070	111
95% CI (U)	166	165	2170	362
Density	0.16	0.27	6.39	0.84
cv	0.863	0.514	0.182	0.308
c	2.582	1.750	1.542	1.812
Fin whale				
Abundance	542	677	2610	1241
95% CI (L)	283	415	1705	842
95% CI (U)	1040	1104	3996	1831
Density	2.27	2.84	10.94	5.21
cv	0.342	0.254	0.220	0.200
c	2.582	1.750	1.542	1.812
Humpback whale				
Abundance	885	1333	461	490
95% CI (L)	571	830	200	302
95% CI (U)	1373	2140	1064	793
Density	3.71	5.59	1.93	2.05
cv	0.227	0.245	0.446	0.250
c	2.582	1.750	1.542	1.812
Gray whale				
Abundance	1302	105	-	-
95% CI (L)	858	46	-	-
95% CI (U)	1976	239	-	-
Density	5.46	0.44	-	-
cv	0.214	0.436	-	-
c	-	-	-	-

	Season			
	Winter	**Spring**	**Summer**	**Fall**
Bottlenose dolphin				
Abundance	11694	2113	5174	9916
95% CI (L)	5222	619	2516	3543
95% CI (U)	26186	7221	10642	27748
Density	49.03	8.86	21.70	41.58
cv	0.421	0.670	0.373	0.553
c	-	-	-	-
Risso's dolphin				
Abundance	2,261	6,481	2,323	3,401
95% CI (L)	1,250	1,764	1,087	1,610
95% CI (U)	4,090	23,814	4,963	7,186
Density	9.48	27.17	9.74	14.26
cv	0.306	0.700	0.392	0.385
c	-	-	-	-
PWS dolphin				
Abundance	7,145	14,157	7,112	2,353
95% CI (L)	2,847	7,750	2,700	579
95% CI (U)	17,932	25,863	18,738	9,552
Density	29.96	59.36	29.82	9.86
cv	0.469	0.312	0.512	0.792
c	-	-	-	-
LBC dolphin				
Abundance	193,849	16,996	50,828	107,663
95% CI (L)	60,808	7,030	24,962	25,299
95% CI (U)	617,973	41,087	103,497	458,173
Density	812.81	71.26	213.12	451.43
cv	0.647	0.474	0.375	0.852
c	1.083	1.342	1.525	1.406
SBC dolphin, ≤ 20				
Abundance	41,406	30,214	40,069	25,259
95% CI (L)	29,399	21,061	29,570	16,367
95% CI (U)	58,318	43,345	54,295	38,982
Density	173.62	126.69	168.01	105.91
cv	0.176	0.186	0.156	0.224
c	1.083	1.342	1.525	1.406

	Season			
	Winter	**Spring**	**Summer**	**Fall**
SBC dolphin, >20				
Abundance	675,464	327,635	253,631	322,887
95% CI (L)	366,039	196,793	156,118	215,693
95% CI (U)	1,246,457	545,469	412,050	483,355
Density	2,832.21	1,373.77	1,063.47	1,353.86
cv	0.320	0.265	0.251	0.208
c	1.083	1.342	1.525	1.406
Dall's porpoise				
Abundance	4,924	9,389	151	785
95% CI (L)	2,887	5,745	48	210
95% CI (U)	8,398	15,344	473	2,933
Density	20.65	39.37	0.63	3.29
cv	0.275	0.253	0.633	0.668
c	-	-	-	-

Table 9. Yearly abundance estimates from CalCOFI visual surveys from 2004 to 2021.
The abundance, lower (L) and upper (U) 95% confidence intervals (CI), density (animals/1000 km^2), coefficient of variation (cv) and unidentified individual correction factor (c) for each species 2004–2021. There were no cruises for winter or spring in 2004, for spring in 2010, for spring, summer, or fall in 2020, or for winter or spring in 2021. Short-beaked common dolphins are divided by group size (≤ 20 or > 20 individuals). Abbreviations: PWS = Pacific white-sided, LBC = long-beaked common, and SBC = short-beaked common.

	Year																	
	2004	**2005**	**2006**	**2007**	**2008**	**2009**	**2010**	**2011**	**2012**	**2013**	**2014**	**2015**	**2016**	**2017**	**2018**	**2019**	**2020**	**2021**
Blue whale																		
Abundance	495	335	340	45	78	641	551	1,303	802	389	517	431	851	1,017	82	450	-	3,807
95% CI (L)	248	220	135	5	24	377	356	370	443	99	167	193	480	406	54	169	-	1,519
95% CI (U)	990	508	855	389	253	1,090	854	4,589	1,452	1,533	1,603	963	1,509	2,547	122	1,199	-	9,540
Density	2.08	1.40	1.43	0.19	0.33	2.69	2.31	5.46	3.36	1.63	2.17	1.81	3.57	4.26	0.34	1.89	-	15.96
cv	0.364	0.215	0.497	1.523	0.660	0.276	0.226	0.715	0.310	0.795	0.629	0.428	0.299	0.496	0.209	0.532	-	0.496
c	2.000	1.141	1.526	1.536	1.273	1.756	1.683	1.607	2.271	2.061	1.600	2.000	1.757	2.200	1.649	1.636	2.250	1.504
Fin whale																		
Abundance	1,025	745	538	550	676	735	3,789	2,850	2,661	1,851	2,184	650	2,351	792	2,779	347	1,331	1,759
95% CI (L)	585	325	240	409	371	415	1,010	1,605	1,445	1,111	971	349	716	355	836	150	372	1,153
95% CI (U)	1,794	1,706	1,204	741	1,233	1,302	14,215	5,061	4,900	3,085	4,912	1,210	7,723	1,769	9,234	803	4,770	2,684
Density	4.30	3.12	2.25	2.31	2.84	3.08	15.89	11.95	11.16	7.76	9.16	2.73	9.86	3.32	11.65	1.45	5.58	7.38
cv	0.292	0.442	0.430	0.152	0.313	0.298	0.759	0.299	0.319	0.265	0.432	0.325	0.667	0.428	0.675	0.449	0.727	0.218
c	2.000	1.141	1.526	1.536	1.273	1.756	1.683	1.607	2.271	2.061	1.600	2.000	1.757	2.200	1.649	1.636	2.250	1.504
Humpback whale																		
Abundance	393	499	347	510	834	349	63	190	189	1,645	1,187	748	320	1,137	1,166	736	1,667	1,026
95% CI (L)	185	214	218	99	222	136	28	53	73	798	625	458	186	728	681	166	725	590
95% CI (U)	836	1,163	554	2,622	3,136	896	139	677	489	3,391	2,257	1,220	552	1,775	1,997	3,259	3,833	1,786
Density	1.65	2.09	1.46	2.14	3.50	1.46	0.26	0.80	0.79	6.90	4.98	3.14	1.34	4.77	4.89	3.08	6.99	4.30
cv	0.399	0.453	0.242	1.004	0.761	0.510	0.424	0.722	0.515	0.382	0.337	0.254	0.283	0.230	0.280	0.883	0.445	0.289
c	2.000	1.141	1.526	1.536	1.273	1.756	1.683	1.607	2.271	2.061	1.600	2.000	1.757	2.200	1.649	1.636	2.250	1.504

	Year																	
	2004	**2005**	**2006**	**2007**	**2008**	**2009**	**2010**	**2011**	**2012**	**2013**	**2014**	**2015**	**2016**	**2017**	**2018**	**2019**	**2020**	**2021**
Gray whale																		
Abundance	-	-	160	425	-	233	87	1,419	130	226	97	902	91	289	118	197	1,983	0
95% CI (L)	-	-	92	114	-	125	12	548	41	37	37	420	12	41	13	81	697	-
95% CI (U)	-	-	279	1,586	-	434	611	3,676	411	1,389	252	1,937	672	2,054	1,051	484	5,642	-
Density	-	-	0.67	1.78	-	0.98	0.36	5.95	0.54	0.95	0.40	3.78	0.38	1.21	0.50	0.83	8.32	0.00
cv	-	-	0.286	0.738	-	0.318	1.240	0.504	0.617	1.090	0.508	0.377	0.375	1.268	1.477	0.470	0.528	-
c	-	-	-	-	-	-	-	-	-	-	-	-	-	-	-	-	-	-
Bottlenose dolphin																		
Abundance	3,280	4,724	1,046	1,390	6,841	10,808	19,449	3,137	3,529	-	8,168	3,190	25,494	-	3,843	18,490	43,436	-
95% CI (L)	537	555	211	1,028	1,179	2,074	3,533	1,381	1,608	-	1,674	910	7,568	-	506	7,348	2,975	-
95% CI (U)	20,026	40,189	5,193	1,879	39,701	56,327	107,076	7,124	7,747	-	39,851	11,188	85,887	-	29,183	46,528	634,155	-
Density	13.75	19.81	4.39	5.83	28.68	45.32	81.55	13.15	14.80	-	34.25	13.38	106.90	-	16.11	77.53	182.13	-
cv	0.953	1.006	0.949	0.152	1.060	0.643	0.982	0.418	0.404	-	0.930	0.641	0.591	-	1.222	0.466	0.740	-
c	-	-	-	-	-	-	-	-	-	-	-	-	-	-	-	-	-	-
Risso's dolphin																		
Abundance	1,444	309	799	3,014	1,563	1,881	-	3,345	2,442	1,528	3,095	13,677	10,597	-	2,747	780	10,371	11,147
95% CI (L)	253	81	273	1,052	154	784	-	565	428	526	934	1	4,436	-	1,457	461	4,713	2,317
95% CI (U)	8,243	1,172	2,335	8,631	15,892	4,511	-	19,797	13,940	4,436	10,258	177,233, 612	25,313	-	5,180	1,319	22,817	53,622
Density	6.05	1.30	3.35	12.64	6.55	7.89	-	14.03	10.24	6.41	12.98	57.35	44.43	-	11.52	3.27	43.48	46.74
cv	0.680	0.700	0.559	0.539	1.534	0.444	-	0.776	1.045	0.365	0.580	0.972	0.451	-	0.315	0.268	0.391	0.813
c	-	-	-	-	-	-	-	-	-	-	-	-	-	-	-	-	-	-

	Year																	
	2004	**2005**	**2006**	**2007**	**2008**	**2009**	**2010**	**2011**	**2012**	**2013**	**2014**	**2015**	**2016**	**2017**	**2018**	**2019**	**2020**	**2021**
PWS dolphin																		
Abundance	12,894	9,467	15,040	7,112	15,651	865	-	1,160	16,350	13,360	4,437	937	9,551	3,602	-	14,963	-	-
95% CI (L)	3,791	3,585	5,104	1,289	5,877	578	-	499	3,862	666	609	140	1,086	2,339	-	5,267	-	-
95% CI (U)	4,3857	24,999	44,317	39,225	41,681	1,296	-	2,700	69,218	268,175	32,329	6,258	83,964	5,547	-	42,512	-	-
Density	54.06	39.69	63.06	29.82	65.62	3.63	-	4.87	68.56	56.02	18.61	3.93	40.05	15.10	-	62.74	-	-
cv	0.658	0.504	0.565	0.785	0.502	0.206	-	0.440	0.793	1.169	0.498	1.208	0.701	0.219	-	0.556	-	-
c	-	-	-	-	-	-	-	-	-	-	-	-	-	-	-	-	-	-
LBC dolphin																		
Abundance	11,627	83,229	1,715	2,197	-	6,357	15,424	18,077	50,364	5,342	5,322	536,655	305,163	31,248	33,408	102,410	35,295	92,422
95% CI (L)	4,711	32,634	742	301	-	896	2,735	1,764	12,889	723	1,103	119,043	61,861	11,100	8,486	25,572	5,314	12,811
95% CI (U)	28,691	212,267	3,964	16,039	-	45,092	86,973	185,198	196,799	39,494	25,682	2,419,278	1,505,383	87,965	131,521	410,118	234,415	666,747
Density	48.75	348.98	7.19	9.21	-	26.66	64.67	75.80	211.18	22.40	22.31	2,250.18	1,279.54	131.02	140.08	429.40	147.99	387.52
cv	0.486	0.506	0.448	1.340	-	1.310	1.086	1.759	0.789	1.354	0.952	0.897	0.970	0.567	0.794	0.807	1.242	1.328
c	1.108	1.239	1.493	1.441	1.185	1.152	1.299	2.839	1.677	1.254	1.475	1.110	1.166	1.264	1.139	1.267	1.139	1.483
SBC dolphin, ≤ 20																		
Abundance	40,046	35,862	50,389	29,073	51,192	27,832	4,739	23,906	22,824	31,521	21,506	27,570	32,468	43,507	27,131	46,143	87,618	19,165
95% CI (L)	26,924	20,273	24,990	15,702	35,171	17,390	538	9,535	13,009	14,731	10,205	16,888	18,182	24,693	16,703	27,217	41,633	10,025
95% CI (U)	59,564	63,437	101,603	53,832	74,511	44,543	41,736	59,937	40,046	67,446	45,321	45,011	57,978	76,656	44,071	78,231	184,394	36,640
Density	167.91	150.37	211.28	121.90	214.65	116.70	19.87	100.24	95.70	132.17	90.17	115.60	136.14	182.42	113.76	193.48	367.38	80.36
cv	0.205	0.297	0.370	0.322	0.193	0.243	1.558	0.496	0.293	0.403	0.394	0.254	0.302	0.295	0.251	0.274	0.394	0.340
c	1.108	1.239	1.493	1.441	1.185	1.152	1.299	2.839	1.677	1.254	1.475	1.110	1.166	1.264	1.139	1.267	1.139	1.483

	Year																	
	2004	**2005**	**2006**	**2007**	**2008**	**2009**	**2010**	**2011**	**2012**	**2013**	**2014**	**2015**	**2016**	**2017**	**2018**	**2019**	**2020**	**2021**
SBC dolphin, >20																		
Abundance	337,417	405,275	273,545	543,135	278,495	138,781	343,565	438,663	283,823	363,291	536,373	645,772	208,125	540,676	253,418	525,670	1,035,914	61,457
95% CI (L)	182,925	175,232	153,632	208,781	78,760	68,858	82,443	212,551	131,650	141,140	295,670	148,271	104,142	335,780	145,755	302,766	644,810	23,026
95% CI (U)	622,386	937,313	487,055	1,412,945	984,754	279,707	1,431,733	905,313	611,888	935,106	973,029	2,812,562	415,931	870,600	440,608	912,684	1,664,239	164,029
Density	1,414.78	1,699.31	1,146.97	2,277.35	1,167.72	581.91	1,440.56	1,839.30	1,190.06	1,523.27	2,249.00	2,707.71	872.66	2,267.04	1,062.58	2,204.12	4,343.57	257.69
cv	0.320	0.448	0.301	0.518	0.717	0.369	0.836	0.383	0.407	0.512	0.311	0.870	0.365	0.247	0.288	0.287	0.245	0.534
c	1.108	1.239	1.493	1.441	1.185	1.152	1.299	2.839	1.677	1.254	1.475	1.110	1.166	1.264	1.139	1.267	1.139	1.483
Dall's porpoise																		
Abundance	3,132	7,801	4,768	8,487	4,033	3,433	-	7,512	7,661	2,823	2,206	2,354	-	401	-	376	-	-
95% CI (L)	941	3,018	2,185	4,717	1,856	1,565	-	2,637	2,214	651	958	426	-	52	-	38	-	-
95% CI (U)	10,429	20,165	10,405	15,269	8,761	7,531	-	21,402	26,502	12,238	5,082	13,021	-	3,103	-	3,713	-	-
Density	13.13	32.71	19.99	35.59	16.91	14.40	-	31.50	32.12	11.84	9.25	9.87	-	1.68	-	1.58	-	-
cv	0.584	0.506	0.406	0.301	0.399	0.410	-	0.558	0.672	0.611	0.422	1.037	-	1.358	-	1.620	-	-
c	-	-	-	-	-	-	-	-	-	-	-	-	-	-	-	-	-	-

Blue Whales

- Sightings of blue whales were highest in summer and lowest in winter. Sightings primarily occurred along the continental slope or farther offshore, except for in the southern half of the survey region during summer, when sightings were also present closer to shore (Figure 25).
- Blue whale detection probability was highest under 0.4 km (Figure 25).
- Abundance was highest in the summer and lowest in the winter and was generally consistent across years. However, there was a decrease in 2007/2008 and again in 2018, as well as an increase in 2021. There was no abundance estimate for 2020 because the survey only occurred in winter that year, when blue whale sightings are rare (Figure 25).
- Density estimates (Table 9) were generally comparable to those for the California Current Ecosystem (CCE; Becker *et al.*, 2020).

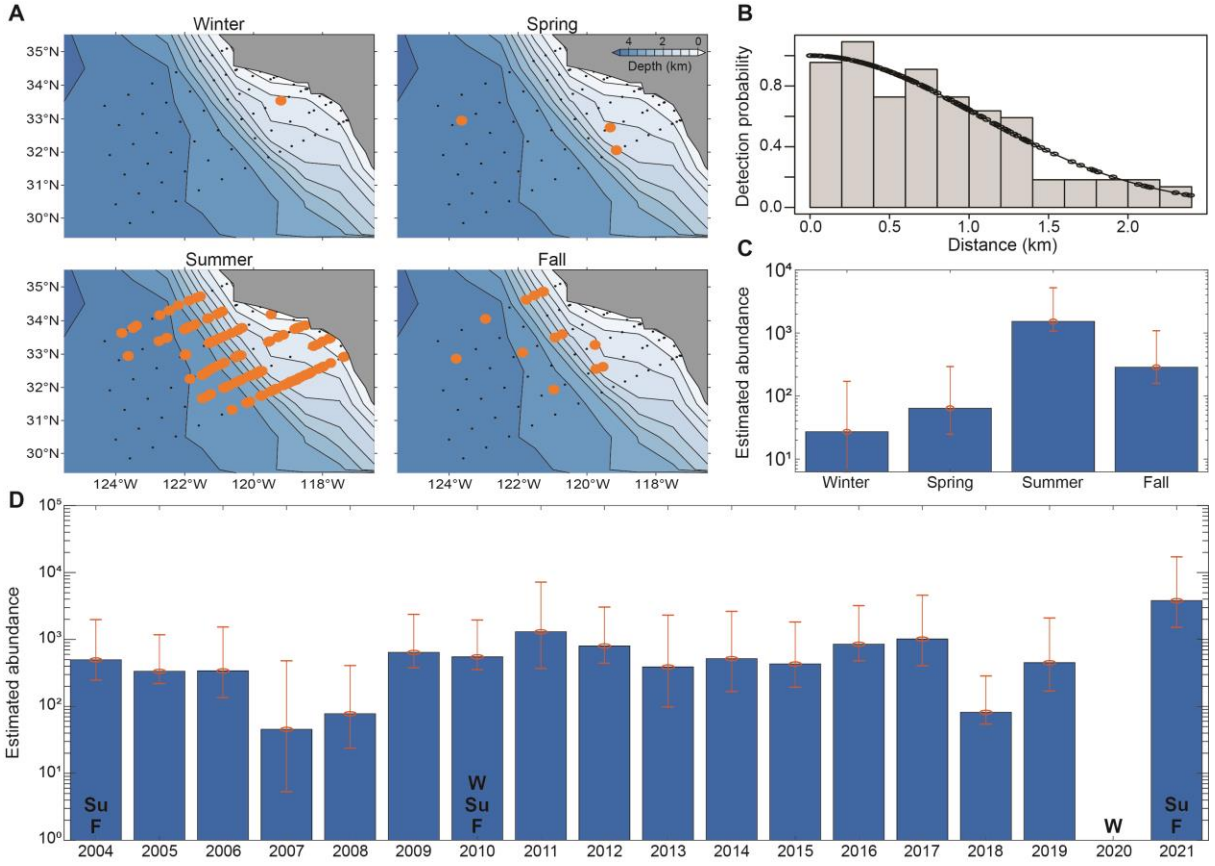

Figure 25. Blue whale sightings, detection probability, and abundance from 2004 to 2021. (A) On-effort, on-transect sightings each season from 2004 to 2021. Black dots represent CalCOFI oceanographic stations and each orange circle represents one visual encounter. (B) Detection function model as a scaled histogram that shows the distribution of perpendicular distances in kilometers. Black circles represent the probability of detection based on perpendicular distance. Estimated abundance each season (C) and year (D) based on quarterly cruises each year except for 2004, 2010, 2020, and 2021 (black abbreviations for these years indicate seasons in which cruises occurred). Red bars represent 95% confidence intervals. Note the y-axes are a log scale.

Fin Whales

- Sightings of fin whales were highest in summer and lowest in winter. During winter and spring sightings primarily occurred inshore, while in fall sightings occurred further offshore (Figure 26).
- Fin whale detection probability was highest under 0.6 km (Figure 26).
- Abundance was highest in the summer and lowest in the winter and increased from 2010 to 2014. Abundance has fluctuated each year since 2014 (Figure 26).
- Density estimates (Table 9) were generally comparable to those for the California Current Ecosystem (Becker *et al.*, 2020).

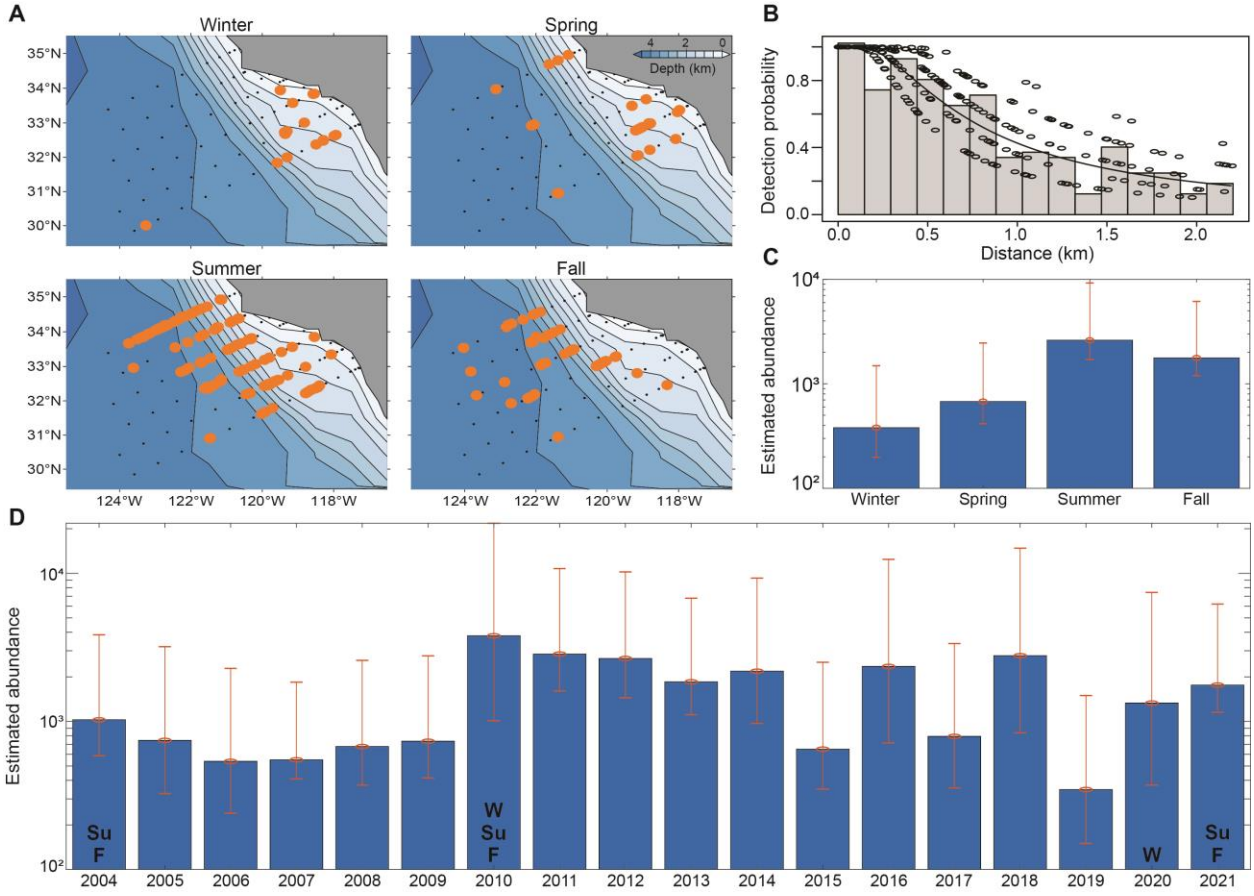

Figure 26. Fin whale sightings, detection probability, and abundance from 2004 to 2021. (A) On-effort, on-transect sightings each season from 2004 to 2021. Black dots represent CalCOFI oceanographic stations and each orange circle represents one visual encounter. (B) Detection function model as a scaled histogram that shows the distribution of perpendicular distances in kilometers. Black circles represent the probability of detection based on perpendicular distance and Beaufort sea state. Estimated abundance each season (C) and year (D) based on quarterly cruises each year except for 2004, 2010, 2020, and 2021 (black abbreviations for these years indicate seasons in which cruises occurred). Red bars represent 95% confidence intervals. Note the y-axes are a log scale.

Humpback Whales

- Sightings of humpback whales were highest in spring and lowest in summer (Figure 27).
- Humpback whale detection probability was highest under 0.6 km (Figure 27).
- Abundance varied slightly between seasons and was highest in the spring and lowest in the summer. Abundance has shown a gradual increase over the period analyzed, except for a decrease from 2010 to 2012 (Figure 27).
- Density estimates (Table 9) were generally comparable to those for the California Current Ecosystem (Becker *et al.*, 2020).

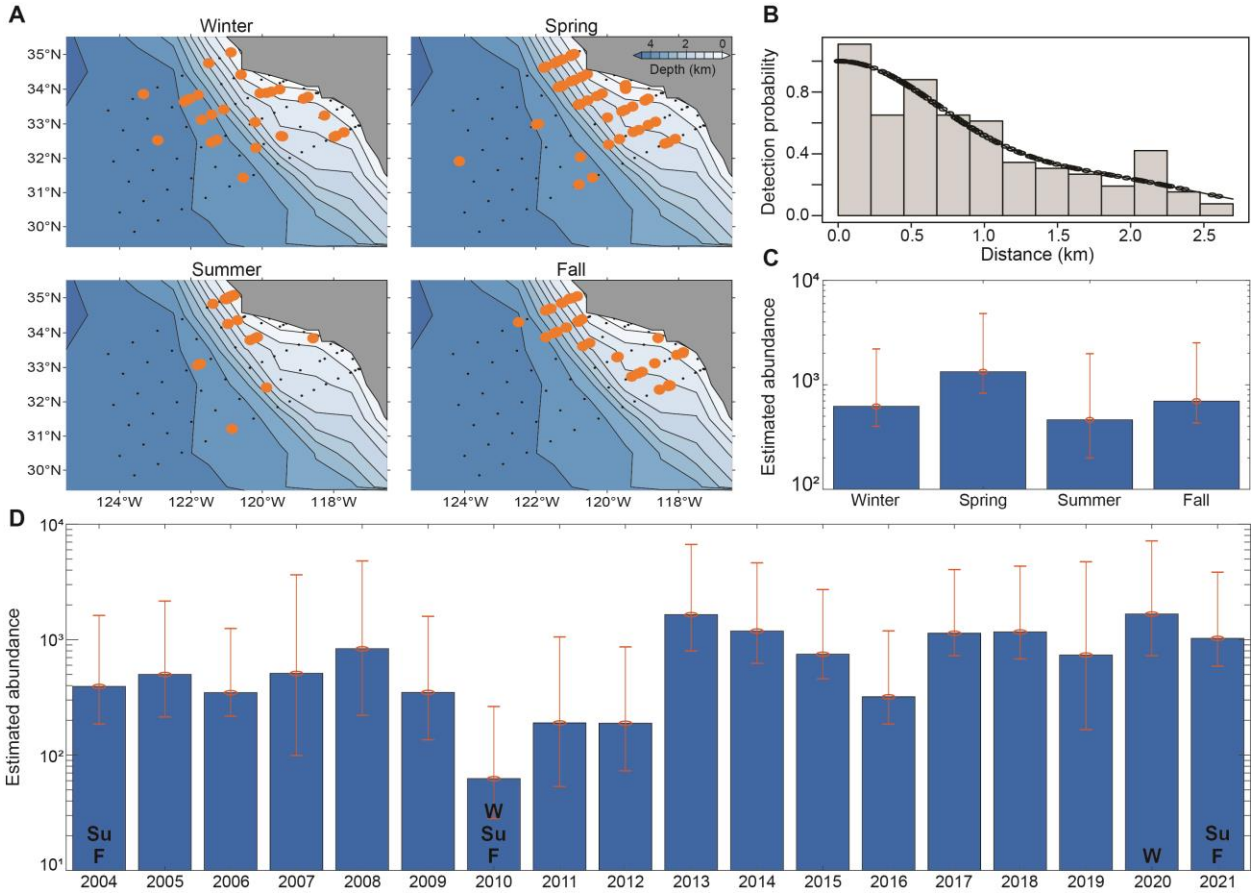

Figure 27. Humpback whale sightings, detection probability, and abundance from 2004 to 2021. (A) On-effort, on-transect sightings each season from 2004 to 2021. Black dots represent CalCOFI oceanographic stations and each orange circle represents one visual encounter. (B) Detection function model as a scaled histogram that shows the distribution of perpendicular distances in kilometers. Black circles represent the probability of detection based on perpendicular distance. Estimated abundance each season (C) and year (D) based on quarterly cruises each year except for 2004, 2010, 2020, and 2021 (black abbreviations for these years indicate seasons in which cruises occurred). Red bars represent 95% confidence intervals. Note the y-axes are a log scale.

Unidentified Large Whales

- Sightings of unidentified large whales were common year round, but were highest in summer and lowest in winter (Figure 28).
- These whales were most likely blue, fin, or humpback whales.

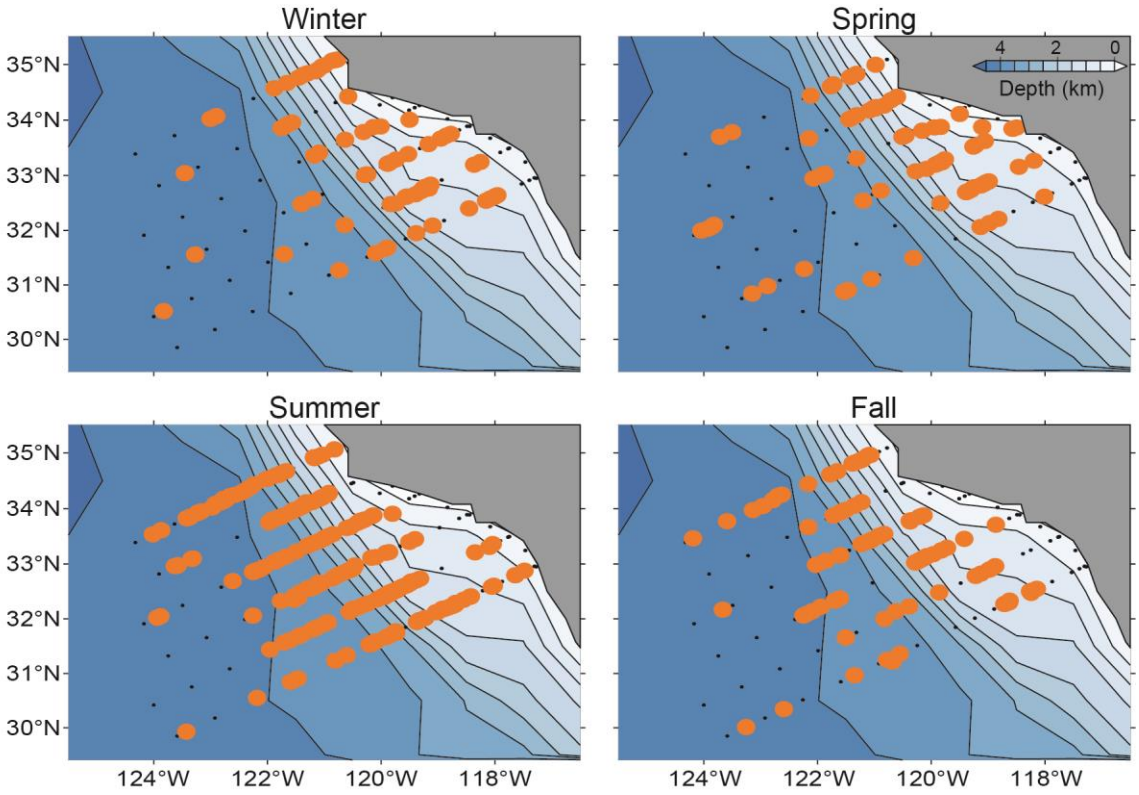

Figure 28. Unidentified large whale sightings from 2004 to 2021.
On-effort, on-transect sightings each season from 2004 to 2021. Black dots represent CalCOFI oceanographic stations and each orange circle represents one visual encounter.

Gray Whales

- Sightings of gray whales were highest in winter and occurred close to shore throughout the survey region. There were also some nearshore sightings in spring in the southern half of the survey region. There were no sightings in summer or fall (Figure 29).
- Gray whale detection probability was highest under 0.6 km (Figure 29).
- Abundance was highest in the winter and shows yearly variation over the study period, with peaks in 2011, 2015, and 2020. There was no abundance estimate for 2021 because surveys did not occur in winter and spring, which have previously been the only seasons with gray whale sightings (Figure 29).
- Previous density estimates of cetacean species in the California Current Ecosystem did not include gray whales (Becker *et al.*, 2020).

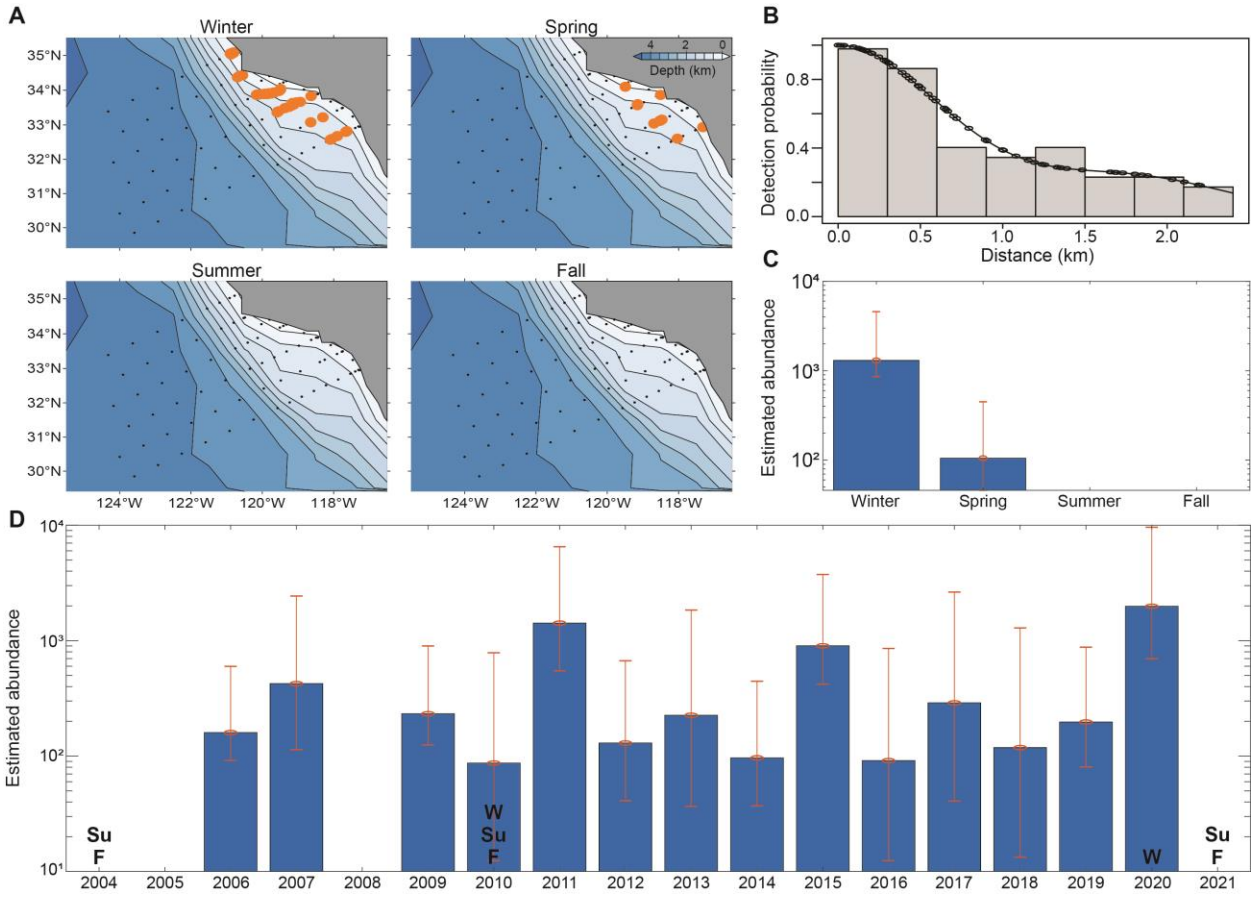

Figure 29. Gray whale sightings, detection probability, and abundance from 2004 to 2021. (A) On-effort, on-transect sightings each season from 2004 to 2021. Black dots represent CalCOFI oceanographic stations and each orange circle represents one visual encounter. (B) Detection function model as a scaled histogram that shows the distribution of perpendicular distances in kilometers. Black circles represent the probability of detection based on perpendicular distance. Estimated abundance each season (C) and year (D) based on quarterly cruises each year except for 2004, 2010, 2020, and 2021 (black abbreviations for these years indicate seasons in which cruises occurred). Red bars represent 95% confidence intervals. Note the y-axes are a log scale.

Bottlenose Dolphins

- Sightings of bottlenose dolphins were lowest in spring and relatively consistent in other seasons. Sightings occurred primarily close to shore (Figure 30).
- Bottlenose dolphin detection probability was highest under 0.2 km (Figure 30).
- Abundance was highest in the winter and fall and lowest in the spring. Abundance has fluctuated over the years of the study but has shown a gradual increase overall (Figure 30).
- Density estimates (Table 9) were higher than those for the California Current Ecosystem (Becker *et al.*, 2020).

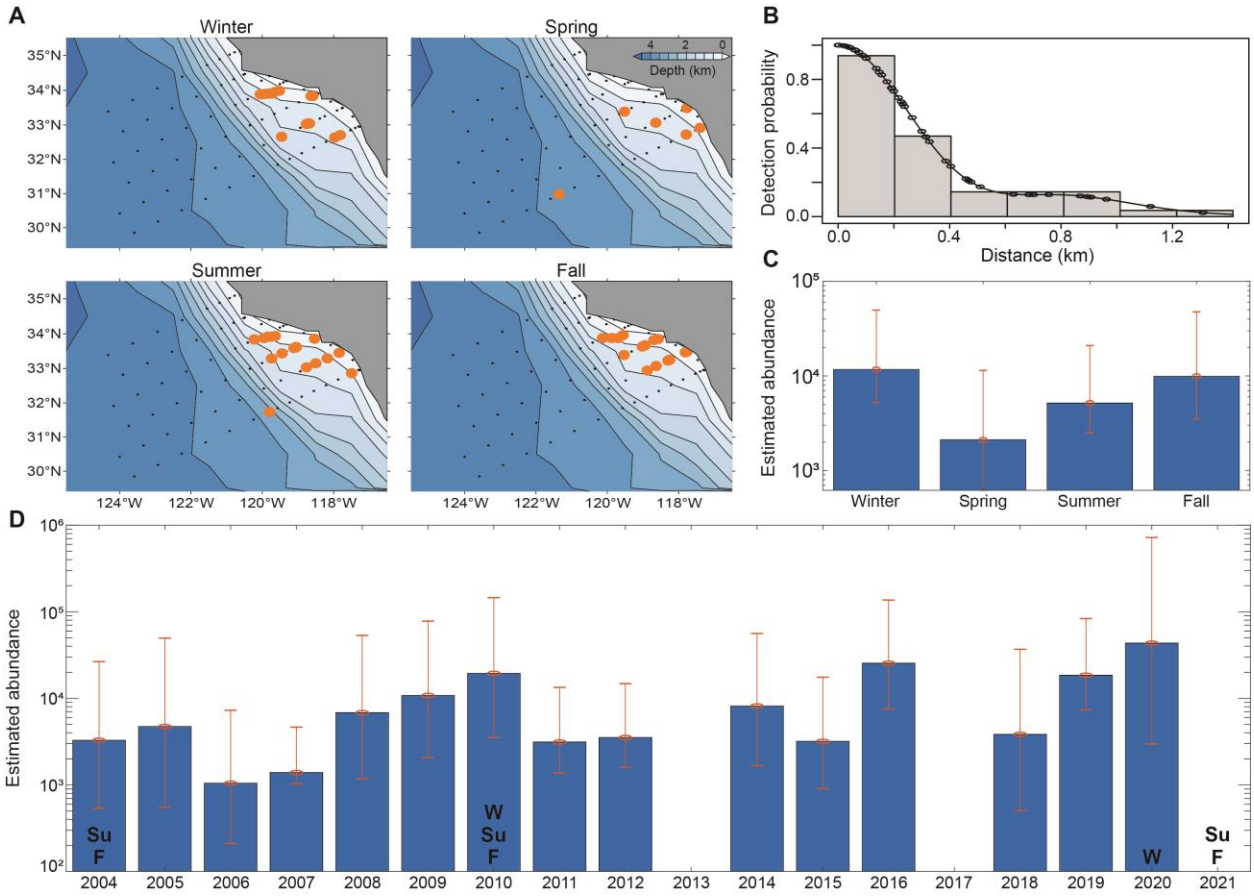

Figure 30. Bottlenose dolphin sightings, detection probability, and abundance from 2004 to 2021. (A) On-effort, on-transect sightings each season from 2004 to 2021. Black dots represent CalCOFI oceanographic stations and each orange circle represents one visual encounter. (B) Detection function model as a scaled histogram that shows the distribution of perpendicular distances in kilometers. Black circles represent the probability of detection based on perpendicular distance. Estimated abundance each season (C) and year (D) based on quarterly cruises each year except for 2004, 2010, 2020, and 2021 (black abbreviations for these years indicate seasons in which cruises occurred). Red bars represent 95% confidence intervals. Note the y-axes are a log scale.

Risso's Dolphins

- Sightings of Risso's dolphins were similar across seasons and occurred primarily close to shore with occasional sightings far offshore (Figure 31).
- Risso's dolphin detection probability was highest under 0.6 km (Figure 31).
- Abundance was highest in the spring and has been relatively stable across years. The high confidence intervals in 2015 are the result of an above average group size estimate during the spring cruise, resulting in a large coefficient of variation for the year (Figure 31).
- Density estimates (Table 9) were generally comparable to those for the California Current Ecosystem (Becker *et al.*, 2020).

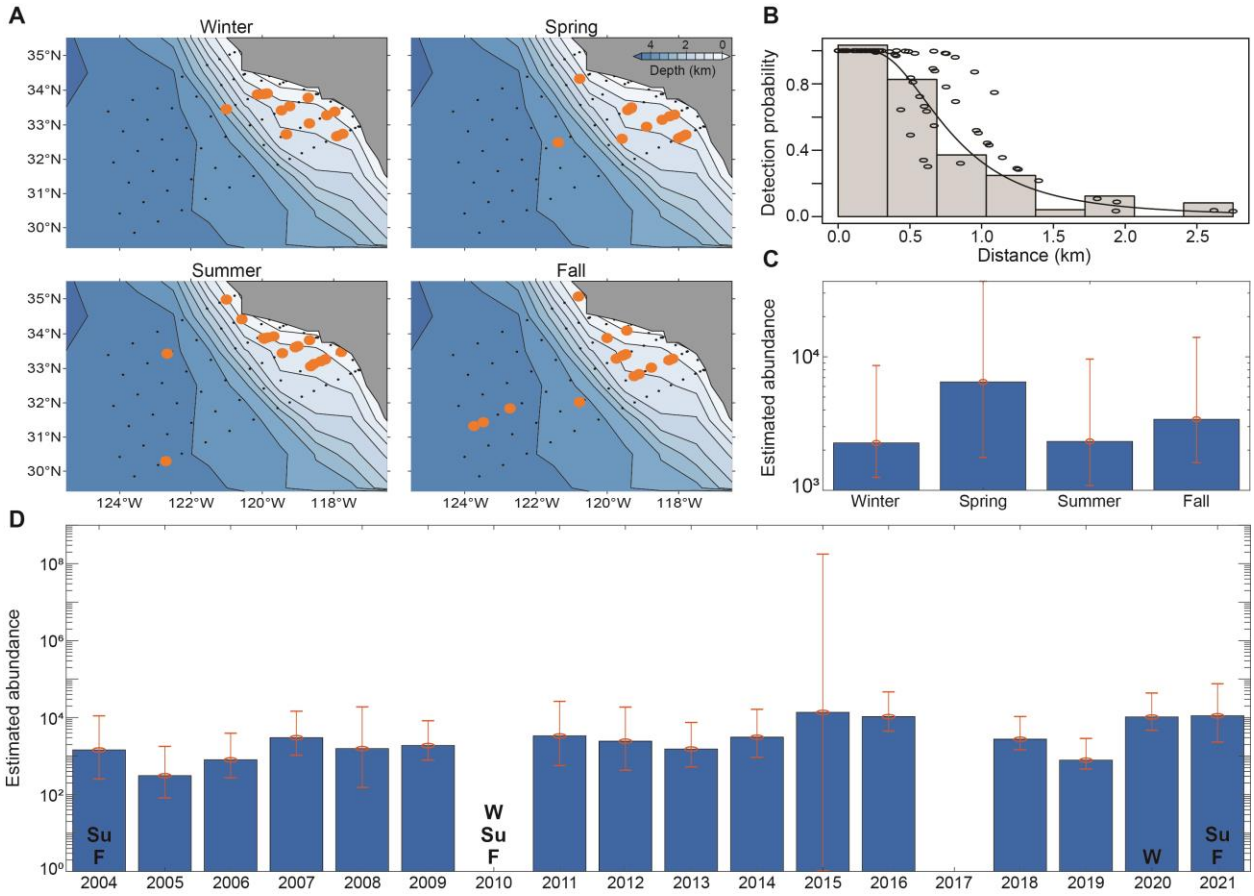

Figure 31. Risso's dolphin sightings, detection probability, and abundance from 2004 to 2021. (A) On-effort, on-transect sightings each season from 2004 to 2021. Black dots represent CalCOFI oceanographic stations and each orange circle represents one visual encounter. (B) Detection function model as a scaled histogram that shows the distribution of perpendicular distances in kilometers. Black circles represent the probability of detection based on perpendicular distance and Beaufort sea state. Estimated abundance each season (C) and year (D) based on quarterly cruises each year except for 2004, 2010, 2020, and 2021 (black abbreviations for these years indicate seasons in which cruises occurred). Red bars represent 95% confidence intervals. Note the y-axes are a log scale.

Pacific White-sided Dolphins

- Sightings of Pacific white-sided dolphins were highest in spring and lowest in fall. Sightings occurred primarily along the continental slope, although in fall detections tended to occur close to shore and only in the southern half of the survey region (Figure 32).
- Pacific white-sided dolphin detection probability was highest under 0.1 km (Figure 32).
- Abundance was highest in the spring and lowest in the fall and was consistent across most years, except for decreases in 2009, 2011 and 2015 (Figure 32).
- Density estimates (Table 9) were generally comparable to those for the California Current Ecosystem (Becker *et al.*, 2020).

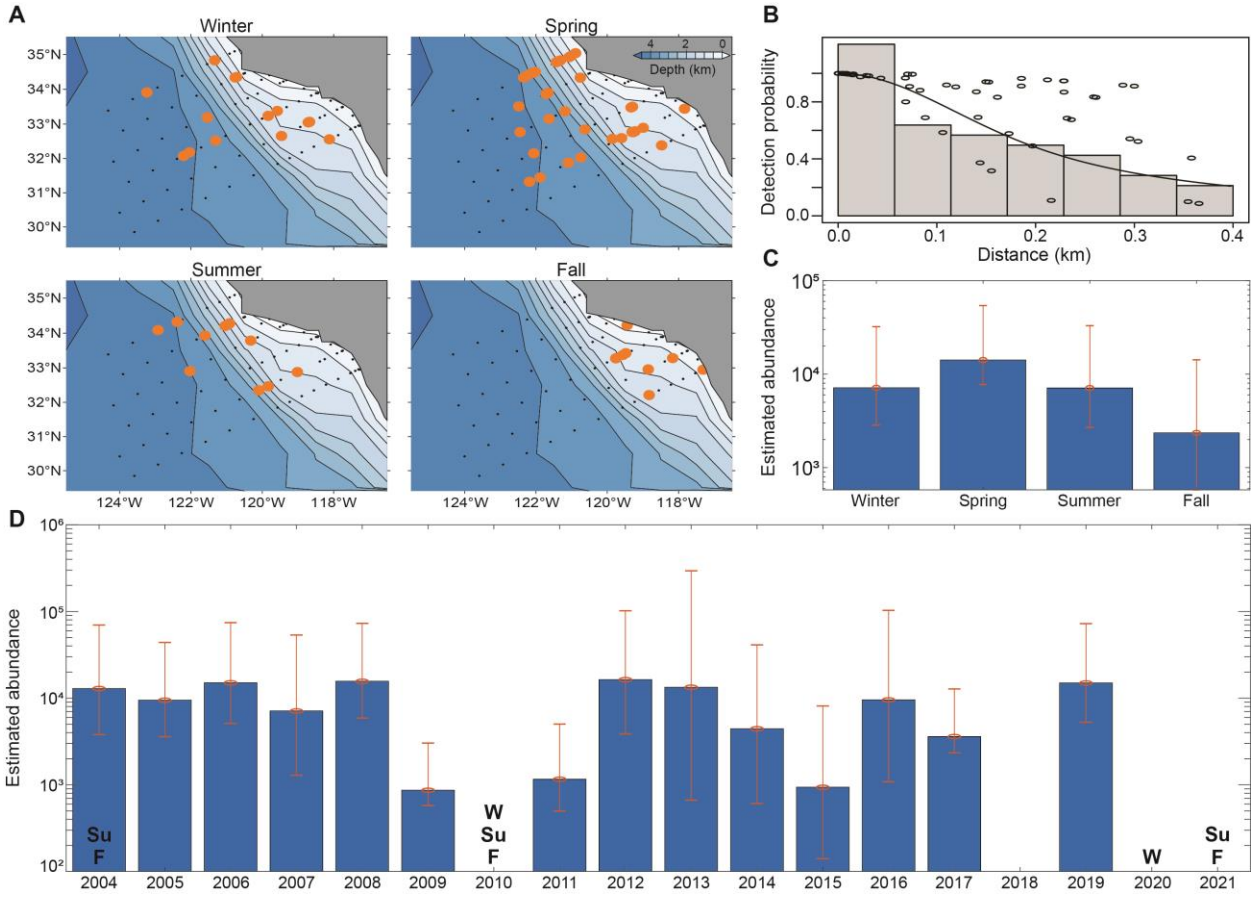

Figure 32. Pacific white-sided dolphin sightings, detection probability, and abundance from 2004 to 2021.
(A) On-effort, on-transect sightings each season from 2004 to 2021. Black dots represent CalCOFI oceanographic stations and each orange circle represents one visual encounter. (B) Detection function model as a scaled histogram that shows the distribution of perpendicular distances in kilometers. Black circles represent the probability of detection based on perpendicular distance and Beaufort sea state. Estimated abundance each season (C) and year (D) based on quarterly cruises each year except for 2004, 2010, 2020, and 2021 (black abbreviations for these years indicate seasons in which cruises occurred). Red bars represent 95% confidence intervals. Note the y-axes are a log scale.

Common Dolphins

Common dolphins were identified as long- or short-beaked when possible and were otherwise classified as unspecified common dolphins. Short-beaked common dolphins were also divided based on group size (≤ 20 or > 20 individuals).

Long-beaked Common Dolphins

- Sightings of long-beaked common dolphins were highest in winter and lowest in spring. In winter sightings occurred exclusively nearshore and summer was the only season in which sightings occurred in the northern portion of the survey area (Figure 33).
- Long-beaked common dolphin detection probability was highest under 0.1 km (Figure 33).
- Abundance was highest in the winter, lowest in the spring, and generally increased over the survey years (Figure 33).
- Density estimates (Table 9) were generally comparable to those for the California Current Ecosystem (Becker *et al.*, 2020).

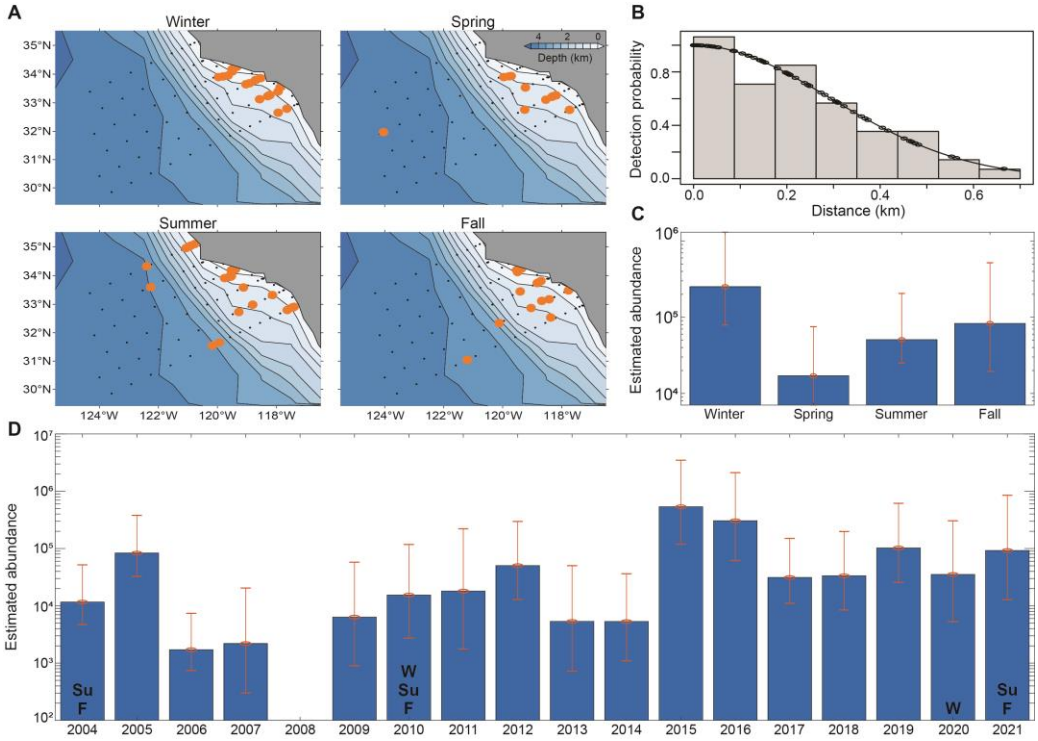

Figure 33. Long-beaked common dolphin sightings, detection probability, and abundance from 2004 to 2021.
(A) On-effort, on-transect sightings each season from 2004 to 2021. Black dots represent CalCOFI oceanographic stations and each orange circle represents one visual encounter. (B) Detection function model as a scaled histogram that shows the distribution of perpendicular distances in kilometers. Black circles represent the probability of detection based on perpendicular distance. Estimated abundance each season (C) and year (D) based on quarterly cruises each year except for 2004, 2010, 2020, and 2021 (black abbreviations for these years indicate seasons in which cruises occurred). Red bars represent 95% confidence intervals. Note the y-axes are a log scale.

Short-beaked Common Dolphins

- Short-beaked common dolphins were regularly sighted throughout the survey region during all seasons, except for along the continental slope offshore of point conception, where sightings were absent during all seasons except fall (Figure 34).
- For short-beaked common dolphin sightings with ≤ 20 individuals, detection probability was highest under 0.03 km. Abundance was highest during winter, lowest during fall, and relatively stable across the survey years, except for a decrease in 2010 (Figure 35).
- For short-beaked common dolphin sightings with > 20 individuals, detection probability was highest under 0.05 km. Abundance was highest during winter and lowest during summer and fall. Over the years of the study, abundance has shown a slight increase, although abundance was low in 2021 (Figure 36).
- Density estimates (Table 9) were generally comparable to those for the California Current Ecosystem (Becker *et al.*, 2020).

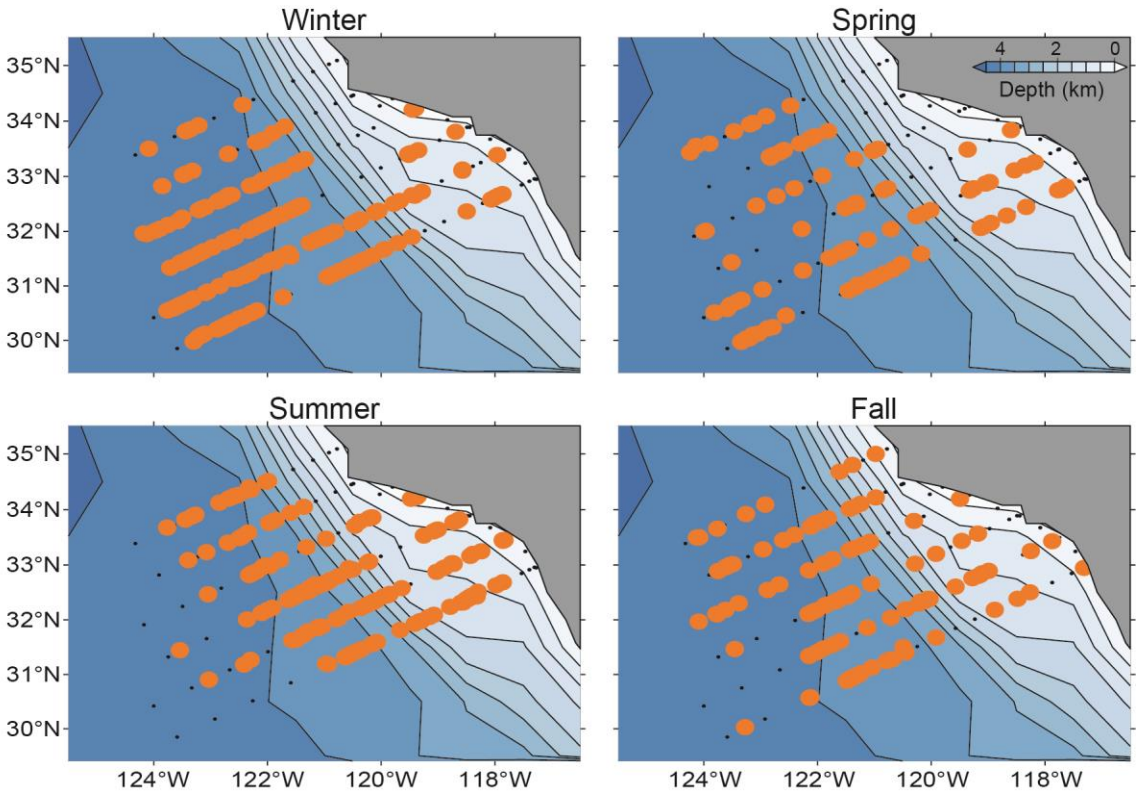

Figure 34. Short-beaked common dolphin sightings from 2004 to 2021.
On-effort, on-transect sightings each season from 2004 to 2021. Black dots represent CalCOFI oceanographic stations and each orange circle represents one visual encounter.

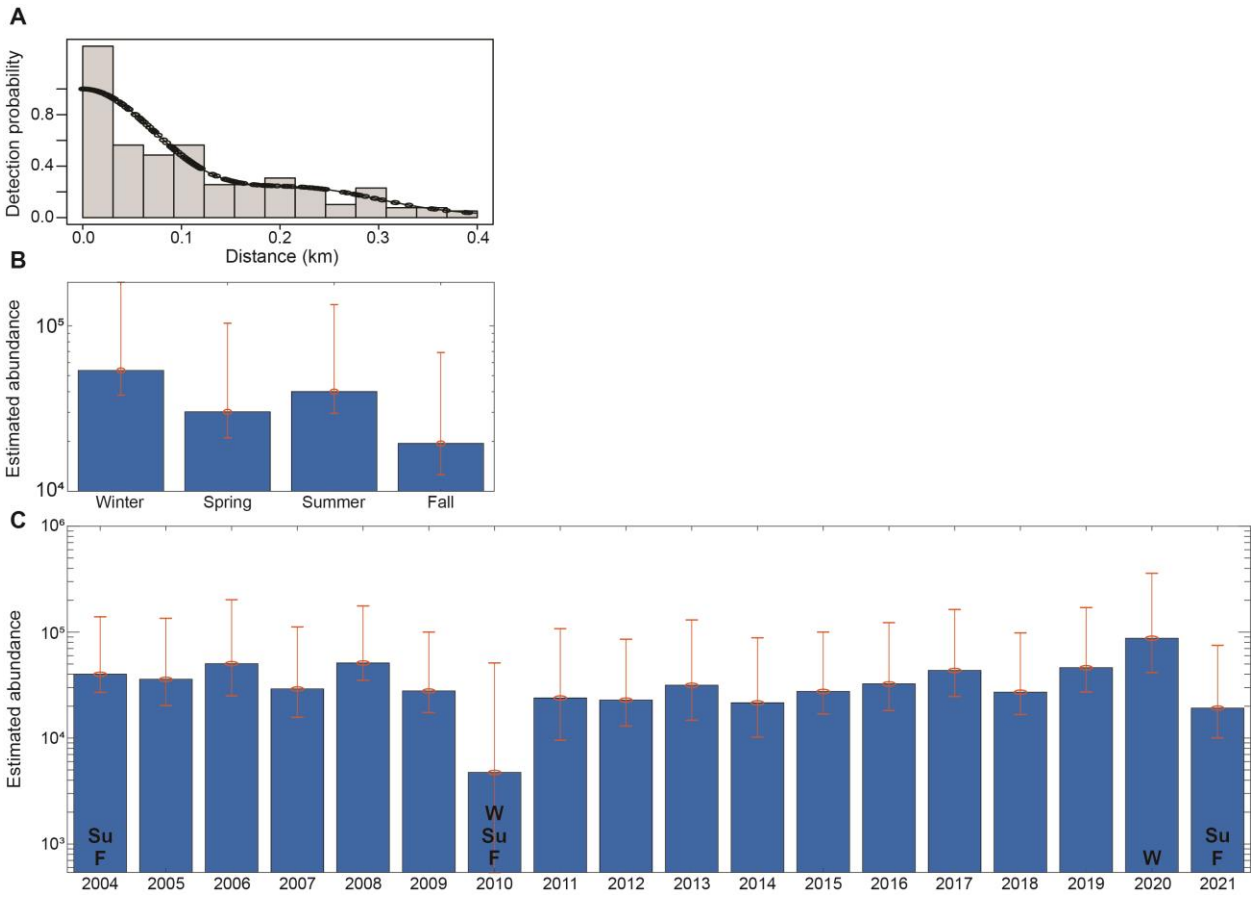

Figure 35. Short-beaked common dolphin detection probability and abundance for groups with 20 individuals or less, from 2004 to 2021.
(A) Detection function model as a scaled histogram that shows the distribution of perpendicular distances in kilometers. Black circles represent the probability of detection based on perpendicular distance. Estimated abundance each season (B) and year (C) based on quarterly cruises each year except for 2004, 2010, 2020, and 2021 (black abbreviations for these years indicate seasons in which cruises occurred). Red bars represent 95% confidence intervals. Note the y-axes are a log scale.

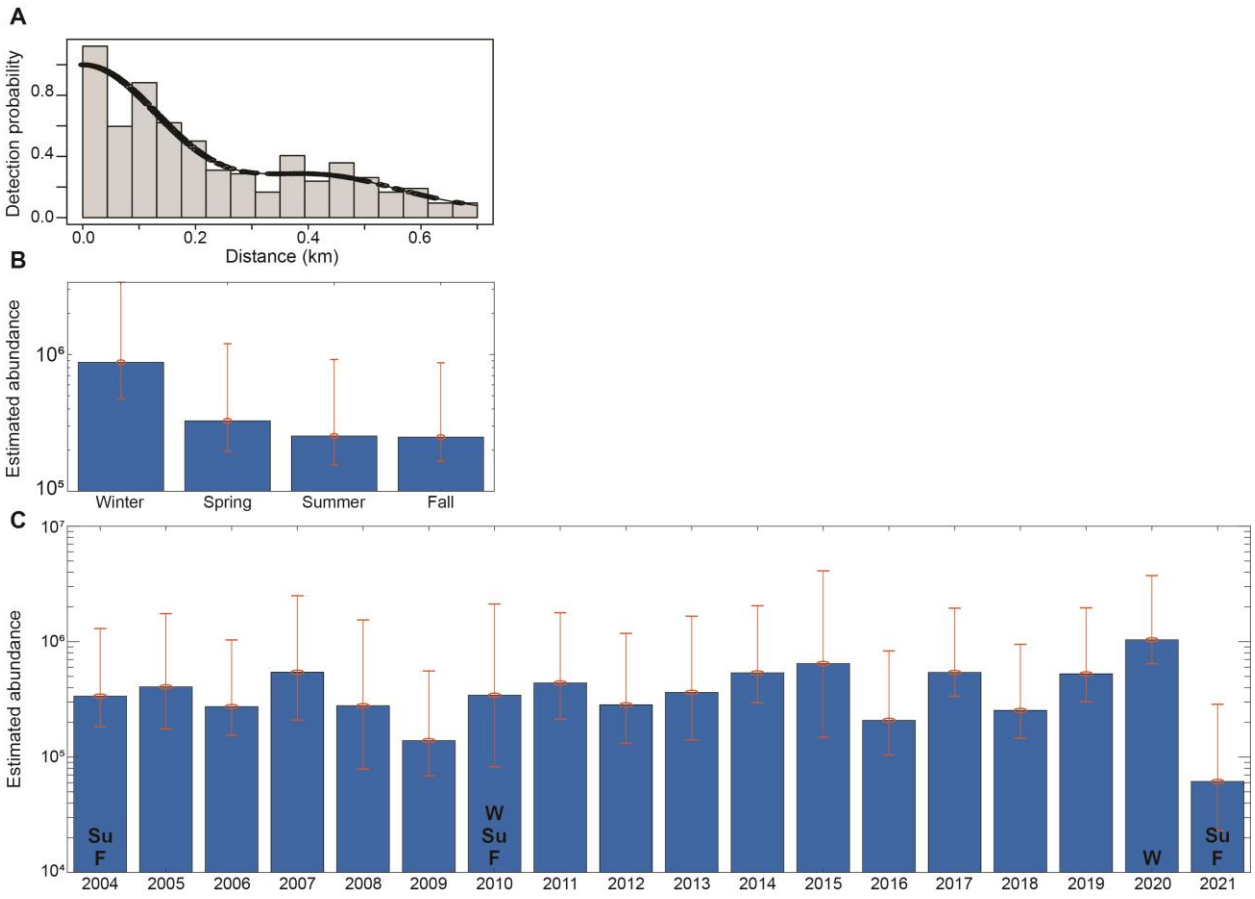

Figure 36. Short-beaked common dolphin detection probability and abundance for groups with more than 20 from 2004 to 2021.
(A) Detection function model as a scaled histogram that shows the distribution of perpendicular distances in kilometers. Black circles represent the probability of detection based on perpendicular distance. Estimated abundance each season (B) and year (C) based on quarterly cruises each year except for 2004, 2010, 2020, and 2021 (black abbreviations for these years indicate seasons in which cruises occurred). Red bars represent 95% confidence intervals. Note the y-axes are a log scale.

Unspecified Common Dolphins

- Sightings of unspecified common dolphins occurred throughout the survey region but were generally highest in summer and lowest in winter (Figure 37).

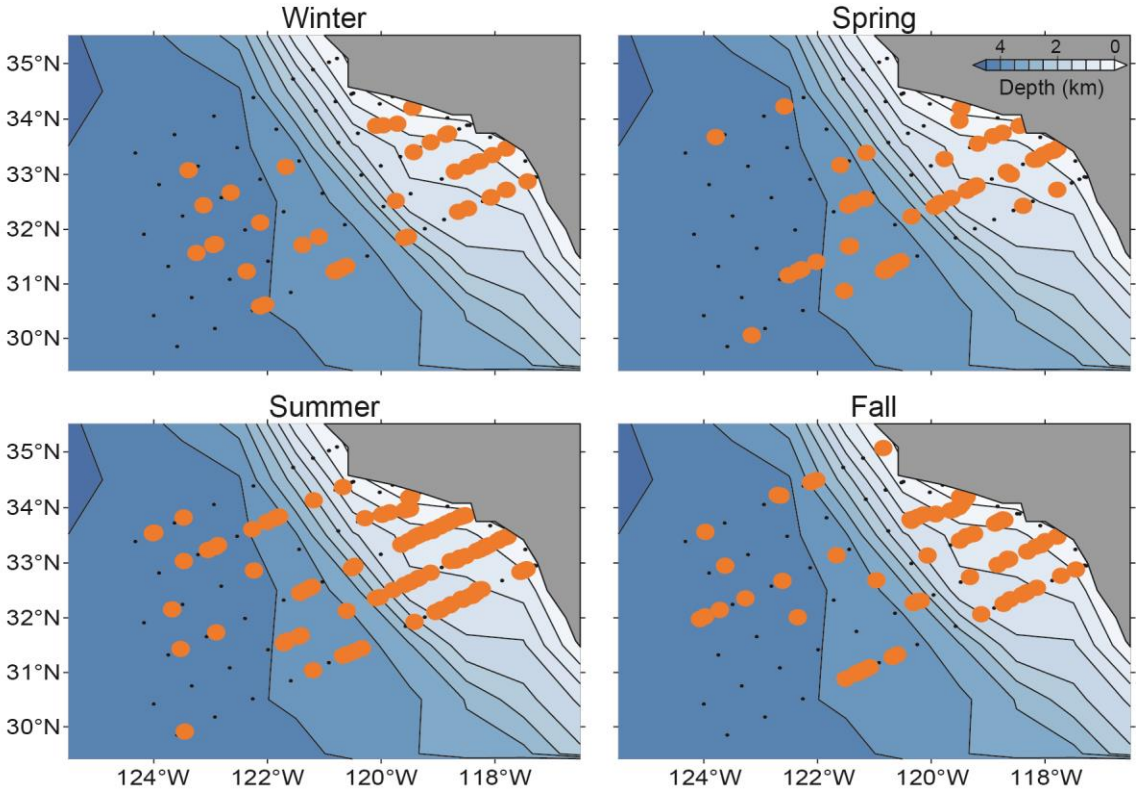

Figure 37. Unspecified common dolphin sightings from 2004 to 2021.
On-effort, on-transect sightings each season from 2004 to 2021. Black dots represent CalCOFI oceanographic stations and each orange circle represents one visual encounter.

Dall's Porpoises

- Sightings of Dall's porpoises were highest in spring and were lowest in summer and fall (Figure 38).
- Dall's porpoise detection probability was highest under 0.1 km (Figure 38).
- Abundance was highest in the winter and spring and lowest in the summer. Abundance was stable from 2004 to 2015 but was low in 2017 and 2019 (Figure 38).
- Density estimates (Table 9) were lower than those for the California Current Ecosystem (Becker *et al.*, 2020).

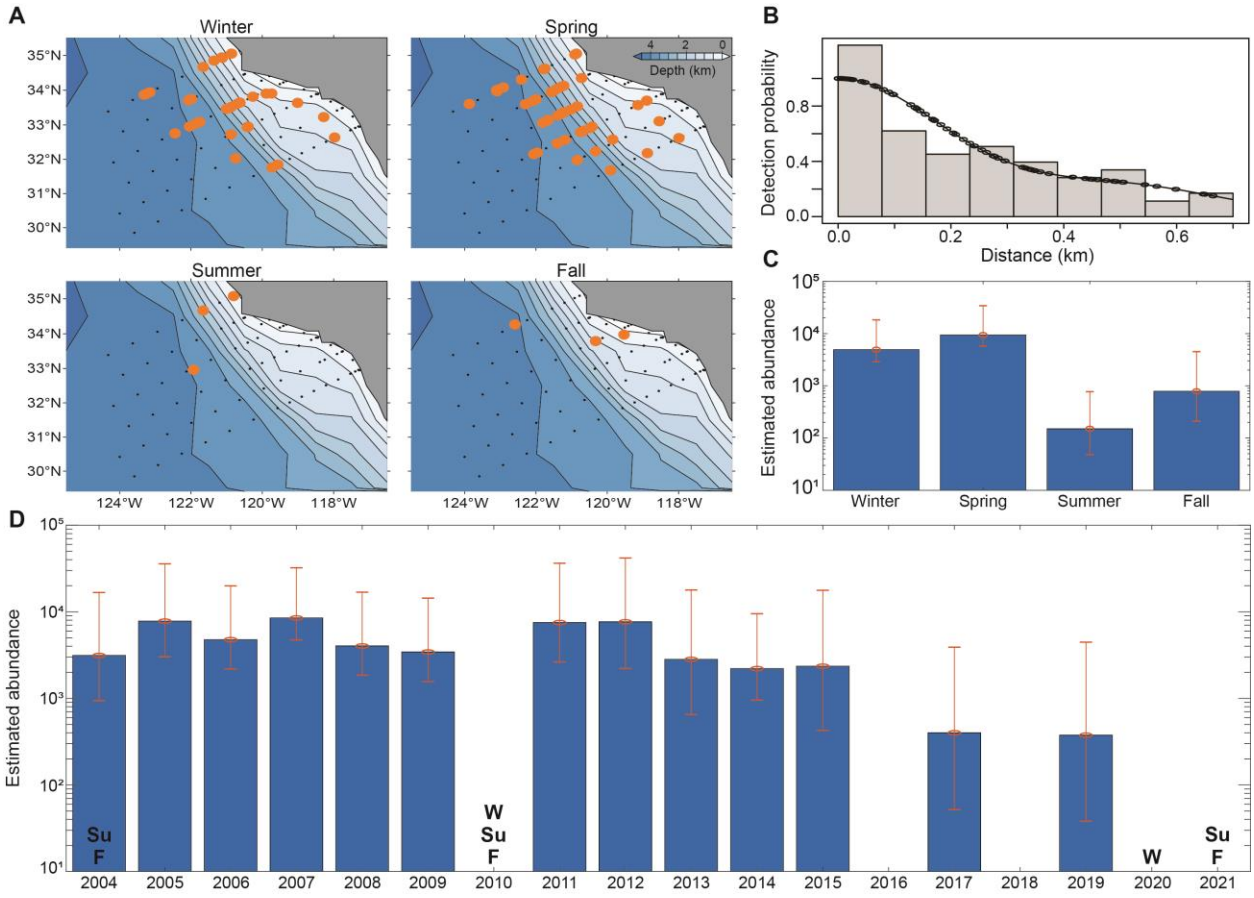

Figure 38. Dall's porpoise sightings, detection probability, and abundance from 2004 to 2021. (A) On-effort, on-transect sightings each season from 2004 to 2021. Black dots represent CalCOFI oceanographic stations and each orange circle represents one visual encounter. (B) Detection function model as a scaled histogram that shows the distribution of perpendicular distances in kilometers. Black circles represent the probability of detection based on perpendicular distance. Estimated abundance each season (C) and year (D) based on quarterly cruises each year except for 2004, 2010, 2020, and 2021 (black abbreviations for these years indicate seasons in which cruises occurred). Red bars represent 95% confidence intervals. Note the y-axes are a log scale.

Conclusions

The passive acoustic monitoring results from this report are generally consistent with previous reports on the SOCAL region. The main differences during this reporting period were the higher number of Cuvier's beaked whale FM pulses at site N and the lack of Hubbs' beaked whale FM pulse detections at sites E and N. As noted during the previous reporting period, site N again had fewer MFA wave trains and packets normalized per year than in previous monitoring periods, while values at site H returned to previously reported levels. Passive acoustic monitoring will continue in the SOCAL range in an effort to document the seasonal presence of this subset of marine mammal species and to record anthropogenic activity as well as the low-frequency ambient soundscape.

CalCOFI visual surveys will also continue in the SOCAL region to further document marine mammal abundance. Of the four mysticete species examined from 2004 to 2021, fin whales were the most commonly sighted. Blue and fin whale abundance was higher in summer and fall, while humpback and gray whale abundance was higher in winter and spring, though detection probability was similar for all four species. Humpback whales showed a possible increase in abundance over time. Of the five odontocete species examined, common dolphins were most often sighted, specifically short-beaked common dolphins. Bottlenose and common dolphin abundance was highest in winter, while Risso's dolphin, Pacific white-sided dolphin, and Dall's porpoise abundance was highest in spring. Bottlenose and common dolphins have shown a potential increase in abundance over time, while Dall's porpoise abundance has declined in recent years.

References

Ballance, L. T., Pitman, R. L., Barlow, J., Pusser, T., DeAngelis, A., Hayslip, C., Irvine, L., Steel, D., Baker, S., Gillies, D., Trickey, J. S., and Baumann-Pickering, S. (**2022**). "Hubbs' beaked whale revealed! Linked acoustic, genetic, and photographic data from *Mesoplodon carlhubbsi*," in *Society of Marine Mammology* (West Palm Beach, FL, USA).

Barlow, J., and Forney, K. A. (**2007**). "Abundance and population density of cetaceans in the California Current ecosystem," Fishery Bulletin **105**, 509-526.

Baumann-Pickering, S., McDonald, M. A., Simonis, A. E., Solsona Berga, A., Merkens, K. P. B., Oleson, E. M., Roch, M. A., Wiggins, S. M., Rankin, S., Yack, T. M., and Hildebrand, J. A. (**2013a**). "Species-specific beaked whale echolocation signals," Journal of the Acoustical Society of America **134**, 2293-2301.

Baumann-Pickering, S., Simonis, A. E., Roch, M. A., McDonald, M. A., Solsona Berga, A., Oleson, E. M., Wiggins, S. M., Brownell, J., Robert, L., and Hildebrand, J. A. (**2014**). "Spatio-temporal patterns of beaked whale echolocation signals in the North Pacific," PLOS One, e86072.

Baumann-Pickering, S., Simonis, A. E., Wiggins, S. M., Brownell, R. L. J., and Hildebrand, J. A. (**2013b**). "Aleutian Islands beaked whale echolocation signals," Marine Mammal Science **29**, 221-227.

Becker, E. A., Forney, K. A., Miller, D. L., Fiedler, P. C., Barlow, J., and Moore, J. E. (**2020**). "Habitat-based density estimates for cetaceans in the California Current Ecosystem based on 1991-2018 survey data," (U.S. Department of Commerce, NOAA Technical Memorandum NMFS-SWFSC-638).

Becker, E. A., Forney, K. A., Thayre, B. J., Debich, A. J., Campbell, G. S., Whitaker, K., Douglas, A. B., Gilles, A., Hoopes, R., and Hildebrand, J. A. (**2017**). "Habitat-based density models for three cetacean species off Southern California illustrate pronounced seasonal differences," Frontiers in Marine Science **4**, 14.

Buckland, S. T., Anderson, D. R., Burnham, K. P., Laake, J. L., Borchers, D. L., and Thomas, L. (**2001**). *Introduction to Distance Sampling: Estimating Abundance of Biological Populations* (Oxford University Press, Oxford, UK).

Campbell, G. S., Thomas, L., Whitaker, K., Douglas, A. B., Calambokidis, J., and Hildebrand, J. A. (**2015**). "Inter-annual and seasonal trends in cetacean distribution, density and abundance off southern California," Deep-Sea Research Part II-Topical Studies in Oceanography **112**, 143-157.

Debich, A. J., Baumann-Pickering, A., Širović, A., Hildebrand, J. A., Herbert, S. T., Johnson, S. C., Rice, A. C., Trickey, J. S., and Wiggins, S. M. (**2015a**). "Passive Acoustic Monitoring for Marine Mammals in the SOCAL Range Complex January - July 2014," (Marine Physical Laboratory, Scripps Institution of Oceanography, La Jolla, CA), p. 43.

Debich, A. J., Baumann-Pickering, S., Širović, A., Hildebrand, J. A., Alldredge, A. L., Gottlieb, R. S., Herbert, S. T., Johnson, S. C., Rice, A. C., Roche, L. K., Theyre, B. J., Trickey, J. S., Varga, L. M., and Wiggins, S. M. (**2015b**). "Passive Acoustic Monitoring for Marine Mammals in the SOCAL Naval Training Area Dec 2012 - Jan 2014," (Marine Physical Laboratory, Scripps Institution of Oceanography, La Jolla, CA), p. 96.

Debich, A. J., Thayre, B., and Hildebrand, J. A. (**2017**). "Marine Mammal Monitoring on California Cooperative Oceanic Fisheries Investigation (CalcOFI) Cruises: Summary of Results 2012-2016," (Marine Physical Laboratory, Scripps Institution of Oceanography, University of California San Diego, La Jolla, CA, MPL Technical Memorandum #609).

Griffiths, E. T., Keating, J. L., Barlow, J., and Moore, J. E. (**2018**). "Description of a new beaked whale echolocation pulse type in the California Current," Marine Mammal Science **35**, 1058-1069.

Hildebrand, J. A. (**2009**). "Anthropogenic and natural sources of ambient noise in the ocean," Marine Ecology Progress Series **395**, 5-20.

Hildebrand, J. A., Baumann-Pcikering, S., Širović, A., Buccowich, J., Debich, A., Johnson, S., Kerosky, S., Roche, L., Berga, A. S., and Wiggins, S. M. (**2012**). "Passive Acoustic Monitoring for Marine Mammals in the SOCAL Naval Training Area 2011-2012," (Marine Physical Laboratory, Scripps Institution of Oceanography, La Jolla, CA).

Jefferson, T. A., Webber, M. A., and Pitman, L. (**2015**). "*Marine Mammals of the World: A Comprehensive Guide to their Identification* (2nd Ed). (Academic Press)."

Jefferson, T. A., Webber, M. A., and Pitman, R. L. (**2008**). "*Marine Mammals of the World: A Comprehensive Guide to their Identification* (Academic Press)."

Johnson, M., Madsen, P. T., Zimmer, W. M. X., Aguilar de Soto, N., and Tyack, P. L. (**2004**). "Beaked whales echolocate on prey," Proceedings of the Royal Society B: Biological Sciences **271**, S383-S386.

Kerosky, S. M., Baumann-Pickering, S., Širović, A., Buccowich, J. S., Debich, A. J., Gentes, Z., Gottlieb, R. S., Johnson, S. C., Roche, L. K., Thayre, B., Wakefield, L., Wiggins, S. M., and Hildebrand, J. A. (**2013**). "Passive Acoustic Monitoring for Marine Mammals in the SOCAL Range Complex during 2012," (Marine Physical Laboratory, Scripps Institution of Oceanography, La Jolla, CA), p. 72.

Marques, T. A., Thomas, L., Fancy, S. G., and Buckland, S. T. (**2007**). "Improving estimates of bird density using multiple-covariate distance sampling," Auk **124**, 1229-1243.

McDonald, M. A., Hildebrand, J. A., Wiggins, S. M., and Ross, D. (**2008**). "A 50 year comparison of ambient noises near San Clemente Island: A bathymetrically complex coastal region off Southern California," Journal of the Acoustical Society of America **124**, 1985-1992.

Miller, D. L., Rexstad, E., Thomas, L., Marshall, L., and Laake, J. L. (**2019**). "Distance sampling in R," Journal of Statistical Software **89**, 1-28.

Rice, A. C., Baumann-Pickering, S., Hildebrand, J. A., Rafter, M., Reagan, E., Trickey, J. S., and Wiggins, S. M. (**2019**). "Passive Acoustic Monitoring for Marine Mammals in the SOCAL Range Complex March 2017 - July 2018," (Marine Physical Laboratory, Scripps Institution of Oceanography, University of California San Diego, La Jolla, CA, MPL Technical Memorandum #636 under Cooperative Ecosystems Study Unit Cooperative Agreement N62473-18-2-0016 for U.S. Navy Pacific Fleet, Pearl Harbor, HI).

Rice, A. C., Baumann-Pickering, S., Širović, A., Hildebrand, J. A., Debich, A. J., Meyer-Lobbecke, A., Thayre, B. J., Trickey, J. A., and Wiggins, S. M. (**2017**). "Passive Acoustic Monitoring for Marine Mammals in the SOCAL Range Complex June 2015 - April 2016," (Marine Physical Laboratory, Scripps Institution of Oceanography, University of California San Diego, La Jolla, CA, MPL Technical Memorandum #610 under Cooperative Ecosystems Study Unit Cooperative Agreement N62473-16-2-0012 for U.S. Navy Pacific Fleet, Pearl Harbor, HI), p. 36.

Rice, A. C., Baumann-Pickering, S., Širović, A., Hildebrand, J. A., Rafter, M., Thayre, B. J., Trickey, J. A., and Wiggins, S. M. (**2018**). "Passive Acoustic Monitoring for Marine Mammals in the SOCAL Range Complex April 2016 - June 2017," (Marine Physical Laboratory, Scripps Institution of Oceanography, University of California San Diego, La Jolla, CA, MPL Technical Memorandum #618 under Cooperative Ecosystems Study Unit Cooperative Agreement N62473-17-2-0014 for U.S. Navy Pacific Fleet, Pearl Harbor, HI), p. 47.

Rice, A. C., Rafter, M., Trickey, J. A., Wiggins, S. M., Baumann-Pickering, S., and Hildebrand, J. A. (**2020**). "Passive Acoustic Monitoring for Marine Mammals in the SOCAL Range Complex July 2018 - May 2019," (Marine Physical Laboratory, Scripps Institution of Oceanography, University of California San Diego, La Jolla, CA, MPL Technical

Memorandum #643 under Cooperative Ecosystems Study Unit Cooperative Agreement N62473-18-2-0016 for U.S. Navy Pacific Fleet, Pearl Harbor, HI).

Rice, A. C., Rafter, M., Trickey, J. S., Wiggins, S. M., Baumann-Pickering, S., and Hildebrand, J. A. (**2021**). "Passive Acoustic Monitoring for Marine Mammals in the SOCAL Range Complex November 2018-May 2020," (Marine Physical Laboratory, Scripps Institution of Oceanography, University of California San Diego, La Jolla, CA, MPL Technical Memorandum #650 under Cooperative Ecosystems Study Unit Cooperative Agreement N62473-19-2-0028 for U.S. Navy Pacific Fleet, Pearl Harbor, HI).

Roch, M. A., Brandes, T. S., Patel, B., Barkley, Y., Baumann-Pickering, S., and Soldevilla, M. S. (**2011a**). "Automated extraction of odontocete whistle contours," Journal of the Acoustical Society of America **130**, 2212-2223.

Roch, M. A., Klinch, H., Baumann-Pickering, S., Mellinger, D. K., Qui, S., Soldevilla, M. S., and Hildebrand, J. A. (**2011b**). "Classification of echolocation clicks from odontocetes in the Southern California Bight," Journal of the Acoustical Society of America **129**, 467-475.

Širović, A., Baumann-Pickering, S., Hildebrand, J. A., Debich, A. J., Herbert, S. T., Meyer-Lobbecke, A., Rice, A., Thayre, B., Trickey, J. S., Wiggins, S. M., and Roch, M. A. (**2016**). "Passive acoustic monitoring for marine mammals in the SOCAL Range Complex July 2014 - May 2015," (Marine Physical Laboratory, Scripps Institution of Oceanography, La Jolla, CA), p. 39.

Soldevilla, M. S., Henderson, E. E., Campbell, G. S., Wiggins, S. M., Hildebrand, J. A., and Roch, M. (**2008**). "Classification of Risso's and Pacific white-sided dolphins using spectral properties of echolocation clicks," Journal of the Acoustical Society of America **124**, 609-624.

Soldevilla, M. S., Wiggins, S. M., Calambokidis, J., Douglas, A., Oleson, E. M., and Hildebrand, J. A. (**2006**). "Marine mammal monitoring and habitat investigations during CalCOFI surveys," California Cooperative Oceanic Fisheries Investigations Reports **47**, 79-91.

Trickey, J. S., Thayre, B. J., Whitaker, K., Giddings, A., Frasier, K. E., Baumann-Pickering, S., and Hildebrand, J. A. (**2020**). "Marine Mammal Monitoring on California Cooperative Oceanic Fisheries Investigation (CalcOFI) Cruises: Summary of Results 2016-2019," (Marine Physical Laboratory, Scripps Institution of Oceanography, University of California San Diego, La Jolla, CA, MPL Technical Memorandum #639 under Cooperative Ecosystems Study Unit Cooperative Agreement N62473-18-2-0016 for U.S. Navy Pacific Fleet, Pearl Harbor, HI).

Wiggins, S. M. (**2015**). "Methods for quantifying mid-frequency active sonar in the SOCAL Range Complex," (Marine Physical Laboratory Technical Memorandum 553, Scripps Institution of Oceanography, University of California San Diego, La Jolla, CA).

Wiggins, S. M., and Hildebrand, J. A. (**2007**). "High-frequency acoustic recording package (HARP) for broadband, long-term marine mammal monitoring," in *International Symposium on Underwater Technology 2007 and International Workshop on Scientific Use of Submarine Cables and Related Technologies 2007* (Institute of Electrical and Electronics Engineers, Tokyo, Japan), pp. 551-557.

Zimmer, W. M. X., Johnson, M. P., Madsen, P. T., and Tyack, P. L. (**2005**). "Echolocation clicks of free-ranging Cuvier's beaked whales (*Ziphius cavirostris*)," Journal of the Acoustical Society of America **117**, 3919-3927.